2015

Effects of Surface Properties on the Charge Regulated Bioenergetic response of Attached Bacteria: Exploration within the Framework of the Chemiosmotic Theory

Lynal Sunila Albert
Lehigh University

Effects of Surface Properties on the Charge Regulated Bioenergetic response of Attached Bacteria: Exploration within the Framework of the Chemiosmotic Theory

by

Lynal Sunila Albert

A Dissertation

Presented to the Graduate and Research Committee

of Lehigh University

in Candidacy for the Degree of

Doctor of Philosophy

In

Environmental Engineering

Lehigh University

(August, 2015)

Approved and recommended for acceptance as a dissertation in partial fulfillment of the requirements for the degree of Doctor of Philosophy.

_____

Date

_____

Dr. Derick G. Brown, Dissertation Director

Professor of Civil and Environmental Engineering

Committee Members:

_____

Date of Acceptance

_____

Dr. Kristen Jellison

Dissertation Committee Chairperson

Professor of Civil and Environmental Engineering

_____

Dr. Arup K. SenGupta

Professor of Civil and Environmental Engineering

_____

Dr. Muhannad Suleiman

Professor of Civil and Environmental Engineering

_____

Dr. Sabrina Jedlicka

Professor of Materials Science and Engineering

Dedicated to my Father…

There is none like you!

Acknowledgements

First and foremost I want to thank my advisor Professor Derick G. Brown without whom this dissertation would not have happened. I wish to express my sincere gratitude for his encouragement, inspiration, and unrelenting support throughout my PhD studies. I am thankful to him for introducing me to a whole new '*academic world'* and teaching me the art of conducting rigorous research. He has spent countless hours reviewing my work, teaching me the craft of publishing, and supporting me in my growth as a researcher, teacher, and student. Most of all, I am thankful for the gracious person he is, and the tremendous positive impact he has had on my life and career. I am greatly indebted to him for all the opportunities he provided me with at Lehigh University and for his commitment to my academic and overall success. I have learned a lot from him, and I hope to someday be able to reflect his qualities, and be a similar blessing to my students.

I would like to thank each of my committee members for their enthusiasm, guidance, and backing throughout my studies. Professor Arup K. SenGupta has always held me to the highest standards both in research and in the classroom. His passion for research and community service is highly contagious, and has greatly influenced me and my career goals. I am grateful to him for his generosity, kindness, and supportive nature. I thank Professor Kristen L. Jellison for her role as my dissertation committee chair, and for actively guiding me throughout my doctoral studies. Most importantly, on several occasions, she has provided me with thoughtful career advice that has been pivotal to my success at and beyond Lehigh. I am extremely grateful to Professor Muhannad Suleiman for his extreme goodness and encouragement. He has always been helpful, thoughtful, and ready to go that extra mile with his support and advice. I very much

appreciate all the guidance and assistance he provided me with during my job interviews. I am thankful to Professor Sabrina Jedlicka for serving as my external committee member, and for providing me with several insights throughout my dissertation preparation. I am immensely honored and fortunate to have each of them in my research committee. Working and interacting with them has been a pleasant and educative experience.

I am grateful to Professor Richard N. Weisman, Professor Gerard Lennon, Mr. William Mushock, Professor John T. Fox and Professor Tara Troy for making valuable contributions to my education at Lehigh. I thank Dr. Sujatha Lamech, Dr. Kalyani Annie and Dr. Florida Tilton from Madras University for having inspired, motivated and challenged me to pursue my research interests. I am immensely grateful to them for having equipped me with the resources required to succeed in my doctoral studies. I am also grateful to my first teacher, Rema Devi whose support and encouragement was indispensable to my academic success.

I thank all my research lab-mates (the current and past) for their support, friendship, and encouragement. I thank Ryan Smith for his friendship and support during my time at Lehigh. I thank Prisca Vidanage, Chrissy Moyer, and Dan Zeroka for their kindness and willingness to always help me.

My time at Pennsylvania was made most beautiful by many friends that became an integral part of my life. I very much enjoyed the memorable dinners and get-togethers with Monica, Gaurav Yajing, Linlin and others. I thank them for being there for me whenever I needed support. I am extremely grateful to Mr. Wesley Jun and Mrs. Sarah Jun for being my guardians, and my parents away from home. I will truly miss them!

I thank Krithi, Mercy, Sreeni, Ranjan and Chalini for being my friends for a life-time, and for always being available when I needed them the most.

I am thankful to my father Mr. M. Albert and my mother Mrs. Regi Albert for their selfless love, sincere devotion, relentless determination and prevailing strength. They have worked hard to provide me with the best education and resources that I may have taken for granted. I thank them for their unconditional love and endless patience. I am truly grateful for all the sacrifices they have made. I thank my Aunt Ms. Magdalene Mary who has always stood by me with her motherly love. I thank my sisters Lumina Albert, Luna Albert, Liji Alex and my brother Alex Albert for their support, friendship and love. They were my cheer leaders all along the way! I also thank my brother-in-law Karan Venayagamoorthy for his support, and for inspiring me to pursue a career in academia.

Finally, I owe immeasurable thanks to my husband and my best friend Saran Kumar Jyothi for all he has done for me. He moved all the way from California so we could be together as I pursued my doctoral studies. I thank him for his unswerving support and patience during my graduate studies. I am truly blessed to have you beside me in this journey of life- you made every step worthwhile!

Above all, I thank my Lord and Savior Jesus Christ for His absolute faithfulness and grace that sustains me every day. All glory be to Him!

This project was funded by the National Science Foundation, I gratefully acknowledge their support.

Table of Contents

List of Tables

List of Figures

Abstract

Microbial adhesion is critical to natural and engineered systems due to the ubiquitous presence of bacteria, their tendency to attach to biotic and abiotic surfaces and their ability to survive in habitats not suitable for most life. Many processes benefit from microbial adhesion, such as attached-growth wastewater treatment and symbiotic nitrogen fixation. In other scenarios, microbial adhesion is highly detrimental and examples include pathogenic biofilm infections on medical implants and devices and bio-corrosion of pipelines and ship hulls. Studies have demonstrated that the metabolic state of adhered bacteria can vary based on the physiochemical properties of the solid surface, but the reasons for this remained ambiguous until recent work by Hong and Brown. They proposed a hypothesis linking the charge regulation effect, which causes the local pH to vary as two surfaces with acid/base functional groups approach each other, and cellular bioenergetics, which stores energy in the form of a proton gradient across the bacterial cytoplasmic membrane. In their initial study, Hong and Brown proposed the hypothesis and demonstrated it for bacteria attachment to glass beads.

Here, we demonstrate the validity of this hypothesis for a range of surfaces with different functional groups using experimental and modelling methods. Initial work focused on depicting that cellular bioenergetics of neutrophilic bacteria is influenced by changes in surface pH. Second, the effect of adhesion on metabolic activity of *Escherichia coli* was studied using a negatively-charged sand surface and a positively-charged goethite-coated sand surface. It was shown that the energy level of *E.coli* was

enhanced upon adhesion to the untreated sand and it was reduced upon adhesion to the coated sand, thus demonstrating the effect of solid surface functional groups on the metabolic activity of attached bacteria.

The hypothesis was extended to study the impact of a range of acidic and basic surfaces on the bacterial metabolic activity making it possible to investigate a wide spectrum of attachment induced surface pH conditions. Adhesion experiments were performed with the Gram-negative *E. coli* and the Gram-positive *Bacillus subtilis* employing various surfaces in granular form. Surface characterization experiments and numerical modelling enabled the identification of the dissociation constants associated with functional groups on the bacterial surface and the solid surface which facilitated demonstration of a direct link between bacterial surface pH and cellular ATP levels.

The results of the study indicated an overall relationship between solid surface functional group properties and bioenergetics of sessile bacteria. To summarize, upon adhesion to negatively-charged (acidic) surfaces, the charge regulated interface results in a proton-rich environment that stimulates ATP synthesis via chemiosmosis. The finite and rapid increase in ATP experimentally observed over the first 48 hours was followed by bacteria exhibiting an enhanced metabolic state through the course of the experiment. Attachment to basic surfaces results in a proton-deficit interface resulting in the depletion of intracellular ATP. The positive surfaces induced a declined metabolic state upon bacterial adhesion resulting in continual depletion of energy reserves over the experiment period.

These findings can serve as the basis in the selection of surfaces and coatings to bring about a desired metabolic activity in attached bacteria based on requirements for the system at hand.

Chapter 1

Introduction and Overview

CHAPTER 1 Introduction and Overview

1.1 Introduction and Background

Microorganisms exist as free planktonic forms or, more commonly, as attached or sessile forms due to a natural tendency to adhere to surfaces [1-4]. Upon adhesion, proliferation of bacteria and secretion of extracellular polymeric matrix substances result in biofilm development [5-9]. Bacterial colonization can occur on different kinds of surfaces including living tissues (plants, animals, human) and abiotic surfaces (pipelines, implants and medical devices, rocks, etc.) [7,10-14].

Microbial adhesion is of critical importance in many natural and engineered systems. In some situations bacterial attachment and the subsequent colonization followed by the establishment of complex microbial communities is desirable [15-24]. In many other scenarios the adhesion of bacteria is highly objectionable and can be problematic [17,24-34]. Interestingly, it has been noted that upon adhesion to surfaces, bacteria demonstrate a change in their metabolic activity levels. This effect was observed initially by Zobell in 1943 and was later identified by many others. If bacterial metabolic activity levels are enhanced, it can encourage colonization and biofilm development at interfaces. Studies have examined the effect of clays [35,36], ion exchange resins [37,38], glass [4,39] plastics [40-42] etc. and demonstrated an enhanced metabolic activity in attached bacteria. However, as other studies have implied, adhesion of bacteria to certain other surfaces can result in lower metabolic activity levels. A decline in metabolic activity has been observed with attachment of

an array of different bacterial species to fluorapatite, amine coated surfaces and other biomaterials [43-46].

Despite several attempts to explain the effect of bacterial attachment on cellular metabolic activity, the reasons for this effect remained uncertain and the underlying mechanism was not clear. The question of why a change in metabolic activity occurs during adhesion and why attachment induced metabolic response is different with various surfaces remained unanswered [47] until recent work by Hong and Brown [39]. Their hypothesis explored a possible link between the charge regulation effect, which occurs when two surfaces bearing functional groups approach each other, and cellular bioenergetics. The basis of the hypothesis development is discussed in the following sections. Hong and Brown experimentally demonstrated an increase in cellular ATP levels when bacteria adhered to a negatively charged glass surface and example results are presented in Figure1.1.

The hypothesis directly links variation in bacterial activity to the functional properties of the adhering surfaces. Understanding the roles surfaces and their associated properties play in causing a variation in bacterial metabolism can be extremely beneficial. This knowledge can be applied in diverse fields where microbial adhesion is relevant. Example areas include environmental engineering, environmental science, medical applications, dental implants, marine engineering, food storage, etc. Within the scope of environmental engineering, it finds application in studies related to

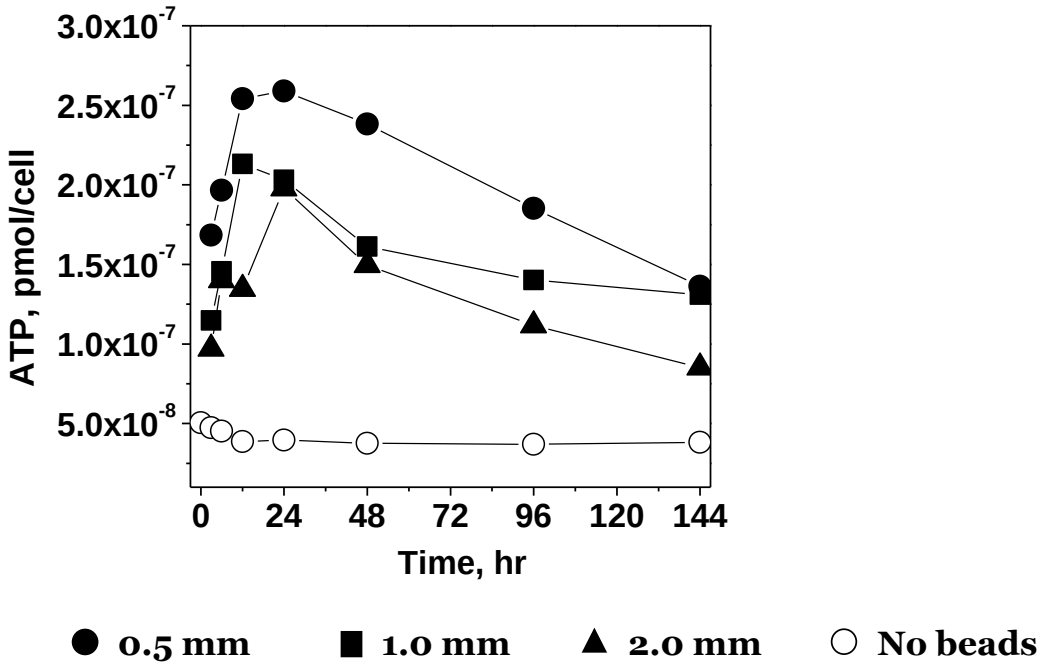

Figure 1.1 – Example results from Hong and Brown [39] demonstrating an enhancement in the metabolic activity of bacteria upon adhesion to glass beads of different diameter. The adenosine triphosphate (ATP) levels for planktonic cells (hollow symbols) and attached cells (solid symbols) show that the ATP levels of sessile bacteria can vary from that of their planktonic counterparts (ATP is a main energy carrier in living organisms).

attached biofilm wastewater treatment plants, microbial fouling in water distribution systems and membranes, oligotrophic survival of bacteria, microbial surface recognition studies, bioremediation, bioaugmentation etc. As will be shown through this thesis, the findings of this research provide a basis for the selection and design of surfaces, materials and coatings for controlling the activity of attached bacteria and for interpreting the interactions of bacteria with natural and engineered surfaces.

The following chapter provides a brief discussion of the two main processes that we build our hypothesis on, cellular bioenergetics and the charge regulation effect. We then lay out the hypothesis that we have developed to explain the mechanism of how attachment of bacteria to surfaces induces a variation in cellular metabolic activity. If activity is enhanced it may help the bacterial cells to colonize the surface and induce biofilm formation, whereas if activity is reduced it can result in a decreased colonization rate and possibly compromise survival and result in cell death. This is followed by a discussion of the specific goals and objectives for this study.

1.2 Cellular Bioenergetics

Microorganisms require energy for growth, division and maintenance of all life processes. Cellular metabolism is the sum total of processes that result in energy generation and energy consumption in the cell. Catabolic processes are those by which complex molecules are degraded into simpler units thereby producing energy. Anabolic processes constitute those that synthesize macromolecules from smaller components thereby consuming the energy provided by the energy releasing

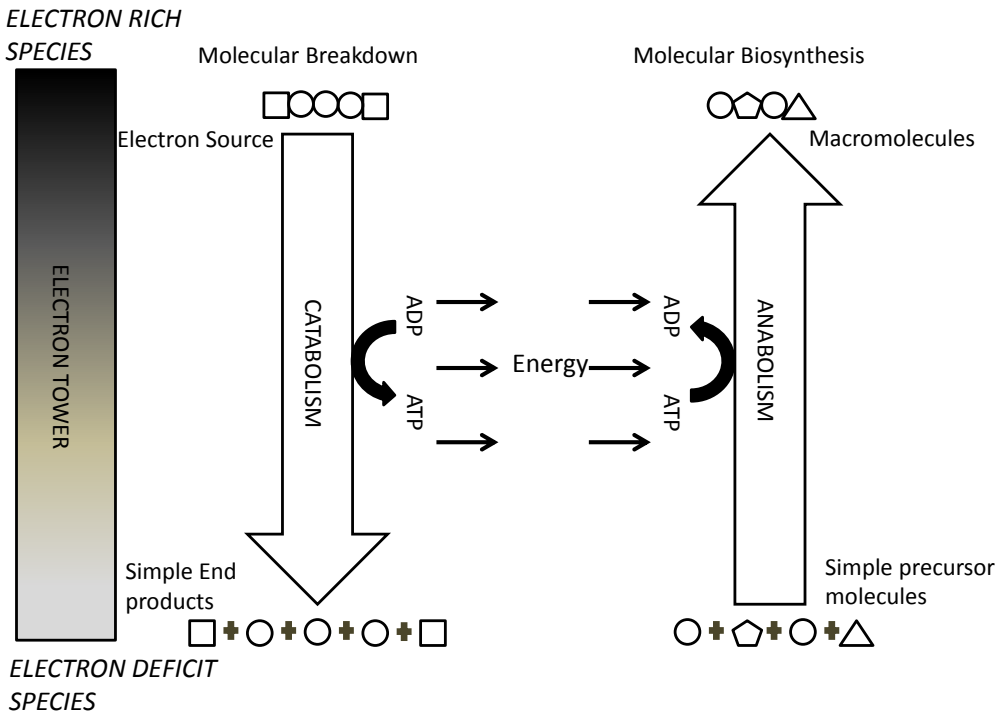

Figure 1.2 – This figure depicts metabolism within the cell. Energy coupling occurs inside the cell with exergonic processes driving endergonic processes. Catabolism is the exergonic breakdown of complex substrate into simpler molecules accompanied by the release of energy which is trapped in energy rich molecules like ATP. The energy is used to drive endergonic anabolic processes that help in macromolecular synthesis.

processes. The interdependent transfer of energy between catabolism and anabolism is termed energy coupling and is represented in Figure1.2.

1.2.1 The Chemiosmosis theory of Mitchell

During the process of catabolism, energy yielding substrate (eg., glucose) is oxidized to produce energy rich molecules like adenosine triphosphate (ATP) which is the chief energy currency in the cell. As a result of the oxidation process, electrons are produced from the substrate and transported along the cytoplasmic membrane toward a terminal electron acceptor (eg., oxygen) via a cascade of membrane proteins. Catabolic pathways deliver chemical energy in the form ATP and other energy carriers such as of NADH, NADPH, and $FADH_2$ which function as carriers along an electron transport chain where electrons are transferred from one protein to another. As electrons are transported towards the terminal electron acceptor, protons are pumped out of the membrane thereby causing a concentration gradient where more protons are outside the membrane than inside. Proton and electrostatic potential gradients are established that together contribute to the proton motive force (Δp) which quantifies the energy stored across the membrane (Equation 1). The proton motive force consisting of an electrical and chemical component is expressed as

$$\Delta p = \Delta\psi - Z\Delta pH \qquad (1)$$

where $\Delta\psi$ is the electrical or membrane potential and ΔpH, the pH gradient across the cell membrane.

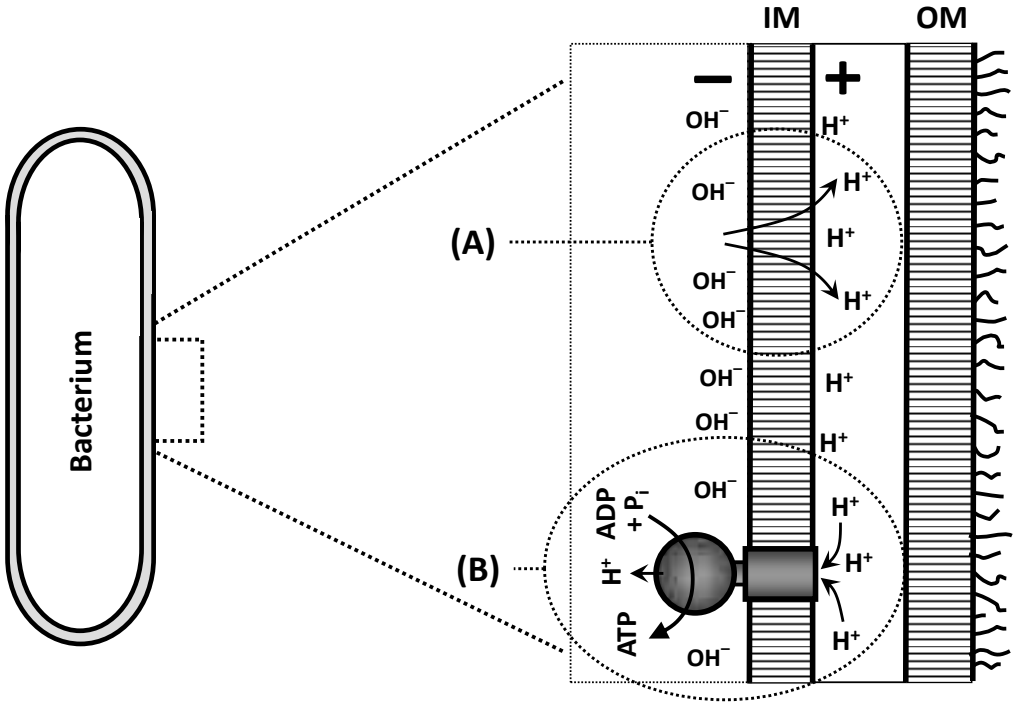

Figure 1.3 - This figure depicts the chemiosmotic theory proposed by Mitchell. Process (A) denotes the pumping out of protons across the cytoplasmic membrane during catabolism that set up the pH and potential gradients that combine to form the proton motive force. Process (B) depicts the synthesis of ATP within the cell as protons are allowed to reenter the cell via the ATP synthase molecule at the expense of the proton motive force.

An enzyme called ATP synthase provides a conduit for the protons to reenter the cell, simultaneously creating energy- rich ATP molecules from adenosine diphosphate (ADP) and inorganic phosphate (P_i). Peter Mitchell was awarded the Nobel Prize in 1978 for postulating this theory referred to as the chemiosmotic theory presented in Figure 1.3.

The energy stored in ATP is used in anabolic pathways to convert small precursor molecules into complex cell macromolecules. Thus, cellular bioenergetics links catabolism to anabolism via pH and electrostatic potential gradients across the cellular plasma membrane that together contributes to the proton motive force. The proton motive force helps form cellular ATP, the most prevalent energy source within a cell.

1.2.2 Proton-Motive Force

The proton motive force consisting of a charge and pH gradient expressed in Equation 1 can be rewritten as

$$\Delta \mathrm{p} = \Delta\psi - 2.303\frac{RT}{F}\Delta \mathrm{pH} \tag{2}$$

where F is the Faraday constant, R is the universal gas constant and T is the temperature.

The free energy required to synthesize ATP termed the phosphorylation potential is depicted as ΔG_p and can be expressed as

$$\Delta G_p = \Delta G^{\circ} + 2.303 \mathrm{RT} \log\left(\frac{[\mathrm{ATP}]}{[\mathrm{ADP}][\mathrm{P}_i]}\right) \tag{3}$$

In the above equation, ΔG_p^o is the standard free energy for ATP hydrolysis with a reported value of 30.1 kJ/mol; $[P_i]$, [ADP] and [ATP] are the concentrations of intracellular inorganic phosphate, ADP and ATP, respectively (mol/L).

The proton motive force is related to the phosphorylation potential via

$$\Delta p = \frac{\Delta G_p}{nF} = -\frac{1}{nF}\left[\Delta G^{\circ} + 2.303RT \log\left(\frac{[ATP]}{[ADP][P_i]}\right)\right] \quad (4)$$

where F is the Faraday constant and n is the number of protons translocated by ATP synthase per ATP molecule synthesized. For bacteria the value of n is typically reported to fall in the range of 2 to 4. The ATP synthase enzyme is reversible, and thus an increase in the Δp will result in an increase in the cellular ATP and a decrease in the Δp will cause a decrease in the cellular ATP.

1.2.3 ATP synthase

ATP synthase is an enzyme present in the membranes of mitochondria and chloroplasts in eukaryotes and in the cytoplasmic membrane of prokaryotes. The enzyme consists of two large multi-peptide units referred to as F_0, the hydrophobic part consisting of 3 subunits and $F_{1,}$ which is hydrophilic with 5 subunits. This complex enzyme serves as a rotatory molecular channel through which protons are allowed to move across the cell membrane. Thus ATP generation occurs within the cell at the expense of the proton motive force that is created at the membrane. The ATP synthase mediated ATP synthesis from ADP and P_i is reversible and protons can be allowed to move across to the outside of the membrane via ATP hydrolysis.

1.3 Charge regulation

Charge regulation is a physiochemical process that takes place when two surfaces bearing acid/base functional groups approach each other, such as a bacterium approaching a sand grain surface. The degree of ionization of the acidic and basic groups on the two surfaces is a function of the local pH at the interface. It is worthwhile to first briefly discuss the bacterial surface prior to describing the charge regulation effect.

1.3.1 The Bacterial Cell Surface

Bacteria are generally classified into two broad categories based on a differential method of staining introduced by Christian Gram in 1884. Due to differences in the composition of the cell wall, Gram positive bacteria retain the purple color of the primary stain (crystal violet) while Gram negative bacteria appear pink or red as a result of the counter stain (safranin or fuchsin). The structure of the Gram positive cell wall composed mainly of peptidoglycan is less complex than that of the Gram negative cell wall. Peptidoglycan is primarily responsible for the rigidity, shape and protection of the bacteria apart from the plasma membrane. Teichoic acids, teichuronic acids, polysaccharides and some proteins are also associated with the wall of the Gram positive bacteria. The Gram negative cell wall on the other hand has three regions: the outer membrane, the relatively thinner peptidoglycan layer and a periplasmic membrane. The outer membrane possesses phospholipids, lipopolysaccharides and polysaccharides. In many cases the bacterial surface bears extracellular appendages

like pili, fimbriae and flagella that help in conjugation, adhesion and locomotion. The cytoplasmic or periplasmic membrane limits the cytoplasm and its contents. The bacterial surface is associated with various acidic and basic functional groups including carboxylic, phosphoric, amine and hydroxyl groups. Studies have demonstrated that bacteria generally possess a net negative surface charge at pH values found in most natural habitats.

1.3.2 The Charge Regulation Effect

When a charged particle is present in an electrolyte solution, counter ions bearing the opposite charge tend to aggregate around the particle. An inner layer of ions aggregates directly at the surface and this is called the stationary (or Stern layer) as it moves with the particle in solution. A second layer of counter ions and co-ions form a diffuse layer around the Stern layer, thereby resulting in an ionic double layer. Several theories have been introduced in an attempt to determine the surface potential of charged species, with most based on the Poisson-Boltzmann equation. Here, the ions are treated as point charges and the uniform distribution of charges is assumed.

When a bacterium approaches another surface, the surface charge and potential will vary. The surface charge and surface potential at both of the interacting interfaces are a function of the ionization of the functional groups on the surfaces and the distance between the surfaces. The effect of the functional groups can be modelled using the Poisson Boltzmann equation, which can be written as:

$$\frac{d^2\psi}{dx^2} = -\frac{1}{\varepsilon_o \varepsilon}\sum_{i=1}^{I} n_{ri} \cdot z_i \cdot e \cdot \exp\left(\frac{-z_i e \psi}{kT}\right) \tag{5}$$

where ψ is the electrostatic potential, x is the distance from the charged surface, ε_o is the permittivity of vacuum; ε is the dielectric constant of the medium, n_{ri} is the number of ions of species i per unit volume; z_i is the valence of ion i, k is the Boltzmann constant and T is the temperature and e is the electron charge. The boundary conditions at the two surfaces are based on Gauss's Law, where the change in potential at the surface is related to the surface charge by:

$$\left.\frac{d\psi}{dx}\right|_s = -\frac{1}{\varepsilon_o \varepsilon}\sigma \tag{6}$$

where σ is the surface charge per unit area of the surface. The net surface charge of the cell can be obtained by summing the individual functional groups creating the positive and negative surface charges:

$$\frac{\sigma}{e} = \sum_j [R_{bj}H^+] - \sum_i [R_{ai}^-] \tag{7}$$

where R_{ai} are the acidic ionizable sites of type I, R_{bj} are the basic ionizable sites of type b. R_{ai} and R_{bj} can be represented based on the ionization of the various functional groups as a function of surface pH and their site densities. In this case, Equations 6 and 7 lead to the following boundary [48,49]conditions:

$$\left.\frac{d\psi}{dx}\right|_{x=0} = -\frac{e}{\varepsilon_o \varepsilon}\cdot\left\{\sum_j\left[\frac{[H^+]N_{bj}}{[H^+]+K_{bj}\exp\left(\frac{e\psi_s}{kT}\right)}\right]-\sum_i\left[\frac{K_{ai}N_{ai}}{K_{ai}+[H^+]\exp\left(\frac{-e\psi_s}{kT}\right)}\right]\right\} \quad (8)$$

In this equation K_{ai} and K_{bj} are the dissociation constants for the different acidic and basic functional groups, respectively. The local hydrogen ion concentration is expressed by the Boltzmann distribution where $[H^+]$ is the concentration of the hydrogen ions in the bulk solution and ψ_S is the surface potential. Using Equation 8, the surface charge and surface pH can be modeled as the bacterial cell approaches the adhering surface. The model can also be validated by considering the bacterial cell surface in the bulk solution (i.e., no adhesion) and comparing the pH response of the modeled surface charge to electrophoretic mobility measurements of the bacterial cell as a function of pH.

Based on modelling, we expect to obtain a decrease in pH at the bacterial surface upon adhesion to a negatively charged acidic surface. Alternatively, when bacteria adhere to a positively charged basic surface, we expect an increase in the local pH. Example modelling results for an *E.coli* bacterium upon approaching a negatively charged and a positively charged surface is depicted in Figure 1.4.

A more prominent decline in surface pH is observed as the dissociation constant becomes more acidic and as the density of the functional group increases. Simultaneously the dotted lines show an increase in surface pH as the dissociation

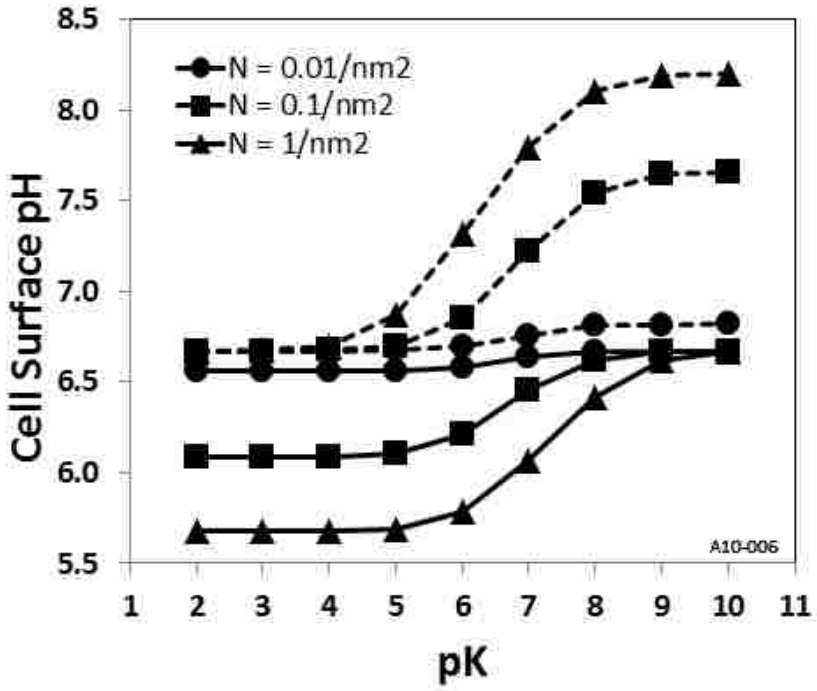

Figure 1.4 - Numerical Modelling of an *Escherichia coli* cell approaching a surface containing a single type of ionizable functional group. Dashed lines represent basic (positively-charged) groups and solid lines represent acidic (negatively-charged) groups. The results indicate that the cell surface pH is a function of the type and density of the acid and base functional groups present on both the interacting surfaces.

constant increases in basicity. This pH variation will result in a corresponding difference in the cellular ATP concentration.

1.4 The hypothesis Statement

To summarize, Δp generated during cellular bioenergetics is composed of both charge and pH gradients across the cell cytoplasmic membrane. The charge-regulation effect results in variation of the cell surface charge and pH as the bacteria approaches another surface. Our hypothesis suggests a link between these two processes and that a change in Δp (measured via cellular ATP levels) will occur in direct response to changes in cell surface pH and potential. A decrease in surface pH will result in an increase in proton motive force while an increase in surface pH will cause a decrease in the proton motive force. This change in Δp will result in the attached cells having a different metabolic level compared to their planktonic counterparts. The effect of the physiochemical charge regulation on cellular bioenergetics is represented in Figure 1.5.

The variation in the local pH at the bacterial surface is a function of the surface properties of the two adhering surfaces.

Understanding how the adhesion of bacteria to a surface with a defined charge can affect Δp and thus the cellular ATP is desirable and can find various applications. Using a series of experiments and numerical modeling methods we propose to establish that relationship. This knowledge will help us design surfaces according to the metabolic activity we desire the adhered bacteria to possess. An increase in

cellular metabolic activity will result in colonization and biofilm formation whereas a decrease in ATP can even affect bacterial survival and viability.

1.5 Goals and Objectives of Study

The primary goal of this study was to validate the hypothesis using different surfaces that would provide a range of cell surface pH values, from acidic to basic. A secondary goal was to establish a direct link between cell surface pH and changes in cellular bioenergetics and ATP formation. The objectives used to meet these goals are as follows.

1.5.1 Objective 1: Establish a relationship between the local pH at the bacterial surface and intracellular ATP concentration.

As per our hypothesis, changes in surface pH of the bacteria can trigger a variation in the cellular ATP concentration. It is essential to test if this part of the hypothesis is valid. We have achieved this by performing experiments that artificially manipulate the bulk pH of the bacterial sample, thus duplicating the effect of charge regulation at the bacterial surface by creating a proton rich or deficit condition.

1.5.2 Objective 2: Characterize the cellular surface of Escherichia coli Bacillus subtilis and obtain data required for Charge Regulation and Bioenergetics modeling

For this project, the Gram negative *Escherichia coli* k12 (ATCC 29181) and Gram positive *Bacillus subtilis* (ATCC23059) were used as the model bacterial strains. The *E.coli* and *B. Subtilis* surfaces were characterized to determine the N and pK values

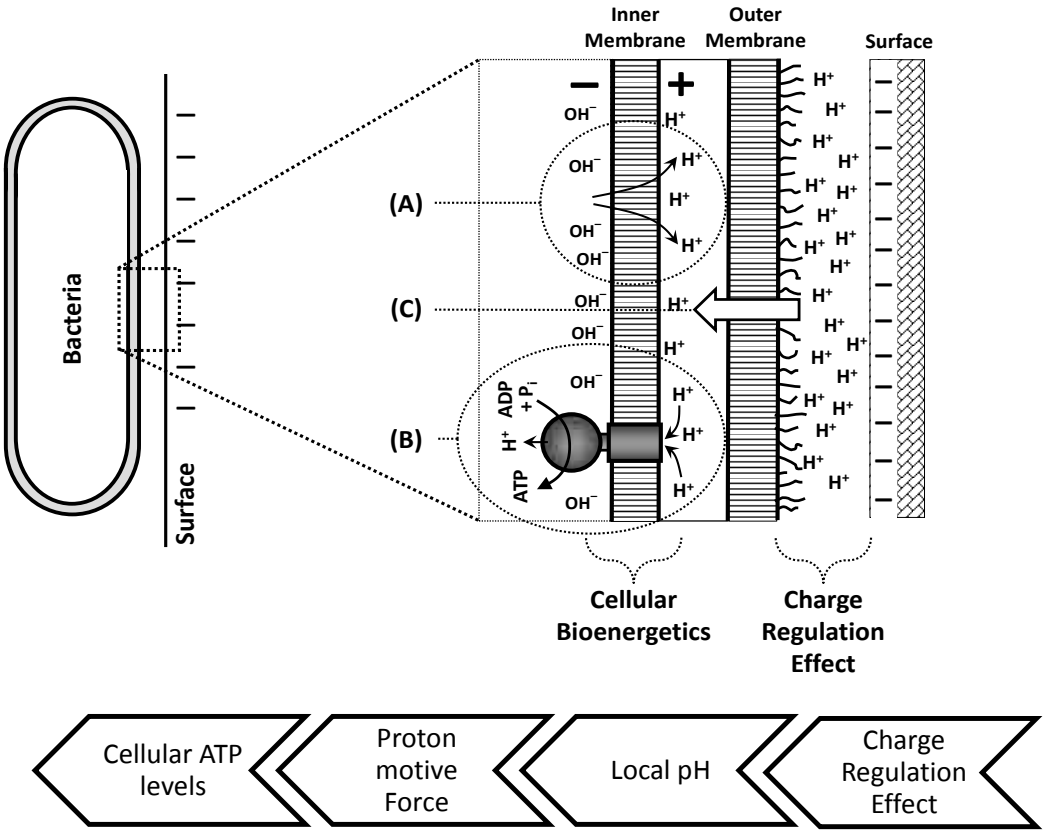

Figure 1.5 - The hypothesis linking the charge-regulation effect to cellular bioenergetics is depicted here for a bacterium adhering to a negatively-charged surface. (A) During catabolic processes, protons are pumped outside the inner (cytoplasmic) membrane (IM), generating the proton motive force (B) The protons are allowed to reenter the cell through ATP synthase that drives ATP synthsis. During adhesion, the charge-regulation effect alters the proton concentration at the cell surface. We hypothesize that this variation in pH at the cell surface (c) propagates through the outer membrane and affects the pH gradient across the IM thus impacting cellular bioenergetics.

that best represent the cell surfaces. This was done using zeta potential measurements for the bacteria by titrating across a wide pH range.

1.5.3 Objective 3: Identify and Characterize different materials of varying surface charge, ranging from positive to negative.

Granular forms of multiple surfaces with different electrostatic properties were identified. The use of surfaces spanning a range of surface charge from positive to negative were used to gain a better understanding of the effect of surface charge on the metabolic activity of adherent bacteria. These surfaces consisted of both naturally-occurring minerals and surface coatings on sand grains. These materials were characterized in order to obtain the pK and N values that best represent their charge properties using zeta potential measurements and the surfaces were characterized using scanning electron microscopy with energy dispersive X-ray analysis.

1.5.4 Objective 4: Experimentally explore how ATP levels of adhered and planktonic bacteria vary with surfaces selected under Objective 3.

The effect of bacterial adhesion on metabolic activity was characterized by measuring the ATP levels of planktonic bacteria and bacteria adhered to the various surfaces. The results from these experiments allow us to determine if the ATP levels changed upon adhesion in agreement with the working hypothesis.

1.5.5 Objective 5: Apply the Charge Regulation and Bioenergetics models to experimental data to determine if results follow the working hypothesis.

The impact of the selected materials on bacterial surface pH and electrostatic potential were accessed through the use of the charge-regulation and bioenergetics models. This allowed examination of the relationship between the surface charge density and the effect it causes on the local pH.

1.6 Dissertation organization

This dissertation is organized in a paper format, with the main chapters presenting a discrete set of findings that have been published, are currently in peer review, or are in preparation for submission. Each chapter is summarized below.

Chapter 2: Central to our hypothesis is the concept that variation in pH at the surface of the bacterium can result in the generation or hydrolysis of ATP via the ATP synthase complex. During bacterial attachment to various surfaces, the local pH between the adhering surfaces will vary as a function of the functional groups on the surfaces of attachment. As per our hypothesis, this variation in proton gradient can induce a metabolic response from the bacterium. In this chapter we artificially reproduce a surface pH variation by manipulating the bulk pH and testing for a corresponding difference in cellular ATP concentration.

Chapter 3: In this chapter the hypothesis was demonstrated for a positively-charged surface using *E.coli* as a model organism. Here the bacterial bioenergetics of *E.coli* was studied upon adhesion to different masses of sand and iron hydroxide (goethite)

coated sand. These materials provided negatively-charged (acidic) and positively-charged (basic) surfaces, respectively. The results followed the hypothesis and demonstrated that chemically-stable iron hydroxides can lower the metabolic activity of attached bacteria.

Chapter 4: In this chapter we examined the effects of multiple surfaces on the ATP levels of both *E. coli* and *B. subtilis*. These materials ranged from sand, with an isoelectric point near 2 (acidic surface), to aluminum-coated sand, with an isoelectric point near 9 (basic surface). The results demonstrate that our hypothesis is able to predict the bioenergetic response of bacteria adhering to surfaces with different charge properties.

Chapter 5: The dissertation concludes with this chapter, which summarizes the overall contributions of this study and makes recommendations for future research work based on current findings and knowledge.

1.7 Reference List

[1] J. Costerton, G. Gessey, Microbial contamination of surfaces, in: Anonymous Surface Contamination, Springer, 1979, p Reference Listp. 211-221.

[2] G. Geesey, R. Mutch, J.t. Costerton, R. Green, Sessile bacteria: An important component of the microbial population in small mountain streams 1, Limnol. Oceanogr. 23 (1978) 1214-1223.

[3] T. Ladd, J. Costerton, G. Geesey, Determination of the heterotrophic activity of epilithic microbial populations, Native aquatic bacteria: enumeration, activity and ecology.ASTM STP. 695 (1979) 180-195.

[4] C.E. Zobell, The Effect of Solid Surfaces upon Bacterial Activity, J. Bacteriol. 46 (1943) 39-56.

[5] S.S. Branda, Å Vik, L. Friedman, R. Kolter, Biofilms: the matrix revisited, Trends Microbiol. 13 (2005) 20-26.

[6] R.M. Donlan, Biofilms: microbial life on surfaces, Emerging Infect. Dis. 8 (2002).

[7] J. Palmer, S. Flint, J. Brooks, Bacterial cell attachment, the beginning of a biofilm, J. Ind. Microbiol. Biotechnol. 34 (2007) 577-588.

[8] P. Stoodley, K. Sauer, D. Davies, J.W. Costerton, Biofilms as complex differentiated communities, Annual Reviews in Microbiology. 56 (2002) 187-209.

[9] G. Cheng, Z. Zhang, S. Chen, J.D. Bryers, S. Jiang, Inhibition of bacterial adhesion and biofilm formation on zwitterionic surfaces, Biomaterials. 28 (2007) 4192-4199.

[10] L. Hall-Stoodley, J.W. Costerton, P. Stoodley, Bacterial biofilms: from the natural environment to infectious diseases, Nature Reviews Microbiology. 2 (2004) 95-108.

[11] R.M. Donlan, J.W. Costerton, Biofilms: survival mechanisms of clinically relevant microorganisms, Clin. Microbiol. Rev. 15 (2002) 167-193.

[12] A.A. Gorbushina, Life on the rocks, Environ. Microbiol. 9 (2007) 1613-1631.

[13] J.W. Costerton, K. Cheng, G.G. Geesey, T.I. Ladd, J.C. Nickel, M. Dasgupta, T.J. Marrie, Bacterial biofilms in nature and disease, Annual Reviews in Microbiology. 41 (1987) 435-464.

[14] M. Ghannoum, G.A. O'Toole, Microbial Biofilms. ASM Press, 2004.

[15] A. Bartrolí, J. Carrera, J. Pérez, Bioaugmentation as a tool for improving the start-up and stability of a pilot-scale partial nitrification biofilm airlift reactor, Bioresour. Technol. 102 (2011) 4370-4375.

[16] S.J. Edwards, B.V. Kjellerup, Applications of biofilms in bioremediation and biotransformation of persistent organic pollutants, pharmaceuticals/personal care products, and heavy metals, Appl. Microbiol. Biotechnol. 97 (2013) 9909-9921.

[17] T.R. Garrett, M. Bhakoo, Z. Zhang, Bacterial adhesion and biofilms on surfaces, Progress in Natural Science. 18 (2008) 1049-1056.

[18] V. Lazarova, J. Manem, Biofilm characterization and activity analysis in water and wastewater treatment, Water Res. 29 (1995) 2227-2245.

[19] S.V. Mohan, N.C. Rao, K.K. Prasad, P. Sarma, Bioaugmentation of an anaerobic sequencing batch biofilm reactor (AnSBBR) with immobilized sulphate reducing bacteria (SRB) for the treatment of sulphate bearing chemical wastewater, Process Biochemistry. 40 (2005) 2849-2857.

[20] C. Nicolella, M. Van Loosdrecht, J. Heijnen, Wastewater treatment with particulate biofilm reactors, J. Biotechnol. 80 (2000) 1-33.

[21] S. Radwan, R. Al-Hasan, S. Salamah, S. Al-Dabbous, Bioremediation of oily sea water by bacteria immobilized in biofilms coating macroalgae, Int. Biodeterior. Biodegrad. 50 (2002) 55-59.

[22] H. Watling, The bioleaching of sulphide minerals with emphasis on copper sulphides—a review, Hydrometallurgy. 84 (2006) 81-108.

[23] M. Zhang, J.H. Tay, Y. Qian, X.S. Gu, Coke plant wastewater treatment by fixed biofilm system for COD and NH 3-N removal, Water Res. 32 (1998) 519-527.

[24] J.W. McClaine, R.M. Ford, Characterizing the adhesion of motile and nonmotile Escherichia coli to a glass surface using a parallel-plate flow chamber, Biotechnol. Bioeng. 78 (2002) 179-189.

[25] J.D. Brooks, S.H. Flint, Biofilms in the food industry: problems and potential solutions, Int. J. Food Sci. Tech. 43 (2008) 2163-2176.

[26] K. Cooksey, B. Wigglesworth-Cooksey, Adhesion of bacteria and diatoms to surfaces in the sea: a review, Aquat. Microb. Ecol. 9 (1995) 87-96.

[27] J.W. Costerton, P.S. Stewart, E.P. Greenberg, Bacterial biofilms: a common cause of persistent infections, Science. 284 (1999) 1318-1322.

[28] R.M. Donlan, J.W. Costerton, Biofilms: survival mechanisms of clinically relevant microorganisms, Clin. Microbiol. Rev. 15 (2002) 167-193.

[29] H. Flemming, Reverse osmosis membrane biofouling, Exp. Therm. Fluid Sci. 14 (1997) 382-391.

[30] H. Flemming, Biofouling in water treatment, in: Anonymous Biofouling and Biocorrosion in Industrial Water Systems, Springer, 1991, pp. 47-80.

[31] H. Flemming, Biofouling in water systems–cases, causes and countermeasures, Appl. Microbiol. Biotechnol. 59 (2002) 629-640.

[32] G.G. Geesey, Biofouling and Biocorrosion in Industrial Water Systems, CRC Press, 1994.

[33] R. Whitehouse, E. Peters, J. Lizotte, C. Lilge, Influence of biofilms on microbial contamination in dental unit water, J. Dent. 19 (1991) 290-295.

[34] A.C.L. Wong, Biofilms in food processing environments, J. Dairy Sci. 81 (1998) 2765-2770.

[35] G. Stotzky, L. Rem, Influence of clay minerals on microorganisms: I. Montmorillonite and kaolinite on bacteria, Can. J. Microbiol. 12 (1966) 547-563.

[36] G. Stotzky,P.M Huang, M.Schnitzer, Influence of soil mineral colloids on metabolic processes, growth, adhesion, and ecology of microbes and viruses, Interactions of soil minerals with natural organics and microbes, SSSA, USA (1986) 305-428.

[37] S. Underhill, J. Prosser, Surface attachment of nitrifying bacteria and their inhibition by potassium ethyl xanthate, Microb. Ecol. 14 (1987) 129-139.

[38] R. Hattori, T. Hattori, Effect of a liquid-solid interface on the life of microorganisms, Ecol. Rev. 16 (1963) 64-70.

[39] Y. Hong, D.G. Brown, Variation in bacterial ATP level and proton motive force due to adhesion to a solid surface, Appl. Environ. Microbiol. 75 (2009) 2346-2353.

[40] M. Fletcher, A microautoradiographic study of the activity of attached and free-living bacteria, Arch. Microbiol. 122 (1979) 271-274.

[41] B. Kefford, S. Kjelleberg, K. Marshall, Bacterial scavenging: utilization of fatty acids localized at a solid-liquid interface, Arch. Microbiol. 133 (1982) 257-260.

[42] A.S. Gordon, F.J. Millero, Measurement of the activity of attached bacteria using a sorption microcalorimeter, J. Microbiol. Methods. 1 (1983) 291-296.

[43] B. Gottenbos, D.W. Grijpma, H.C. van der Mei, J. Feijen, H.J. Busscher, Antimicrobial effects of positively charged surfaces on adhering Gram-positive and Gram-negative bacteria, J. Antimicrob. Chemother. 48 (2001) 7-13.

[44] A.A. Dispirito, P.R. Dugan, O.H. Tuovinen, Inhibitory effects of particulate materials in growing cultures of Thiobacillus ferrooxidans, Biotechnol. Bioeng. 23 (1981) 2761-2769.

[45] A. Terada, A. Yuasa, S. Tsuneda, A. Hirata, A. Katakai, M. Tamada, Elucidation of dominant effect on initial bacterial adhesion onto polymer surfaces prepared by radiation-induced graft polymerization, Colloids and Surfaces B: Biointerfaces. 43 (2005) 99-107.

[46] R. Kugler, O. Bouloussa, F. Rondelez, Evidence of a charge-density threshold for optimum efficiency of biocidal cationic surfaces, Microbiology. 151 (2005) 1341-1348.

[47] M.C. van Loosdrecht, J. Lyklema, W. Norde, A.J. Zehnder, Influence of interfaces on microbial activity, Microbiol. Rev. 54 (1990) 75-87.

[48] Y. Hong, D.G. Brown, Cell surface acid–base properties of Escherichia coli and Bacillus brevis and variation as a function of growth phase, nitrogen source and C: N ratio, Colloids and Surfaces B: Biointerfaces. 50 (2006) 112-119.

[49] Y. Hong, D.G. Brown, Electrostatic behavior of the charge-regulated bacterial cell surface, Langmuir. 24 (2008) 5003-5009.

Chapter 2

Variation in bacterial ATP concentration during rapid changes in extracellular pH and implications for the activity of attached bacteria

This Chapter was published as:

Albert, L. S.; Brown, D. G., 2015 Variation in bacterial bioenergetics during rapid changes in extracellular pH and implications for the activity of attached bacteria. Colloids Surf. B**.** 132, 111-116.

CHAPTER 2 Variation in bacterial ATP concentration during rapid changes in extracellular pH and implications for the activity of attached bacteria

2.1 Introduction

In recent work, we demonstrated that bacterial attachment to a surface can impact cellular bioenergetics, with the effect related to the types and surface densities of acid/base functional groups on the bacterial and solid surfaces [1-5]. Specifically, we have demonstrated that surfaces with acidic functional groups can enhance bacterial activity, measured as an increase in cellular adenosine triphosphate (ATP), whereas surfaces with basic functional groups can decrease cellular ATP.

The current theory describing this effect is based on the charge-regulated nature of the two surfaces [1-5]. When a surface with ionizable groups approaches another surface, electroneutrality requires the counterion concentration to increase in the solution between the surfaces to offset the decrease in inter-spatial volume. As H+ and OH- are counterions for negatively- and positively-charged surfaces, respectively, their concentrations next to the surface will vary, altering the local pH and electrostatic potential (Figure 2.1) [6-8].

Through charge-regulation modeling, we have shown that the local pH at the adhesion interface can drop below pH 5 or rise above pH 9, depending on the acid/base characteristics of the bacterial and solid surfaces [1, 2, 4]. This is illustrated in Figure 2.2 for an *Escherichi coli* bacterium as it approaches both a glass (negatively-charged, acidic) surface and an amine (positively-charged, basic) surface.

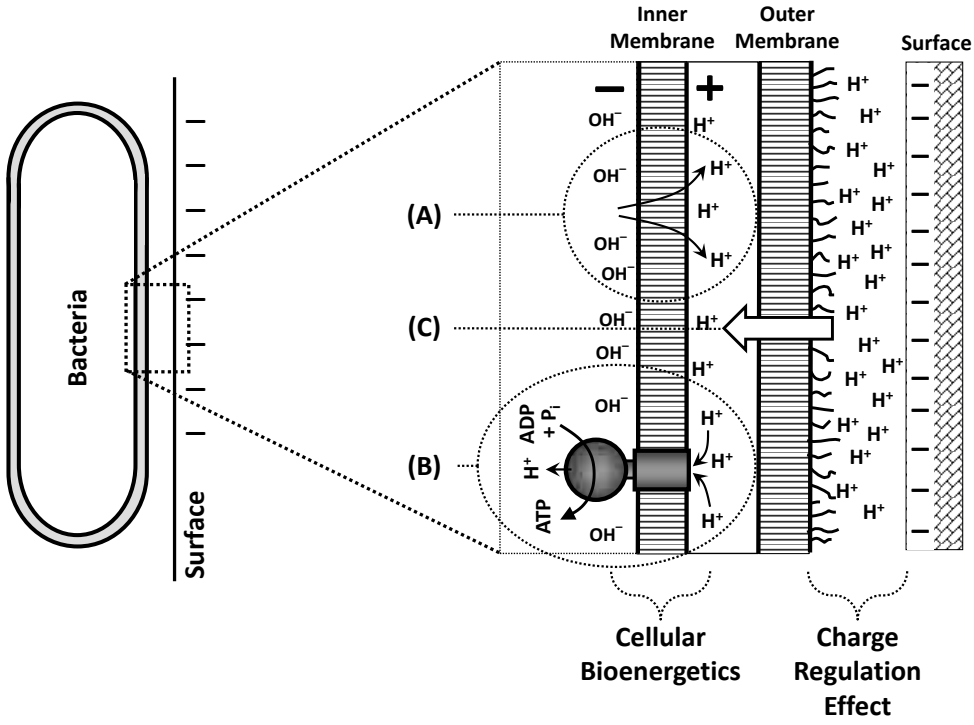

Figure 2.1 - The working hypothesis describing the effect of adhesion on bacterial metabolic activity, depicted here for a Gram-negative bacterium adhering to a negatively-charged surface, links cellular bioenergetics to the charge-regulation effect. (a) In cellular bioenergetics, protons are pumped across the inner (cytoplasmic) membrane (IM) during respiration, setting up pH and electrostatic gradients across the IM, which are quantified as the proton motive force (Δp). We hypothesize that the alteration in proton concentration at the cell surface (c) propagates through the outer membrane and affects the pH gradient across the IM. Similar results would be expected with Gram-Positive bacteria.

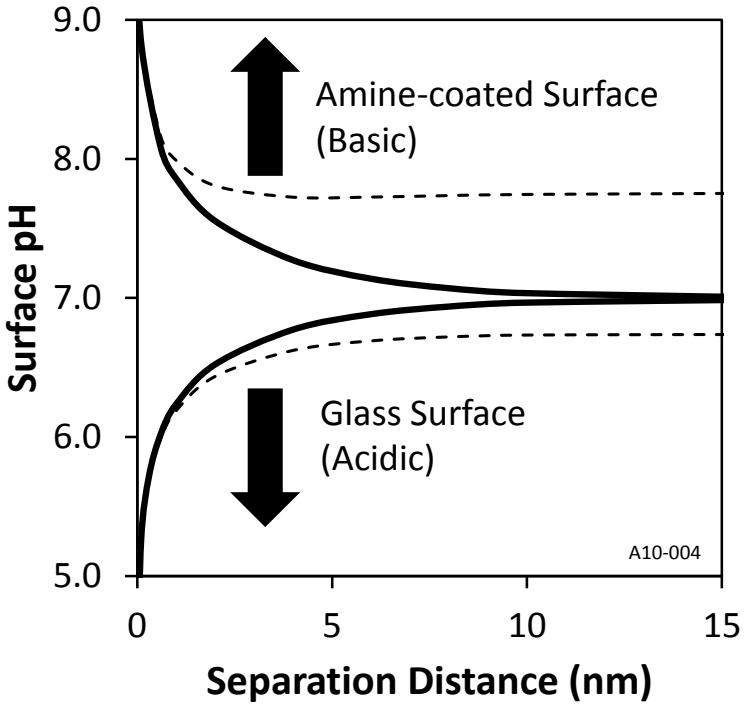

Figure 2.2 - Example charge-regulation results showing the pH at the *E. coli* cell surface (solid lines) and glass and amine-coated surfaces (dashed lines) as the bacterium approaches each of the two surfaces. Following the hypothesis outlined in Figure 2.1, the decrease in pH upon adhesion to the glass surface should result in an increase in cellular ATP and the increase in pH upon adhesion to the amine surface should result in a decrease in cellular ATP.

The hypothesis states that this variation in pH between the bacteria and solid surface can affect cellular bioenergetics, which links catabolic and anabolic reactions. During bacterial respiration, catabolic reactions establish an electrochemical proton gradient across the cytoplasmic membrane by pumping protons to the outside of the cytoplasmic membrane (process A in Figure 2.1) [9-11]. This is analogous to charging a capacitor, with the energy stored in a proton gradient rather than an electron gradient. The energy stored in this electrochemical gradient is termed the proton motive force (Δp, in units of mV) and is composed of both a charge gradient (Δψ) and a pH gradient (ΔpH) and can be expressed using the Nernst equation [12, 13]:

$$\Delta p = \Delta \psi - \frac{2.3RT}{F} \Delta pH \qquad (1)$$

where R is the ideal gas constant, T is temperature and F is the Faraday constant. The energy stored in Δp is used to create ATP, which is used to drive many anabolic reactions. In this process, protons are allowed to cross back into the cytoplasm through the ATP Synthase enzyme complex and the energy stored in the proton gradient is used to convert adenosine diphosphate (ADP) to ATP (process B in Figure 2. 1). Thus, an increase in ΔpH should increase Δp and be observed as an increase in cellular ATP concentration. Conversely, a decrease in ΔpH should decrease Δp and cellular ATP.

We have experimentally demonstrated that adhesion of bacteria under non-growth conditions results in significant shifts in cellular ATP, and numerical modeling of the

charge-regulation effect indicates that these shifts were due to local pH variations up to two units away from the pH of the bulk solution [1-3]. Full development of this hypothesis, however, requires development of the relationship describing how cellular ATP concentration responds to external pH shifts under non-growth conditions (process C in Figure 2. 1). There has been research with actively growing cells that examined the effects of bulk pH on Δp. These studies examined acidophiles, neutrophiles and alkaliphiles, using a variety of electron donors and acceptors [14-26]. In these studies, the extracellular pH was varied within the optimal range for growth of the different species and the results demonstrated that Δp is highest under acidic pH (with acidophilic bacteria) and it decreases as the pH increases through neutral pH (with neutrophilic bacteria) to basic pH (with alkaliphilic bacteria).

We have identified three studies that demonstrated the effects of a large external pH shift on the ATP levels of non-growing bacteria. In these studies, the pH of a suspension of E. coli cells was lowered from ~8 to ~3 in a single, rapid step and this resulted in an increase in cellular ATP concentrations [27-29]. One study then increased the pH back to pH ~8 and the cellular ATP concentration returned to a lower level [28]. This data is in agreement with the working hypothesis (Figure 2.1), but given that these studies focused on a single data point, the relationship between changes in external pH and cellular ATP levels (process C in Figure 2.1) remained unresolved.

A goal of this study was to develop a general form of this relationship. We can approach this mathematically by considering the free energy of phosphorylation, ΔG_p (kJ/mol), which provides a mathematical relationship between Δp and ATP [30]:

$$\Delta p = -\frac{\Delta G_P}{nF} = -\frac{1}{nF}\left[\Delta G_p^o + RT \cdot \ln\left(\frac{[ATP]}{[ADP][P_i]}\right)\right] \quad (2)$$

Here, ΔG_p^o is the standard free energy for ATP hydrolysis with a reported value of 30.1 kJ/mol [31]; $[P_i]$ is the intracellular inorganic phosphate concentration (mol/L); [ATP] and [ADP] are the concentrations of ATP and ADP, respectively (mol/L), and n is the number of protons translocated by the ATP synthase to generate one ATP molecule. The value of n is typically reported in the range of 2 to 4 for bacteria [31-35] and there is strong evidence that n varies as an inverse function of Δp, i.e., n decreases as Δp increases [35]. It is important to note that the relationship described by equation 2 is a reversible thermodynamic process: if Δp increases, then the concentration of ATP will increase, and if Δp decreases, then ATP will decrease [36].

Combination of equations 1 and 2 then provides a relationship describing the cellular ATP concentration as a function of ΔpH:

$$[ATP] = [ADP][P_i]\exp\left\{\frac{nF}{RT}\Delta\psi - 2.3n\Delta pH - \frac{\Delta G_P^o}{RT}\right\} \quad (3)$$

While this is a simplistic analysis, as [ADP] and $[P_i]$ will vary inversely with [ATP] [1, 3, 31, 37-39], it does demonstrate that the ATP concentration should be

exponentially related to the pH gradient across the cytoplasmic membrane. Assuming changes in extracellular pH affect ΔpH, we would then anticipate an exponential relationship between external pH and the cellular ATP concentration.

The focus of this study was to experimentally elucidate this exponential relationship for neutrophilic bacteria by varying extracellular pH and rapidly measuring cellular ATP concentrations. These experiments were conducted under non-growth conditions, with local pH values varied both within and well outside of the cell's optimal range, thus allowing exploration of process C in Figure 2.1. Specifically, this was accomplished by artificially manipulating the external (bulk) pH between the values of 3.5 to 10.5 and rapidly measuring changes in cellular ATP levels in four different neutrophilic bacterial strains (two Gram-Negative and two Gram-Positive). The results provide further evidence in support of the working hypothesis by elucidating process C in Figure 2.1, and demonstrate that an exponential relationship between pH and cellular ATP concentrations was observed in agreement with equation 3.

2.2 Materials and Methods

2.2.1 Bacterial Cultivation

Four neutrophilic bacterial strains were used in this study, including the Gram-Negative strains *Escherichia coli* K-12 (ATCC29181) and *Pseudomonas putida* (ATCC12633) and the Gram-Positive strains *Bacillus subtilis* (ATCC23059) and *Staphylococcus epidermidis* (ATCC 35984). Bacterial cultures were grown to the

exponential phase in 500 mL of Luria Bertini broth (LB broth, Fisher Scientific) and then stored with 15% glycerol at -86°C using the glass bead method [3, 4, 40]. For each experiment, bacteria from the frozen stock were cultivated in 500 mL of LB broth at 30°C. After 20 hours of growth the bacteria were harvested and washed by centrifuging the suspension at 3500xg for 15 minutes, followed by re-suspension of the bacterial pellet in phosphate buffer solution (PBS, 0.258g KH_2PO_4 and 0.470g K_2HPO_4 in 1 liter of deionized water with the pH adjusted to 7.2 using 1M NaOH). The bacterial suspension was sampled into 50 mL centrifuge tubes and placed on a rotatory shaker at room temperature. The test tubes were removed after either a 24 hour (1 day) starvation period or a 168 hour (1 week) starvation period and the bacteria were washed a second time. The use of two starvation periods was to demonstrate if cells respond differently after undergoing extended depletion of their energy reserves. The resulting bacterial suspensions were diluted with PBS to a concentration of approximately 10^8 cells, determined via Acridine Orange direct counts [41]. These final bacterial suspensions were used as described below.

2.2.2 Experimental Methods

For each experimental condition, an 8 ml sample of the bacterial suspension was withdrawn and its pH was adjusted from its current value of 7.2 to a desired value in the range of 3.5 to 10.5 using 1 M HCl or 1 M NaOH. After a specified waiting period (discussed below), 1 mL of the sample was removed and treated with 1 mL of nucleotide releasing buffer solution (NRB) [3]. NRB consists of 0.05% alkyl-dimethyl-benzyl-ammonium-chloride (benzalkonium chloride) in Tris-Mg^{2+} buffer (20

mM Tris, 2 mM EDTA and 10 mM magnesium acetate adjusted to a pH of 7.75) and it is used to lyse the bacterial cells and inactivate ATPase so that the enzyme does not degrade the released ATP. The samples treated with NRB were shaken well for 15 seconds and then analyzed for ATP as described below.

2.2.3 Analysis of Bacterial ATP

The ATP assay was performed following Hong and Brown [3] using a Sirius Luminometer (Titertek-Berthold) and freshly prepared Luciferin-Luciferase solution. Luciferase solution was prepared by adding 1 ml Tris buffer (20 mM Tris and 2 mM EDTA, adjusted to a pH of 7.75) to 1 mg of Luciferase (Sigma). 25 µl aliquots of this Luciferase solution were stored at -20°C in amber colored bottles until required for use. Prior to each experiment, the Luciferin-Luciferase solution was prepared by adding 1 mg of Luciferin (Sigma) and 10 ml of Tris Albumin buffer (20 mM Tris, 2 mM EDTA, 150 mM magnesium acetate, 50 µM dithiothreitol and 1 g bovine serum albumin adjusted to a pH of 7.75) to a Luciferase aliquot. The solution was gently mixed and allowed to sit at room temperature for 30 minutes before use.

For the ATP measurement, 100 µl of Tris Mg^{2+} buffer was pipetted into a luminometer tube containing 200 µl of the bacterial-NRB sample. The contents were mixed thoroughly for 15 seconds using a vortex mixer. The tube was then placed in the luminometer and 100 µl of the Luciferin-Luciferase solution was injected into the sample. The light generated by the reaction of ATP and the Luciferin-Luciferase was measured by the luminometer and quantified as Relative Light Units (RLU), which is

a direct measure of the ATP concentration in the vial. To allow comparison of the change in ATP as a function of solution pH between the four different bacterial strains, the RLU values obtained at different pH values for each strain were normalized by the RLU value obtained at a pH of 7.2 and the units are provided as normalized RLU (nRLU).

2.3 Results and Discussion

2.3.1 Temporal variation in cellular ATP during rapid extracellular pH change

In prior studies, it was demonstrated that the bacterial ATP concentration rose and quickly plateaued after a rapid drop in pH, and then began to decrease after a few minutes, presumably due to protein denaturation [27, 28]. The first experimental series in this study examined these temporal changes for the four different bacterial strains, with the goal of selecting a specific waiting period between the rapid change in solution pH and the ATP measurement. Variations in ATP as a function of time are shown in Figure 2.3 for *E. coli* K-12 at a solution pH of 7.2 and when the solution pH was rapidly changed from 7.2 to both 4.5 and 9.2. As anticipated, the ATP concentration increased upon lowering the solution pH and it decreased when the pH was increased.

Temporal variations in ATP were observed upon changing the pH, with notable differences for the one-day and one-week starvation periods. With one-day starvation, the ATP concentrations rapidly reached a stable value within 30 seconds (the time of

the first measurement) and remained stable for approximately 2-3 minutes, after which they started to decline. With one-week starvation, the ATP concentrations took 2-4 minutes to reach a stable value (which was very similar to the stable value for the one-day starvation), with a decline in ATP then starting soon afterwards. Similar temporal results were found with the other bacterial strains, and based on the results of these experiments the remaining analyses used ATP values obtained during the stable period (90 seconds for the one-day starvation period and up to four minutes for the one-week starvation period).

2.3.2 Response of ATP concentration to rapid changes in extracellular pH

The second experimental series measured the bacterial ATP concentration after a rapid change from a pH of 7.2 to values within the range of 3.5 to 10.5. It was anticipated that a rapid decrease in bulk pH would induce an increase in the proton gradient across the cell membrane, enhancing Δp and increasing the cellular ATP concentration, and as shown in Figure 2.4 this was directly observed. The nRLU values obtained for various

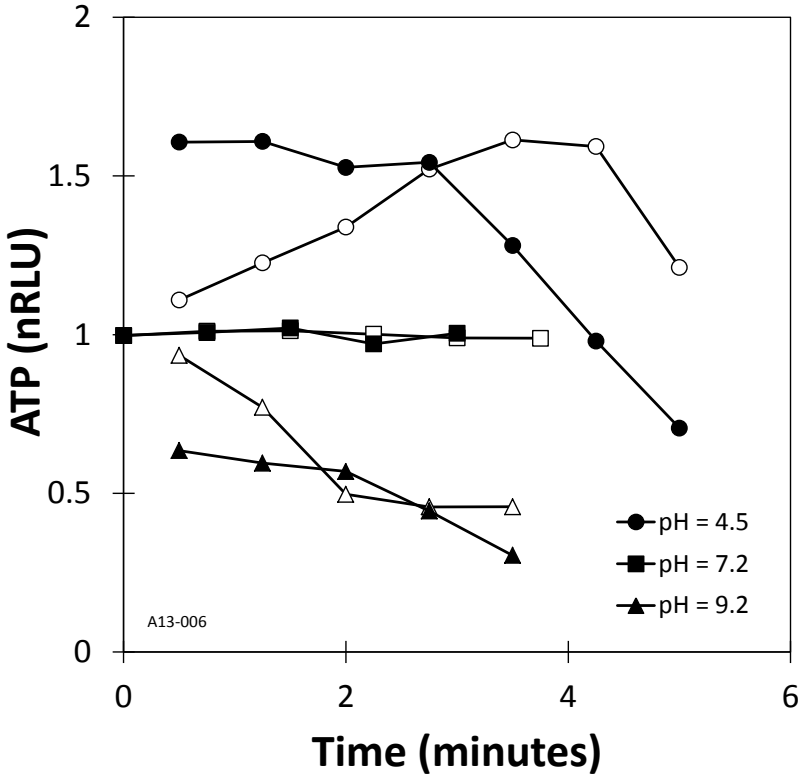

Figure 2.3 - Total ATP concentration of *E. coli* suspensions as a function of time at three solution pH values. Data presented as RLU normalized to the average RLU value at pH 7.2 (nRLU) for both one-day (solid symbols) and one-week (hollow symbols) starvation periods. For the pH 4.5 and 9.2 data, zero minutes represents the time when the pH was changed from 7.2 to the specified pH.

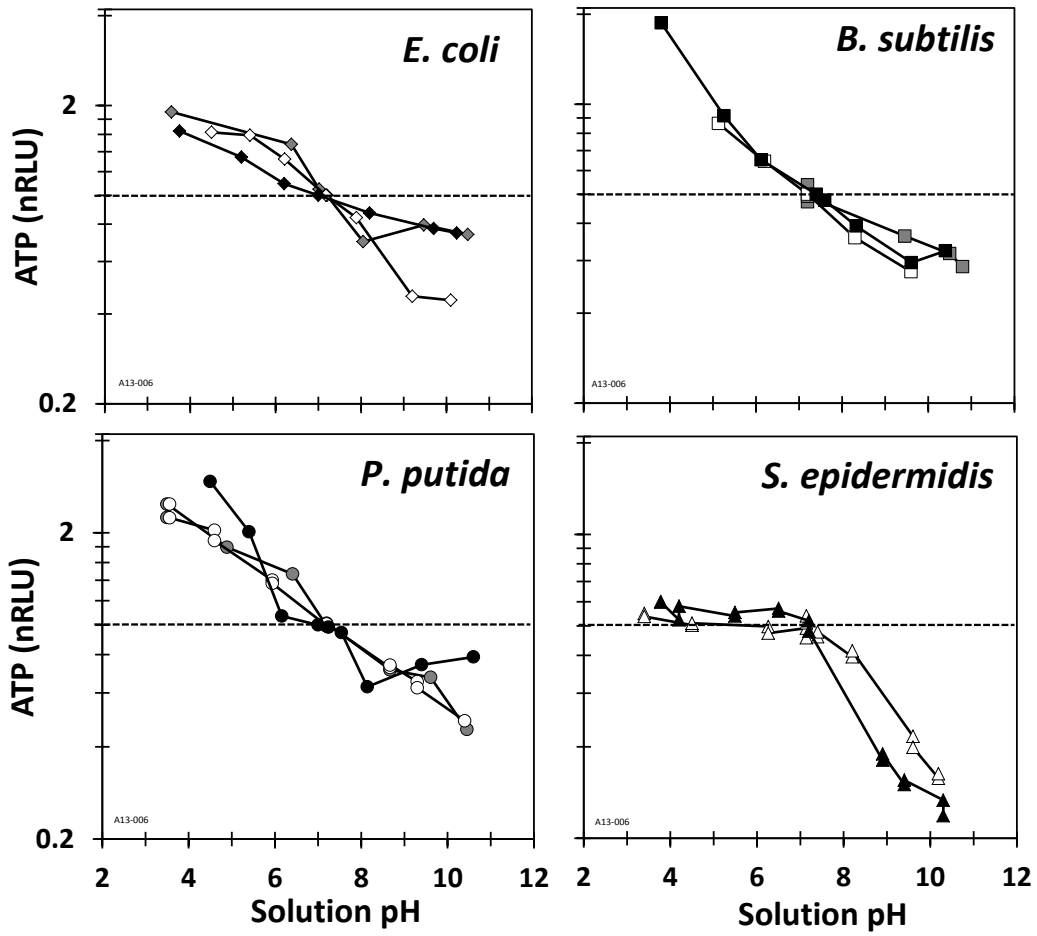

Figure 2.4 - ATP concentration, presented as Relative Light Units normalized to the value at pH 7.2 (nRLU), as a function of the solution pH. Grey and black symbols are replicate experiments with bacteria starved for one day. White symbols are bacteria starved for one week.

pH levels are in direct proportion to the H^+ concentration in the bulk solution and, with the exception of *S. epidermidis*, which will be discussed below, the ATP concentrations showed a two- to four-fold increase as the pH of the sample was decreased to 3.5. Conversely, it was anticipated that a rapid increase in bulk pH would decrease the proton gradient across the cell membrane, depleting Δp and decreasing cellular ATP. As shown in Figure 2.4, the ATP decreased as the bulk H^+ concentration decreased, with the ATP concentrations dropping by 20% to 70% as the pH was increased to 10.5. The results also demonstrate that the response to the rapid change in pH was identical under both the one-day and one-week starvation periods. Overall, these results are consistent with the hypothesis shown in Figure 2.1 and suggest a distinct relationship between bacterial ATP content and solution pH, with the ATP concentration inversely related to the pH.

2.3.3 Relationship between ATP and extracellular pH

To test for the exponential relationship between ATP and ΔpH suggested by equation 3, the data for each bacterial strain were aggregated and examined for their ability to be fit via a general exponential function. The results, shown in Figure 2.5, demonstrate that the exponential function accurately describes the experimentally-observed ATP/pH relationship.

To examine this relationship further, a comparative analysis of the four bacterial strains was performed and the results are presented in Figure 2.6. *E. coli*, *B. subtilis* and *P. putida* all demonstrated similar metabolic responses across the entire pH range.

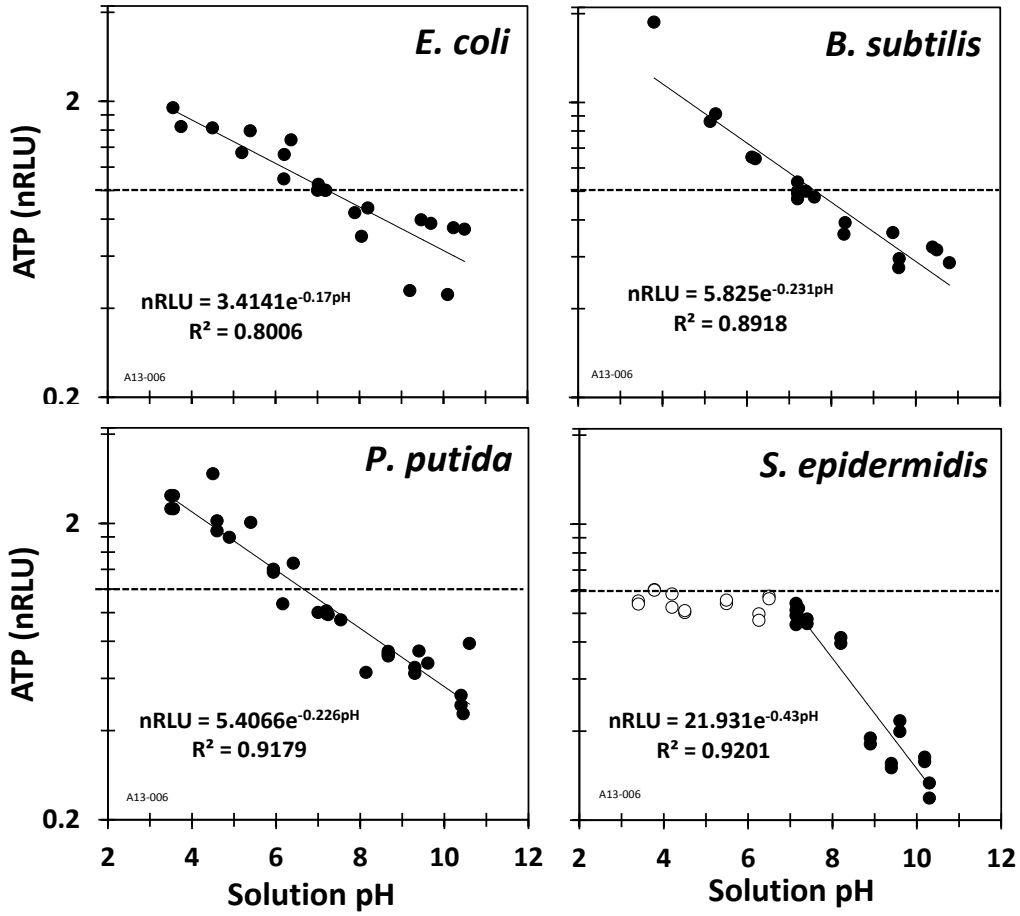

Figure 2.5 - Exponential curve fits of the consolidated experimental data. Hollow symbols for *S. epidermidis* were not included in the curve fit.

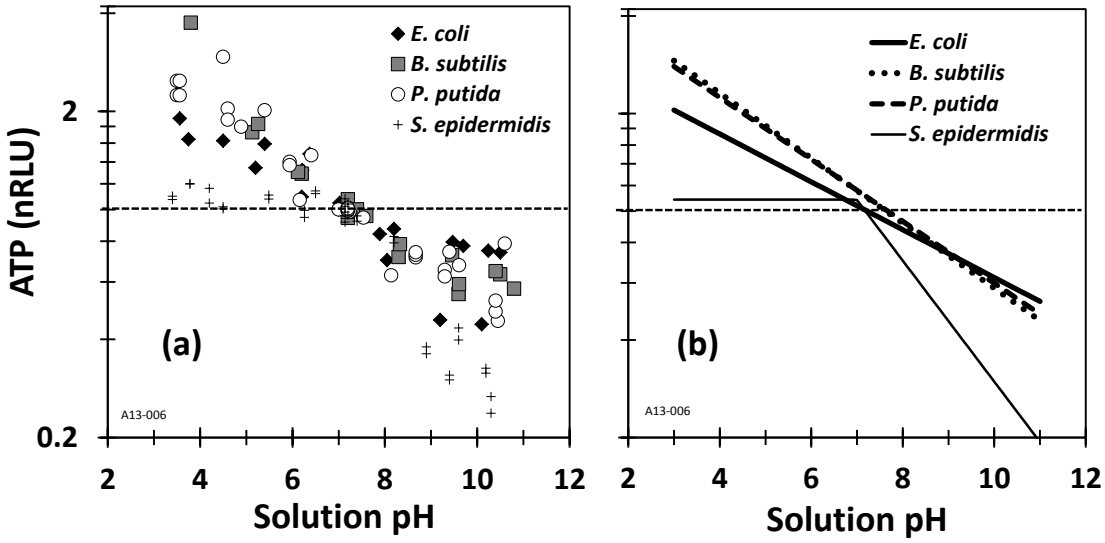

Figure 2.6 - Comparison of ATP levels between the four bacterial species as a function of solution pH. (a) Experimental data. (b) Exponential curve fits.

This finding indicates that the hypothesis outlined in Figure 2.2 is a common mechanism for influencing Δp via changes in pH outside of the cell and occurs with both Gram-Negative and Gram-Positive bacteria. *S. epidermidis*, on the other hand, showed no response under acidic conditions and a steeper slope under basic conditions than the other three bacterial strains. *S. epidermidis* is a well-studied inhabitant of human skin, which has a pH range of 4.0 to 5.6 with an average value around 4.7 [42-47]. This indicates that this species, although neutrophilic, has adapted to survive and grow under acidic conditions [48]. *S. epidermidis* has been shown to grow at both pH 7.0 and 5.5 with an identical growth rate and minimal lag period, whereas at a pH of 8.5 it had a an extensive lag period and a much lower growth rate [49]. The results found here, with no variation in *S. epidermidis* ATP levels under acidic conditions and an enhanced decrease in ATP under basic conditions, are consistent with these prior studies.

Statistical analysis of the data of the four bacterial species supports the similarity between the bacterial strains and the difference with *S. epidermidis*. Linearization of the exponential relationships in Figure 2.5 gives

$$\ln(\mathrm{nRLU}) = \mathrm{m}\cdot\mathrm{pH} + \mathrm{b} \tag{4}$$

where m is the slope and b is the intercept of the line fits. The 95% confidence intervals on m and b for each of the bacterial strains are presented in Figure 2.7. *E. coli*, *B. subtilis* and *P. putida* responded similarly to changes in pH and this is seen by the grouping of their confidence intervals, whereas *S. epidermis* shows distinct

deviation from this grouping. When considered in context with our prior work on the variation in bacterial ATP upon adhesion [1-5], these results suggest that *S. epidermis* adhesion to acidic surfaces would have no effect on cellular bioenergetics, while its adhesion to basic surfaces will have an enhanced effect compared to other neutrophilic bacteria. This information may be useful in identifying and developing antibacterial materials, coatings and solutions to discourage *S. epidermidis* colonization of surfaces.

2.4 Implications to bioenergetic response of attached bacteria

We have previously demonstrated that bacterial adhesion to surfaces results in changes in cellular ATP, with the variation a function of the surface properties as described by the working hypothesis [1-3]. However, the direct elucidation of the link between surface pH changes and variation in cellular ATP had not been established (process C in Figure 2.1). The results provided herein demonstrated that a distinct response in cellular ATP to changes in pH at the cell surface does exist. This finding fills in a key knowledge gap in the hypothesis suggesting that charge-regulation-induced pH changes at the cell surface can induce a bioenergetic response in bacteria [1-5].Specifically, and most importantly, this study elucidated a means to predict changes in cellular ATP as a function of changes in the local pH. Charge-regulation modeling can provide an estimate of the local pH upon a bacterium adhering to a surface [1, 2, 4, 6-8] and an example was provided in Figure 2.2. The exponential relationship elucidated in Figures 2.5 and 2.7 provides a means to estimate the relative variation in cellular ATP that may occur during this adhesion-induced pH change. In summary,

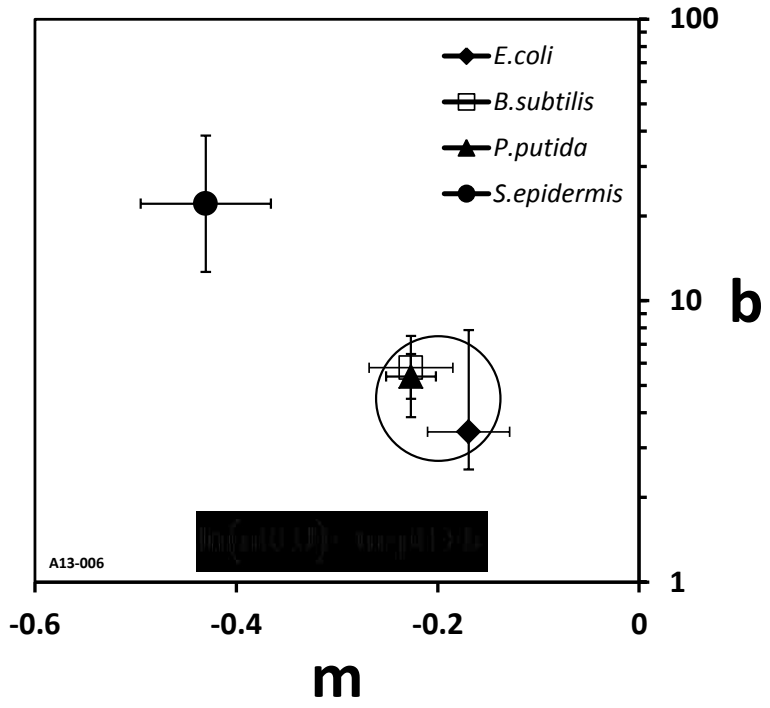

Figure 2.7 - Comparative analysis of the slope (m) and intercept (b) from equation 4 for the four bacterial species. Error bars represent the 95% Confidence Intervals. Results demonstrate that *E. coli*, *B. Subtilis* and *P. putida* have similar responses to pH changes (delineated by circle) and *S. epidermis* deviates from this response. The data for *S. epidermidis* was obtained using the upper pH range indicated in Figure 2.5.

we have demonstrated how cellular ATP levels are influenced by rapid changes in the extracellular pH, and this information may aid in the selection and design of surfaces that provide a desired bioenergetic response in bacteria (e.g., a passively antimicrobial surface) through local pH variations via the charge-regulation effect [1-4].

2.5 Acknowledgments

This project was funded by the National Science Foundation through Grant 0828356. The authors gratefully acknowledge their valuable support during this work.

2.6 Reference List

[1] D.G. Brown and Y. Hong, Impact of the Charge-Regulated Nature of the Bacterial Cell Surface on the Activity of Adhered Cells, J. Adhesion Sci. Technol., 25 (2011) 2199-2218.

[2] Y. Hong and D.G. Brown, Alteration of bacterial surface electrostatic potential and pH upon adhesion to a solid surface and impacts to cellular bioenergetics, Biotechnol. Bioeng., 105 (2010) 965-972.

[3] Y. Hong and D.G. Brown, Variation in bacterial ATP level and proton motive force due to adhesion to a solid surface, Appl. Environ. Microbiol., 75 (2009) 2346-2353.

[4] Y. Hong and D.G. Brown, Electrostatic behavior of the charge-regulated bacterial cell surface, Langmuir, 24 (2008) 5003-5009.

[5] Y. Hong and D.G. Brown, Cell surface acid-base properties of *Escherichia coli* and *Bacillus brevis* and variation as a function of growth phase, nitrogen source and C:N ratio, Colloids Surf. B, 50 (2006) 112-119.

[6] D.C. Prieve and E. Ruckenstein, Role of surface chemistry in particle deposition, J. Coll. Interface Sci., 60 (1977) 337-348.

[7] D.C. Prieve and E. Ruckenstein, The double-layer interaction between dissimilar ionizable surfaces and its effect on the rate of deposition, J. Coll. Interface Sci., 63 (1978) 317-329.

[8] D.C. Prieve and E. Ruckenstein, The surface potential of and double-layer interaction force between surfaces characterized by multiple ionizable groups, J. Theoret. Biol., 56 (1976) 205-228.

[9] P. Mitchell, Coupling of phosphorylation to electron and hydrogen transfer by a chemi-osmotic type of mechanism, Nature, 191 (1961).

[10] P. Mitchell, Chemiosmotic coupling in oxidative and photosynhetic phosphorylation, Biol. Rev., 41 (1966) 445-502.

[11] P. Mitchell, Possible molecular mechanisms of the protonmotive function of cytochrom systems, J. Theoret. Biol., 62 (1976) 327-367.

[12] E.R. Kashket, The proton motive force in bacteria: a critical assessment of methods, An. Rev. Microbiol., 39 (1985) 219-242.

[13] D.G. Nicholls and S.J. Ferguson, Bioenergetics 3, Academic Press, London, 2002.

[14] J.C. Cox, D.G. Nicholls and W.J. Ingledew, Transmembrane electrical potential and transmembrane pH gradient in the acidophile *Thiobacillus Ferro-oxidans*, Biochem. J., 178 (1979) 195-200.

[15] I. Friedberg and H.R. Kaback, Electrochemical proton gradient in *Micrococcus lysodeikticus* cells and membrane vesicles, J. Bacteriol., 142 (1980) 651-658.

[16] F.M. Harold, E. Pavlasova and J.R. Baarda, A transmembrane pH gradient in *Streptococcus faecalis*: Origin, and dissipation by proton conductors and N,N'-dicyclohexylcarbodiimide, Biochim. Biophys. Acta, 196 (1970) 235-244.

[17] E.R. Kashket, Proton motive force in growing *Streptococcus lactis* and *Staphylococcus aureus* cells under aerobic and anaerobic conditions, J. Bacteriol., 146 (1981) 369-376.

[18] S. Khan and R.M. Macnab, Proton chemical potential, proton electrical potential and bacterial motility, Journal of Molecular Biology, 138 (1980) 559-614.

[19] C.H. Kuhner, P.A. Hartman and M.J. Allison, Generation of a proton motive force by the anerobic oxalate-degrading bacterium *Oxalobacter formigenes*, Appl. Environ. Microbiol., 62 (1996) 2494-2500.

[20] P.C. Maloney, Relationship between phosphorylation potential and electrical H^+ gradient during glycolysis in *Streptococcus lactis*, J. Bacteriol., 153 (1983) 1461-1470.

[21] E. Padan, D. Zilbertstein and H. Rottenberg, The proton electrochemical gradient in *Escherichia coli* cells, European J. Biochem., 63 (1976) 533-541.

[22] E. Padan, D. Zilbertstein and S. Schuldiner, pH homeostasis in bacteria, Biochim. Biophys. Acta, 650 (1981) 151-166.

[23] J.B. Russell, Effect of extracellular pH on growth and proton motive force of *Bacteroides succinogenes*, a cellulolytic ruminal bacterium, Appl. Environ. Microbiol., 53 (1987) 2379-2383.

[24] J.-I. Shioi, S. Matsuura and Y. Imae, Quantitative measurements of proton motive force and motility in *Bacillus subtilis*, J. Bacteriol., 144 (1980) 891-897.

[25] M.G. Sturr, A.A. Guffanti and T.A. Krulwich, Growth and bioenergetics of alkaliphilic *Bacillus firmus* OF4 in continuous culture at high pH, J. Bacteriol., 176 (1994) 3111-3116.

[26] D. Zilberstein, S. Schuldiner and E. Padan, Proton electrochemical gradient in *Escherichia coli* cells and its relation to active transport of lactose, Biochem. J., 18 (1979) 669-673.

[27] A.P. Singh and P.D. Bragg, ATP synthesis driven by a pH gradient imposed across the cell membranes of lipoic acid and unsaturated fatty acid auxotroophs of *Escherichia coli*., FEBS Letters, 98 (1979) 21-24.

[28] L. Grinius, R. Slusnyté and B. Griniuviené, ATP synthesis driven by protonmotive force imposed across *Escherichia coli* cell membranes, FEBS Letters, 57 (1975) 290-293.

[29] D.M. Wilson, J.F. Alderete, P.C. Maloney and T.H. Wilson, Protonmotive force as the source of energy for adenosine 5'-triphosphate synthesis in *Escherichia coli*, J. Bacteriol., 126 (1976) 327-337.

[30] C.W. Jones, Membrane-associated energy conservation in bacteria: a general introduction, in: C. Anthony (Ed.) Bacterial Energy Transduction, Academic Press, New York, 1988.

[31] E.R. Kashket, Stoichiometry of the H+-ATPase of growing and resting, aerobic Escherichia coli, Biochem., 26 (1982) 5534-5538.

[32] P.C. Maloney and F.C. Hansen III, Stoichiometry of proton movements coupled to ATP synthesis driven by a pH gradient in *Streptococcus lactis*, J. Membrane Biol., 66 (1982) 63-75.

[33] D.S. Perlin, M.J.D. San Fransisco, C.W. Slayman and B.P. Rosen, H+/ATP stoichiometry of proton pumps from Neurospora crassa and Escherichia coli, Arch. Biochem. Biophys., 248 (1986) 53-61.

[34] R. Vink, M.R. Bendall, S.J. Simpson and P.J. Rogers, Estimation of H+ to adenosine 5'-triphosphate stoichiometry of Escherichia coli ATP synthase using 31P NMR, Biochem., 23 (1984) 3667-3675.

[35] J.J. Tomashek and W.S.A. Brusilow, Stoichiometry of energy coupling by proton-translocating ATPases: A history of variability, J. Bioenerg. Biomembr., 32 (2000) 493-500.

[36] M.T. Madigan, J.M. Martinko and J. Parker, Brock Biology of Microorganisms, Ninth ed., Prentice Hall, Upper Saddle River, NJ, 2000.

[37] W.J. Ball, Jr. and D.E. Atkinston, Adenylate energy charge in Saccharomyces cerevisiae during starvation, J. Bacteriol., 121 (1975) 975-982.

[38] D.N. Dietzler, C.J. Lais and M.P. Leckie, Simultaneous increases of the adenylate energy charge and the rate of glycogen synthesis in nitrogen-starved Escherichia coli W4597, Arch. Biochem. Biophys., 160 (1974) 14-25.

[39] C. Petersen and L.B. Møller, Invariance of the nucleoside triphosphate pools of Escherichia coli with growth rate, J. Biol. Chem., 275 (2000) 3931-3935.

[40] D. Jones, P.A. Pell and P.H.A. Sneath, Maintenance of bacteria on glass beads at -60°C to -76°C, in: B.E. Kirsop, A. Doyle (Eds.) Maintenance of microorganisms and cultured cells: A manual of laboratory methods, Academic Press, San Diego, 1991.

[41] J.E. Hobbie, R.J. Daley and S. Jasper, Use of nuclepore filters for counting bacteria by fluorescence microscopy, Appl. Environ. Microbiol., 33 (1977) 1225-1228.

[42] H. Lambers, S. Piessens, A. Bloem, H. Pronk and P. Finkel, Natural skin surface pH is on average below 5, which is beneficial for its resident flora, Int. J. Cosmetic Sci., 28 (2006) 359-370.

[43] M.-H. Schmid and H.C. Korting, The concept of the acid mantle of the skin: Its relevance for the choice of skin cleansers, Dermatology, 191 (1995) 276-280.

[44] A. Zlotogorski, Distribution of skin surface pH on the forehead and cheek of adults, Arch. Dermatol. Res., 279 (1987) 398-401.

[45] J.L. Matousek and K.L. Campbell, A comparative review of cutaneous pH, Veterinary Dermatology, 13 (2002) 293-300.

[46] C. Surber, P. Itin and T. Rufli, Skin surface pH after short exposure to model solutions, in: R. Marks, G. Plewig (Eds.) The Environmental Threat to the Skin, The University Press, Cambridge, 1992.

[47] H.C. Korting and O. Braun-Falco, The effects of detergents on skin pH and its consequences, Clinics in Dermatology, 14 (1996) 23-27.

[48] P.D. Cotter and C. Hill, Surviving the Acid Test: Responses of Gram-Positive Bacteria to Low pH, Microbiol. Molec. Biol. Rev., 67 (2003) 429-453.

[49] H.C. Korting, A. Lukacs, N. Vogt, J. Urban, W. Ehret and G. Ruckdeschel, Influence of the pH-value on the growth of *Staphylococcus epidermidis*, *Staphylococcus aureus* and *Propionibacterium acnes* in continuous culture, Int. J. Hyg. Environ. Med., 193 (1992) 78-90.

Chapter 3

Variation in *E. coli* energy levels during attachment to iron hydroxide (goethite) coated sand: Identification of a charge-regulated mechanism for bacterial inactivation.

Chapter 3 Variation in *E. coli* energy levels during attachment to iron hydroxide (goethite) coated sand: Identification of a charge-regulated mechanism for bacterial inactivation.

3.1 Introduction

Owing to their low cost, relative abundance in nature and physiochemical properties, iron minerals and iron (hydr)oxides are used in a range of environmental engineering applications. Iron particles and nanoparticles have been shown to efficiently remove heavy metals and arsenic from industrial waste effluent and contaminated water [1-8]. Iron-based permeable reactive barriers are used for remediation of oxidized groundwater contaminants, such as chlorinated compounds, by mediating redox reactions [9-12]. Iron nanoparticles have been proposed for stabilizing biosolids from wastewater treatment plants [13]. And iron and iron-coated surfaces, including iron-impregnated activated carbon, readily remove bacteria and viruses from water through sorption [14-19].

In aqueous systems, bacteria are typically negatively charged and iron surfaces exhibit positive charges, resulting in favorable adhesive forces between the two surfaces [20]. Studies have shown that iron surfaces exhibit antimicrobial properties to the adhered bacteria, with much of the work being performed with iron nanoparticles [21-24]. These studies have mainly focused on ferrous and zero-valent iron nanoparticles and have demonstrated that these forms of iron are highly cytotoxic to bacteria, with the

antimicrobial effects attributed to oxidative stress caused by oxygen radical formation, membrane disruption, and interference with ionic transport chains across the cell wall.

When considering antimicrobial properties of chemically stable forms of iron, such as goethite (FeOOH), magnetite (Fe_3O_4), and maghemite (γ-Fe_2O_3), the results are mixed. A few studies showed no bactericidal effects[21-23] while some demonstrated a decrease in bacterial viability [25, 26]. There experimental durations and approaches varied between these studies, and to date there is no consensus on antimicrobial properties of stable iron forms.

In this study we examine the effects of chemically-stable iron on the activity of attached bacteria by considering the relationship between cellular bioenergetics and the physiochemical charge-regulation process that occurs during bacterial adhesion (Figure 3.1) [27-30]. Bioenergetics describes the link between catabolic and anabolic reactions. During respiration, catabolic reactions pump protons across the cytoplasmic membrane (process A in Figure 3.1), setting up an electrochemical proton gradient composed of both pH (ΔpH) and electrostatic potential ($\Delta\psi$) gradients [31-33]. The energy stored in this gradient is termed the proton motive force (Δp) and is used to create chemical energy in the form of adenosine triphosphate (ATP) from adenosine diphosphate (ADP) via the membrane-bound enzyme complex ATP synthase (process B in Figure 3.1). ATP is a main energy carrier in living organisms and is used by the cell to drive anabolic processes.[34] It is important to note that cellular bioenergetics is a reversible process: a rise in Δp will increase ATP and a drop in Δp will result in a

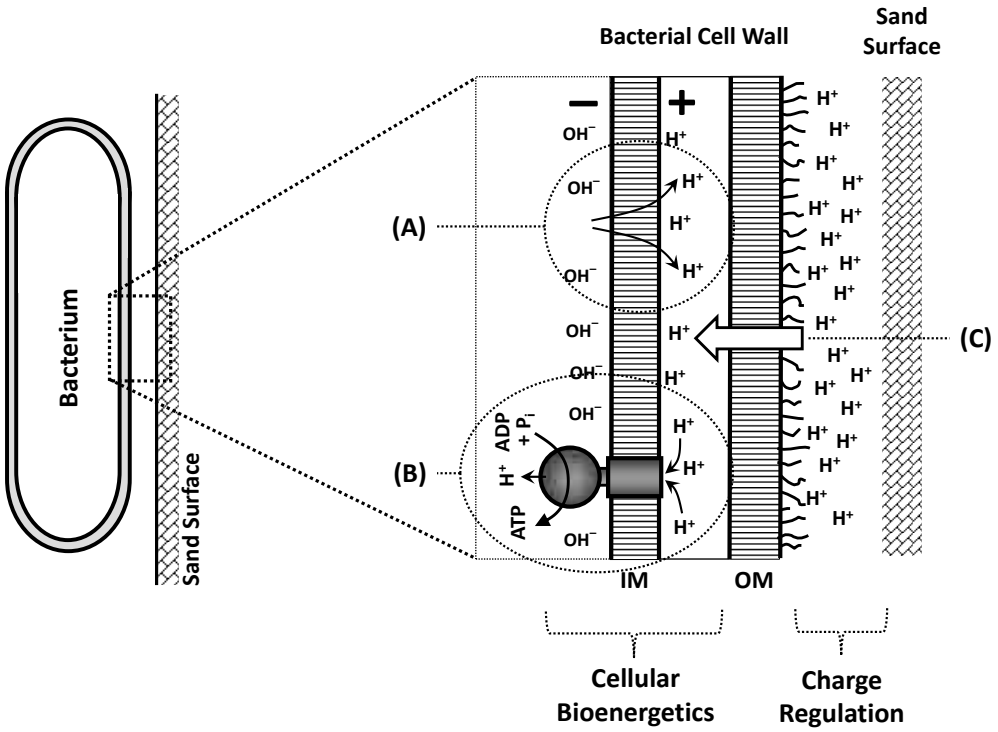

Figure 3.1 - The working hypothesis, depicted here for a Gram-negative bacterium adhering to a negatively-charged sand surface, links cellular bioenergetics to the charge-regulation effect. (Process A) In cellular bioenergetics, protons are pumped across the inner (cytoplasmic) membrane (IM) during respiration, setting up pH and electrostatic gradients across the IM. (Process B) The protons are then allowed back across the IM via the ATP-Synthase enzyme complex and the energy is captured to produce ATP from ADP. When cells approach the negatively-charged sand grain surface, the charge-regulation effect results in decrease in pH at the cell surface, which (Process C) propagates through the outer membrane (OM) and enhances the pH gradient across the IM. This enhancement in Δp increases the formation of ATP. The exact opposite is expected for the positively-charged iron-hydroxide surface, where a rise in pH due to the charge-regulation effect results in a decrease in Δp and ATP.

decrease in ATP, and as will be discussed below, this is a key component of how attachment to iron (hydr)oxide surfaces affects bacterial bioenergetics.

We recently demonstrated that changes in the pH at the bacterial cell surface can directly impact bioenergetics and cellular ATP levels, with the relationship following the reversible thermodynamics of cellular bioenergetics. Specifically, the cellular ATP concentration increased when the external pH was reduced (i.e., H^+ concentration increased, enhancing Δp) and the ATP decreased when the external pH was increased (i.e., H^+ concentration decreased, depleting Δp) [27]. While this study used an artificially-induced extracellular pH change, the local pH at the bacterial surface can also vary during adhesion due to the charge-regulation effect, which occurs as two surfaces with acid/base functional groups approach each other [28-30, 35-41], and this is the basis of our working hypothesis. The bacterial cell surface contains an array of functional groups including carboxylic, phosphoric, hydroxyl and amine groups. As the separation distance decreases between a bacterium and solid surface, which can also contain ionizable functional groups, the charge and electrostatic potential at the two surfaces will vary as a result of electroneutrality constraints between the surfaces. This charge-regulated surface response depends on the type and quantity of functional groups on the two surfaces and it results in a change in surface pH.

Our working hypothesis is that this charge-regulated change in pH at the bacterial cell surface will influence cellular bioenergetics by providing a local proton-rich or proton-deficient environment. In a recent study with the Gram negative *Escherichia coli* and

the Gram positive *Bacillus brevis*, we found that charge-regulation modeling predicted a pH decrease upon adhesion to negatively-charged glass beads, and experimentally demonstrated that the cellular ATP concentrations of the adhered cells were greater than for their planktonic counterparts [28-30]. Further charge-regulation modeling indicated that positively-charged surfaces should result in a pH rise and thus our working hypothesis predicts a decrease in Δp and cellular ATP levels.

As stable iron forms in aqueous systems exhibit positively-charged surface oxides, this suggests that they may reduce the activity of attached bacteria by lowering Δp and ATP levels. This was the focus of this study, where we examined the bioenergetics of *E. coli* cells adhered to FeOOH (goethite) coated sand and to untreated sand. Through a combination of experimental studies, and numerical modeling of cellular bioenergetics and the charge-regulation process, we demonstrate that *E. coli* attachment to untreated sand results in enhanced cellular ATP concentrations, while attachment to the FeOOH-coated surface results in depleted ATP levels, with the results in agreement with the working hypothesis. We summarize with a discussion of the implications of these findings.

3.2 Materials and Methods

3.2.1 Bacterial Cultivation

Gram-Negative *Escherichia coli* K-12 (ATCC29181) was grown in 500 mL of Luria Bertini broth (LB broth, Fisher Scientific) and stored in 15% glycerol at -86°C using the glass bead method [42]. In preparation for each experiment, bacteria from the

frozen stock were grown in 500 mL of LB broth at 30°C for 20 hours. The bacterial culture was then washed twice by centrifuging at 3500×g for 15 minutes, followed by re-suspension of the bacterial pellet in phosphate buffer solution (PBS, 0.258g KH_2PO_4 and 0.470g K_2HPO_4 in 1 L of deionized water with the pH adjusted to 7.2 using 1M NaOH). The bacteria samples were starved for 48 hours and subjected to another wash before being diluted with PBS to a concentration of approximately 10^8 cells, determined via Acridine Orange direct counts [43].

3.2.2 Sand Surface Preparation

Two 200 g batches of silica sand (AGSCO 000 sand) were rinsed with deionized water, autoclaved and dried in an oven at 105°C. One batch was coated with synthetic FeOOH (Goethite) according to the method described by Kim et al [44, 45]. Briefly, 200 g of sand was treated with 100 mL ferric hydroxide precipitate solution, which was prepared by raising the pH of a 0.2 M ferric chloride solution ($FeCl_3 \cdot 6H_20$) to 7.8. The sand suspension was mixed in a shaker at 60°C for 12 hr, after which it was dried for 24 hr at 105°C. The iron-coated sand was then rinsed with deionized water a minimum of five times, dried at 105°C and stored in centrifuge tubes. The untreated and iron-coated sand samples were rinsed one final time with DI immediately prior to use.

3.2.3 Surface Analysis

The iron surface coverage on both untreated and iron-coated sand grains was mapped using scanning electron microscopy (SEM, Hitachi 4300 SE/N) and Energy Dispersive

X-ray Spectroscopy (EDS, Zeiss LEO 1550). The zeta potentials of the *E. coli* cells and of colloidal fines from the sand and iron-coated sand samples (obtained during the washing process) were measured using a Malvern Zetasizer Nano ZS in a 10 mM NaCl solution at pH values ranging from ~2 to ~11 (adjusted with NaOH and HCl).

3.2.4 Experimental Methods

Bacterial attachment and ATP experiments were conducted using three different masses (0.3 g, 0.6 g, and 1.2 g) of sand and iron-coated sand, providing variation in the surface area available for adhesion. Glass vials were prepared by adding the specified sand mass with 4 mL of bacterial suspension and control vials contained only the bacterial suspension. The vials were placed on an Orbitron shaker at 25 rpm, maintained at 30°C in an incubator, and they were individually sacrificed at specific times through a total of five days for bacterial counting or determination of the bacterial ATP concentration. The number of adhered cells was determined as the difference between the total cells added to the vial and the planktonic cell count. The ATP was quantified on a total ATP per vial and then converted to ATP/cell for adhered and planktonic bacteria using the cell counts.

The ATP was extracted from the vials by placing the vials in boiling water for 3.5 min followed by rapid cooling in an ice bath for 1 min. This procedure lyses the cells, releasing ATP into solution, and inactivates the ATP synthase enzyme.[46] A 1 mL sample was then pipetted out of the vial and stored immediately in microcentrifuge tubes at -20°C prior to ATP analysis.

3.2.5 Bacterial ATP analysis

The ATP assay was performed according to Hong and Brown [30] using a Sirius Luminometer (Titertek-Berthold) and freshly prepared Luciferin-Luciferase solution. Luciferase solution was prepared adding 1 mL of Tris buffer (20 mM Tris and 2 mM EDTA, adjusted to a pH of 7.75 with acetic acid) to 1 mg of Luciferase (Sigma) and it was stored in 25 μL aliquots at -20°C. The Luciferin-Luciferase solution was then prepared by adding 10 mL of Tris Albumin buffer (20 mM Tris, 2 mM EDTA, 150 mM magnesium acetate, 50 μM dithiothreitol and 1 g bovine serum albumin, adjusted to a pH of 7.75 with acetic acid) to 1 mg of Luciferin (Sigma) and gently mixed with a Luciferase aliquot. The freshly prepared Luciferin-Luciferase solution was incubated at room temperature for a minimum of 30 minutes before performing the ATP analysis.

During ATP measurement, the frozen ATP extract samples were thawed to room temperature using a thermomixer. 100 μL of the bacterial ATP sample was pipetted into a luminometer tube containing 200 μL of Tris Mg^{2+} buffer (20 mM Tris, 2 mM EDTA, and 10 mM Mg^{2+} added as Mg acetate, adjusted to pH 7.75 with acetic acid). The contents of the tube were mixed thoroughly for 15 seconds using a vortex mixer. The tube was then placed in the luminometer and 100 μL of the Luciferin-Luciferase solution was injected into the sample. The Relative Light Units (RLU) obtained from the luminometer is a direct measure of the ATP concentration in the vial and was converted to ATP using standard curves with ATP standard solutions (Sigma).

3.3 Results and Discussion

3.3.1 Surface Characterization

The SEM/EDS analysis of the sand grains showed that the untreated sand had no detectable iron on its surface, while the iron-coated sand showed roughly 30% surface coverage of iron (Figure 3.2). This iron coverage resulted in a shift in the isoelectric point (IEP) of the sand from near 2 for the untreated sand to approximately 8 for the iron-coated sand (Figure 3.3). Additionally, the *E. coli* suspension has an IEP of near 2.5. These values are in agreement with data in the literature, where sand has reported IEP of ~2 [47], synthetic Goethite has reported IEP values in the range of 7.5-9.6 [48], and *E.coli* has an IEP of near 2 [35, 36]. Thus, the sand and *E. coli* both had a net negative charge a neutral pH, whereas the iron-coated sand had a net positive charge (Figure 3.3).

3.3.2 ATP and Cellular Bioenergetics

The shift from a negative charge for the untreated sand to a positive charge for the iron-coated sand had a significant impact on the adhesion of *E. coli*. As shown in Figure 3.4, the iron-coated sand showed a large increase in bacterial adhesion, from 10-20% for the untreated sand to 92-94% adhesion with the coating. Given that the

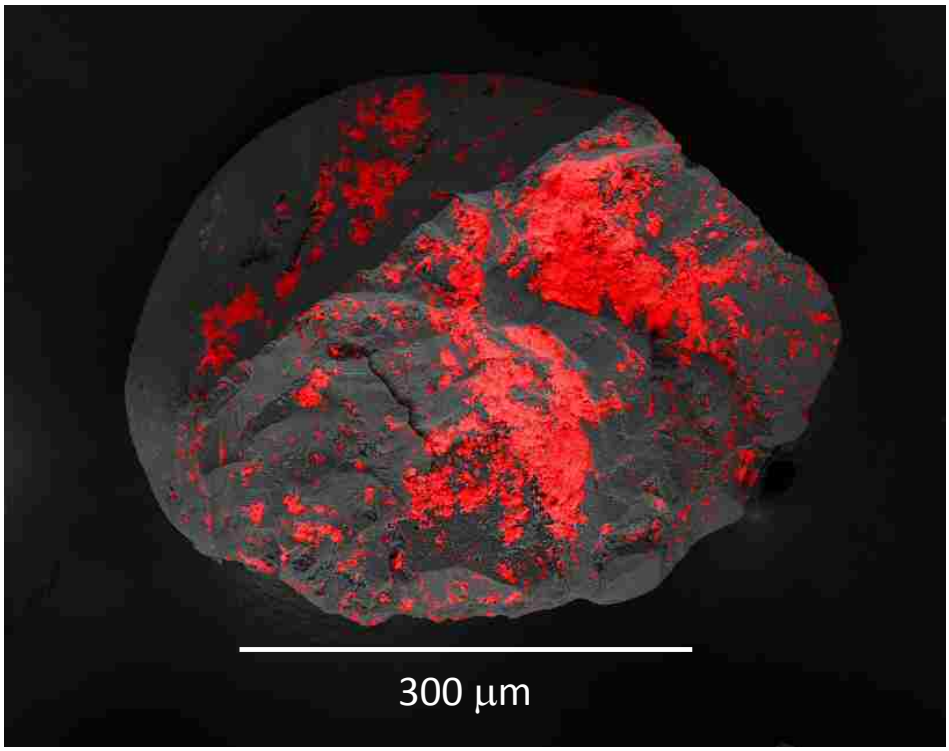

Figure 3.2 - Scanning electron microscope image of an iron-hydroxide coated sand grain particle. The red delineates high surface concentrations of iron as determined via Energy Dispersive X-ray Spectroscopy.

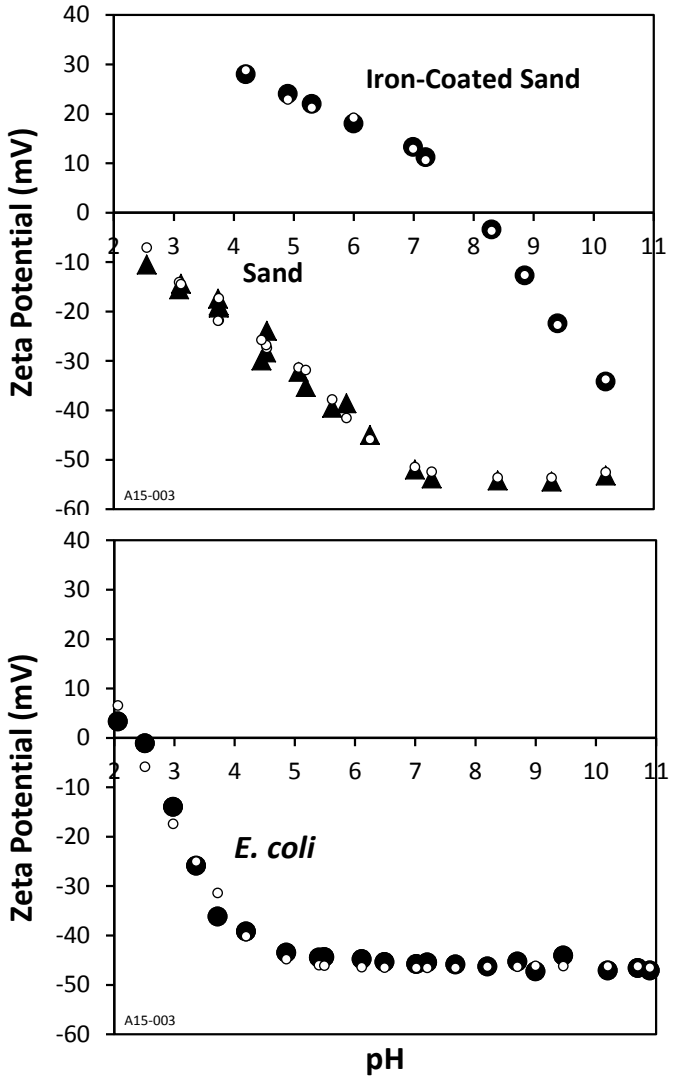

Figure 3.3 - Zeta potential of the sand, iron-coated sand, and *E. coli* suspended in 10 mM NaCl. A large shift in the isoelectric point was observed between the untreated (IEP≈2) and treated (IEP≈8) sands. The black symbols are the experimental data and the small white circles represent the best-fit charge-regulation model of the experimental data for determining the pK and N values for the surfaces.

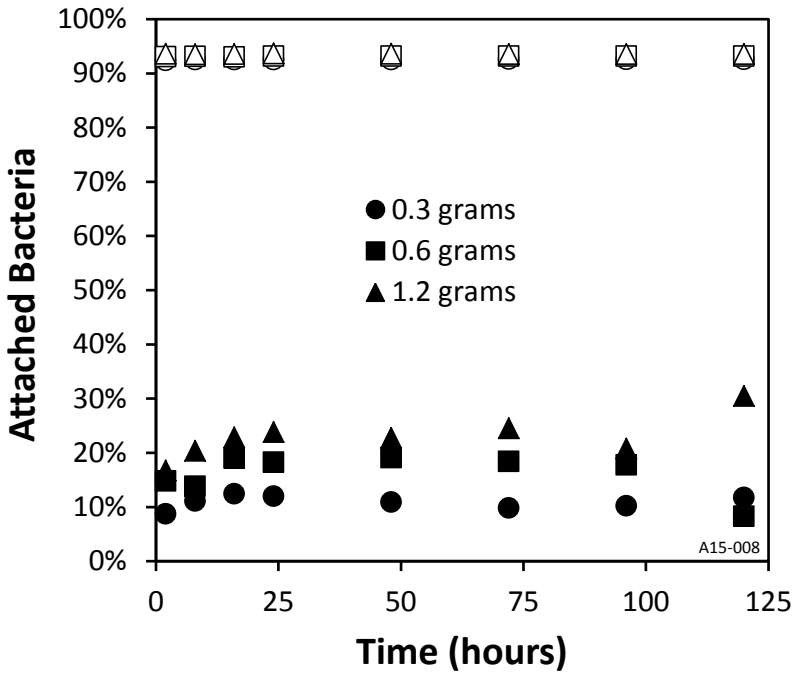

Figure 3.4 - Adhesion of *E. coli* to untreated sand (solid symbols) and iron-coated sand (hollow symbols) with 4 mL of bacteria suspension and three different masses of sand. Results demonstrate a significant increase in adhesion with the iron-hydroxide coating.

sand surface was only partially covered with the iron coating, this indicates that the bacteria had a high affinity for adhering to the positively-charged iron coating.

The ATP results for both the adhered and planktonic bacteria are shown in Figure 3.5. The ATP levels of the planktonic *E. coli* remained relatively constant throughout the 5-day experiment. Conversely, the ATP for *E. coli* adhered onto the untreated sand increased above the planktonic values and the ATP for *E. coli* adhered onto the iron-coated sand decreased, with both findings in agreement with the hypothesis. For the untreated sand, ATP increased throughout the first 24 hours and then slowly declined back towards the planktonic values over the next four days. These results were similar to those from our preliminary study with *E. coli* and *Bacillus brevis* adhesion onto glass beads [28, 30]. For the iron-coated sand, the ATP levels continuously declined below the planktonic levels over the five-day experimental period. These results clearly demonstrated that bacterial adhesion to the sand and iron-coated sand directly impacted cellular bioenergetics.

To explore this further, the change in ΔpH across the cytoplasmic membrane required to achieve these ATP shifts was explored within the framework of the Chemiosmotic Theory. This was done by considering the relationship between Δp (in units of mV) and the free energy of phosphorylation, ΔG_p (kJ/mol):

$$\Delta p = -\frac{\Delta G_P}{nF} \tag{1}$$

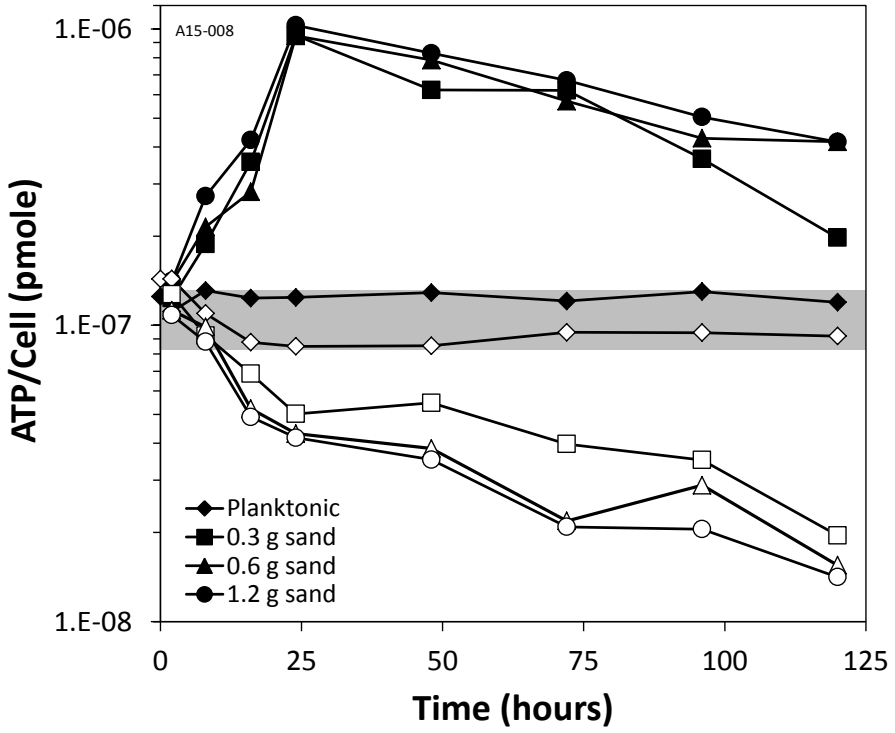

Figure 3.5 - ATP/cell for the planktonic bacteria and bacteria attached to the untreated sand (solid symbols) and iron-coated sand (hollow symbols). Gray shading highlights planktonic bacteria from the controls for each of the two experiments (i.e., from vials with no sand).

where n is the number of protons translocated per ATP synthesized (Process A in Figure 3.1) and F is the Faraday constant. The value of n is typically reported in the range of 2 to 3 for bacteria [49-53], and a value of n = 2 was used to calculate Δp for the following analysis. ΔG_p can be calculated from the following relationship [54]:

$$\Delta G_p = \Delta G_p^o + RT \cdot \ln\left(\frac{[ATP]}{[ADP][P_i]}\right) \tag{2}$$

where ΔG_p^o is the standard free energy for ATP hydrolysis with a reported value of 30.1 kJ/mol [49]; $[P_i]$ is the intracellular inorganic phosphate concentration (mol/L); [ATP] and [ADP] are the concentrations of ATP and ADP, respectively (mol/L); R is the ideal gas constant and T is temperature (K).

To determine Δp from the experimental ATP concentrations via Equations (1) and (2), the ADP and P_i concentrations must be determined. This was done by considering the adenylate relationships (the adenylate pool and the adenylate energy charge) within biological cells. The adenylate pool (AP) is the sum of the molar concentrations of ATP, ADP and adenosine monophosphate (AMP):

$$AP = [ATP] + [ADP] + [AMP] \tag{3}$$

While the distribution of the adenylates will vary as a function of the bacteria's metabolic state, the AP remains fairly constant within a bacterial cell [55-57]. The adenylate energy charge (EC_A) describes the relative distribution of the adenylates in the adenylate pool. It is defined as

$$EC_A = \frac{[ATP] + \frac{1}{2}[ADP]}{AP} \quad (4)$$

and varies from 0 (AP = [AMP]) to 1 (AP = [ATP]) [58]. The three adenylates can also be related through the reaction catalyzed by adenylate kinase, ATP + AMP ↔ 2ADP, represented by the equilibrium equation:

$$K = \frac{[ATP][AMP]}{[ADP]^2} \quad (5)$$

where K has a value of 0.8 [58-60]. Finally, the total intracellular phosphate concentration (C_{T,PO_4}) is the sum of the phosphate distribution between the adenylates:

$$C_{T,PO4} = 3[ATP] + 2[ADP] + [AMP] + [P_i] \quad (6)$$

The following two assumptions were used to solve this system of equations:

i. The EC_A of bacteria during growth has been shown to be ~0.8 and it declines to a constant value of 0.2–0.3 during starvation [49, 55, 61-63]. Here, with the bacteria starved prior to the experiment, it was assumed that the initial EC_A (t = 0) was 0.2.

ii. The P_i of starved *E. coli* has been shown to be ~14 mM and this was used as the initial value at the beginning of the experiment (t = 0) [49].

Using these initial conditions, along with the experimental ATP data for the planktonic bacteria, AP and C_{T,PO_4} were calculated, and these were subsequently used as constant values through the remainder of the analysis.

Results of the adenylate analysis are shown in Figure 3.6, where it can be seen that the *E. coli* adenylate energy charge is enhanced during attachment to the negatively-charged untreated sand, with values ranging from 0.20 up to 0.75, whereas it is depleted during attachment to the positively-charged iron-coated sand, with values ranging from 0.19 down to 0.05. Correspondingly, the ATP increased from ~10% of AP to over 60% during adhesion to the untreated sands, in agreement with our prior results for *E. coli* attachment to glass beads [28, 30]. For the iron-coated sand, the *E. coli* ATP decreased significantly, from ~7% of AP down to <1%.

Using these results, Δp was calculated from Equations (1) and (2) and the results are presented in Figure 3.7. In this figure it can be seen that Δp for the planktonic cells ranged between -190 mV to -195 mV over the course of the experiment. These values are within reported ranges of Δp for bacteria, which extend from -140 mV to over -220 mV [64, 65]. For the cells adhered to the untreated sand, Δp increased to approximately -228 mV over the first 24 hours and then decreased slowly over the next 4 days. For the cells adhered to the iron-coated sand, Δp continuously declined, dropping to approximately -178 mV by the end of the 5-day experiment.

As stated earlier, Δp is composed of both a pH gradient (Δp) and an electrostatic potential gradient ($\Delta\psi$) and it is expected that changes in Δp due to the charge-

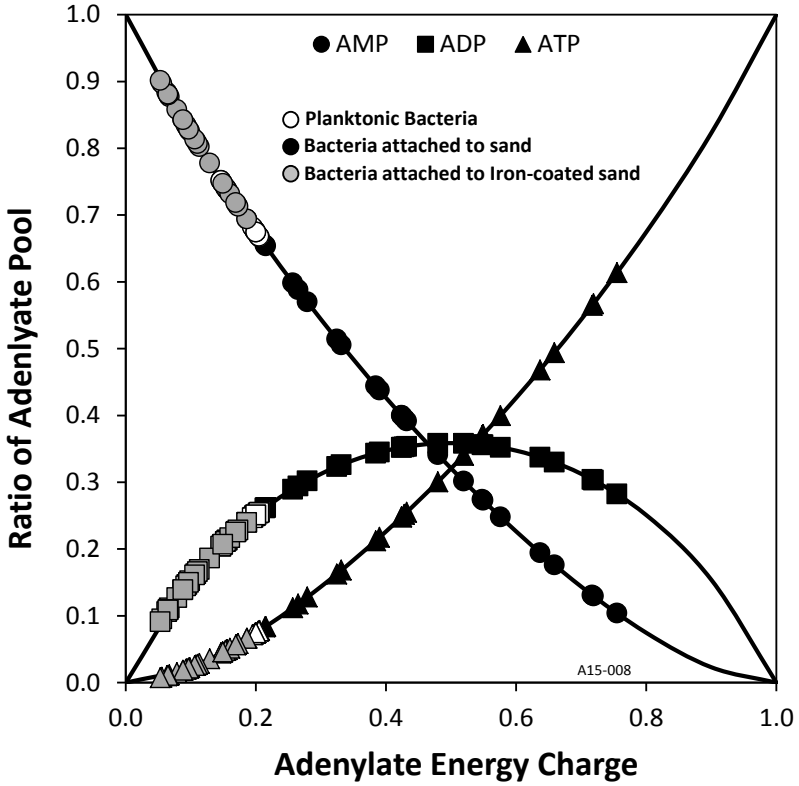

Figure 3.6 - Ratio of ATP, ADP and AMP to the adenylate pool as a function of the adenylate energy charge. Symbols are calculated from the experimental data and the lines are the theoretical model from Atkinson and Walton.[30, 58] Results demonstrate an increase in bioenergetics (i.e., an increase in the adenylate energy charge) for *E. coli* adhered to the uncoated sand (solid symbols) as compared to the planktonic bacteria (hollow symbols), and a decrease in bioenergetics (i.e., a decrease in the adenylate energy charge) during adhesion to the iron-hydroxide coated sand (gray symbols).

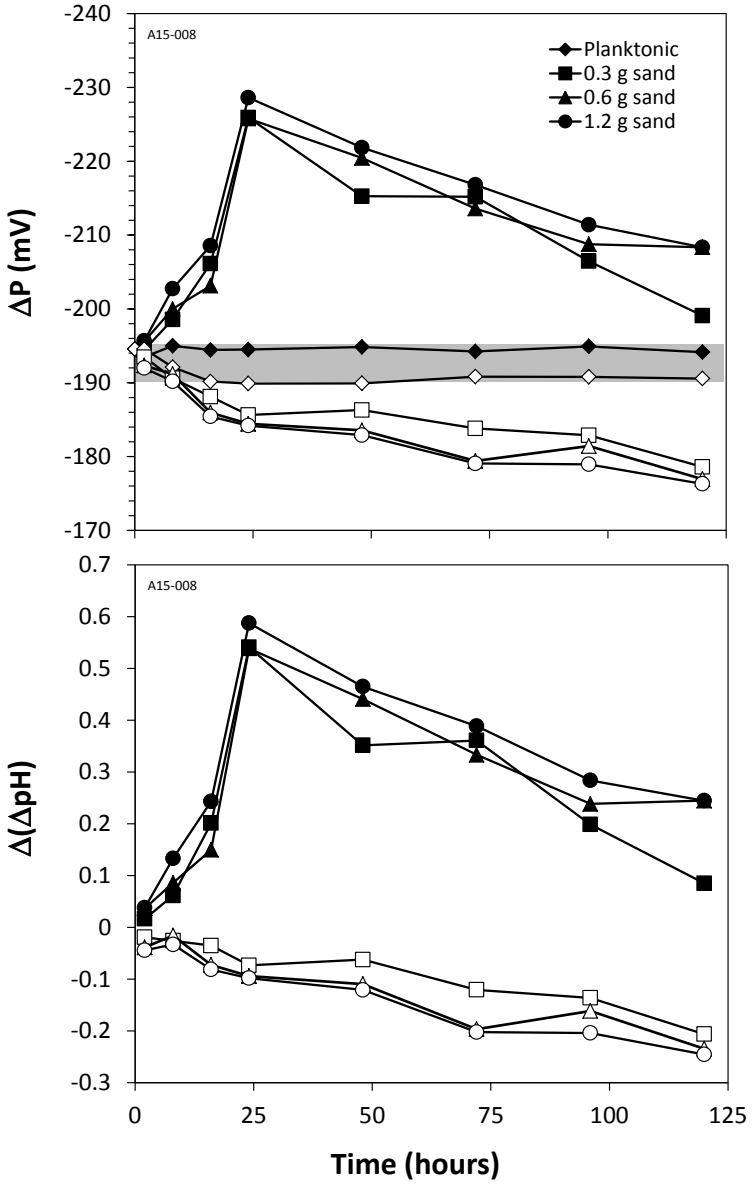

Figure 3.7 - Proton motive force (Δp) and change in ΔpH (Δ(ΔpH)) required to achieve the experimentally-measured ATP values. Gray shading highlights the Δp values for the planktonic bacteria. Solid symbols are with the untreated sand and the hollow symbols are with the iron-hydroxide coated sand.

regulation effect would be to the ΔpH component [28, 30, 65]. When Δp is in units of mV, it can be written as [66]:

$$\Delta p = \Delta\psi - \frac{2.3RT}{F}\Delta pH \tag{7}$$

For neutrophilic bacteria, such as *E. coli* examined here, Δψ accounts for 70-80% of Δp, with ΔpH contributing 20-30% [65]. Here, the change in ΔpH required to give the experimentally-observed ATP values was calculated by assuming that Δψ was equal to 75% of the Δp value t = 0 and the subsequent variation in Δp was due to changes in ΔpH [28, 30, 65]. The results are shown in Figure 3.7, where it can be seen that an increase in ΔpH (i.e., Δ(ΔpH)) of as little as 0.6 pH units is required to achieve the ATP increase observed with untreated sand, and this is similar the values of up to ~0.5 pH units found with *E. coli* and *B. brevis* on clean glass beads [28, 30]. With the iron-coated sand, a decrease in ΔpH of only down to 0.25 pH units results in the experimentally-observed drop in ATP below that of the planktonic cells.

3.3.3 Charge-Regulation Effect

Charge-regulation modeling was performed to determine if the predicted pH change at the *E. coli* surface during adhesion is sufficient to result in the Δ(ΔpH) values calculated from the bioenergetic modeling. The charge-regulation model presented here was developed in Hong and Brown [29, 35] and follows the model proposed by Ninham and Parsegian [67], with modifications to allow modeling of surfaces containing multiple functional groups [29, 35, 38, 68-70]. While this model is

sufficient here for representing the charge-regulated bacterial cell surface [29, 35], other approaches for charge-regulated surfaces are also applicable, such as the soft-particle approach [41, 71-73].

The model used here is based on the Poisson-Boltzmann equation, which describes the electrostatic potential in an electrolyte solution as a function of distance from a charged surface. The one-dimensional Poisson-Boltzmann equation can be written as

$$\frac{d^2\psi}{dx^2} = -\frac{1}{\varepsilon_o \varepsilon} \sum_i n_{ri} z_i e \exp\left(\frac{-z_i e \psi}{kT}\right) \tag{8}$$

where x is the distance from the charged surface; ψ is the electrostatic potential (V); ε_o is the permittivity of vacuum (8.854×10^{-12} C^2/J-m); ε is the dielectric constant of the medium (78.5 for water); n_{ri} is the number of ions of species i per unit volume in the bulk fluid; z_i is the valence of ion i; e is the electron charge (1.602×10^{-19} C); k is the Boltzmann constant (1.381×10^{-23} J/K); and T is the temperature (298 K). Gauss's law is used to provide the boundary conditions to Equation 8:

$$\left.\frac{d\psi}{dx}\right|_\alpha = -\frac{\sigma_\alpha}{\varepsilon_o \varepsilon} \tag{9}$$

where σ is the surface charge density (C/m^2) and subscript α = 1,2 defines the two surfaces.

The surface charge comes from the dissociation of acid/base functional groups at the two surfaces, i.e. $R_{aj}H \leftrightarrow R_{aj}^- + H^+$ and $R_{bk}H^+ \leftrightarrow R_{bk} + H^+$, where R_{aj} are the

acidic ionizable sites of type j (e.g., phosphoric, carboxylic, and hydroxyl groups) and R_{bk} are the basic ionizable sites of type k (e.g., iron hydroxide groups). Given these reactions, the charge-regulated boundary conditions for the electrostatic potential profile can be written as the sum of the positively-charge sites minus the sum of the negatively-charged sites, resulting in the following equation [28, 29, 35, 38]:

$$\sigma_\alpha = e\cdot\left[\sum_{k=1}^{m_{b\alpha}}\frac{[H^+]_\infty N_{bk\alpha}}{[H^+]_\infty + K_{bk\alpha}\exp\left(\frac{e\psi_\alpha}{kT}\right)} - \sum_{j=1}^{m_{a\alpha}}\frac{K_{aj\alpha}N_{aj\alpha}}{K_{aj\alpha} + [H^+]_\infty \exp\left(\frac{-e\psi_\alpha}{kT}\right)}\right] \tag{10}$$

where $N_{aj\alpha}$ and $N_{bk\alpha}$ are the number of acid sites of type j and base sites of type k per unit area of surface α; $K_{aj\alpha}$ and $K_{bk\alpha}$ are the corresponding dissociation constants associated with the acidic and basic functional groups (mole/L); $[H^+]_\infty$ is the bulk proton concentration (mole/L); ψ_α is the electrostatic potential for each surface (V); and $m_{a\alpha}$ and $m_{b\alpha}$ are the number of different acidic and basic groups on each surface, respectively. Finally, the local proton concentration adjacent to each surface ($[H^+]_\alpha$) can be determined using the Boltzmann distribution:

$$[H^+]_\alpha = [H^+]_\infty \exp\left(-\frac{e\psi_{s\alpha}}{kT}\right) \tag{11}$$

To model these charge-regulated surface interactions, the pK and N values for the acidic and basic functional groups on the two surfaces (where pK = -log(K)) were quantified from the zeta potential (ζ) data. The purpose here is to identify values of pK and N that accurately represent the charge and electrostatic potential of the

surfaces as a function of pH, and this is not necessarily the pK and N values for each functional group on the surface. This was accomplished by applying the Grahame equation, which represents the charge as a function of the electrostatic potential and solution electrolyte composition:

$$\sigma_\alpha = \pm\left[2\varepsilon_o\varepsilon kT\sum_i n_{ri}\left\{\exp\left(\frac{-z_i e\psi_\alpha}{kT}\right)-1\right\}\right]^{\frac{1}{2}} \quad (12)$$

Using ζ as an estimate of ψ_α, equations 10 and 12 were coded in C++ and combined with the numerical optimization code PEST (Watermark Numerical Computing) to obtain the pK and N values that best simulate the zeta potential titration data. The resulting pK and N values are presented in Table 1 and the charge-regulation model simulations of the surface potential using these values are presented in Figure 3.3, indicating that the pK and N values are able to accurately represent the electrostatic nature of the surfaces as a function of pH.

The pK and N values in Table 1 were used with equations 8-11 to calculate the *E. coli* surface pH as a function of separation distance from the sand and iron-coated sand surfaces, and the results are shown in Figure 3.8. First, it can be seen that with a bulk pH of 7, the *E. coli* surface pH is approximately 6.2 due to the negatively-charged cell surface and the local distribution of H^+ adjacent to the cell surface via the Boltzmann distribution. As the bacterium then approaches the untreated sand surface, the cell surface pH drops from 6.2 to below 5.

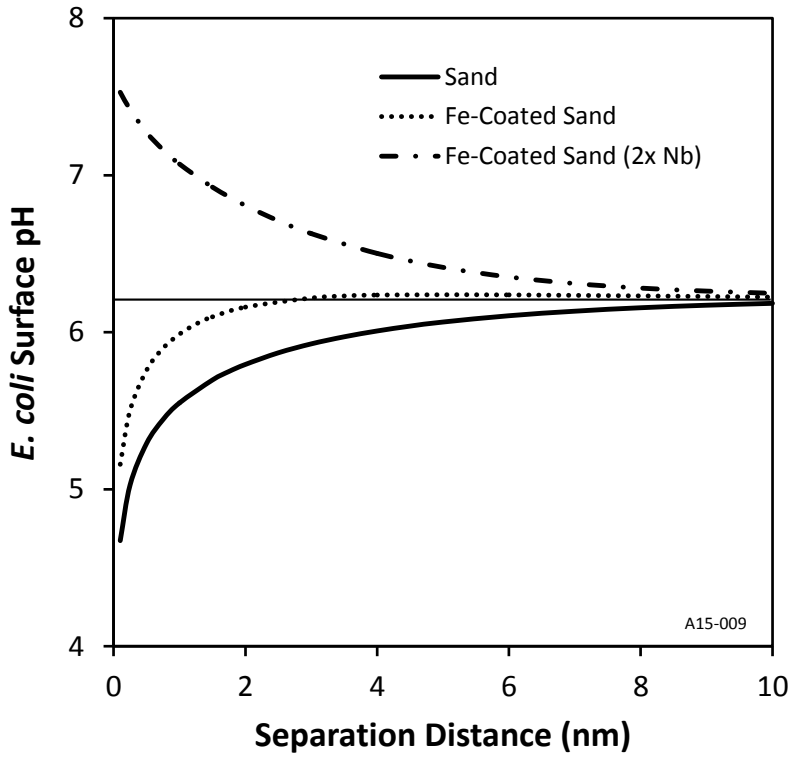

Figure 3.8 - Charge-regulated surface pH of *E. coli* as a function of separation distance from the untreated sand and iron-coated sand (electrolyte is 10 mM NaCl at pH 7). Also presented is the surface pH for the case where the site density of the basic functional group describing the iron-coated surface (N_b, Table 3) was doubled. See text for discussion.

Table 3.1 - Best-fit pK and N values for acidic (a) and basic (b) sites for the three surfaces used in this study. Parentheses indicate 95% confidence intervals. Resulting model fits using these values are presented in Figure 3.3.

	pK	**N (#/nm^2)**
E. coli	pK_a = 2.60 (2.49 – 2.71) pK_b = 11.24 (7.70 – 14.8)	N_a = 0.118 (0.108 – 0.129) N_b = 0.0420 (0.0322 – 0.0547)
Sand	pK_{a1} = 2.75 (2.49 – 3.02) pK_{a2} = 5.16 (4.94 – 5.38)	N_{a1} = 0.0383 (0.0340 – 0.0431) N_{a2} = 0.0532 (0.0460 – 0.0614)
Fe-coated Sand	pK_{a1} = 4.42 (4.04 – 4.81) pK_{a2} = 7.52 (6.86 – 8.18) pK_b = 9.04 (8.40 – 9.68)	N_{a1} = 0.0393(0.0250 – 0.0715) N_{a2} = 0.0303 (0.0122 – 0.0752) N_b = 0.0687 (0.0524 – 0.0901)

For the iron-coated sand, it was anticipated that the cell surface pH would rise as the separation distance decreases, but the model shows a decrease in pH, albeit less of a drop than the uncoated sand. It is important to note that the pK and N values are those that best represent the overall (spatially-averaged) electrostatic properties of the surfaces. For the iron-coated surface, the iron hydroxide only partially coats the surface (Figure 3.2) yet accounts for a significant fraction of the adsorbed bacteria (Figure 3.4). If we make an educated assumption that the local surface density of the basic (positive) functional groups on the iron-coated portions of the sand is higher than the average value obtained from the zeta potential measurements, we can reassess the effects of *E. coli* adhesion to the iron coating. This is shown in Figure 3.8 for a simple doubling of the basic site density (N_b), and the results demonstrate that the pH increases from 6.2 to above 7.5 as the *E. coli* cell approaches the iron-coated surface.

One should not take these as absolute numbers, as the model assumes planar surfaces, but it does suggest the expected trend as the bacterium approaches the sand surface and demonstrates how the charge-regulated surfaces result in a variation in the cell surface pH with separation distance. Specifically, *E. coli* adhesion to the negatively-charged (acidic) sand surface results in a decrease in surface pH, causing an increase in ΔpH and Δp, with a corresponding rise in cellular ATP. Conversely, E. coli adhesion to the positively-charged (basic) iron hydroxide surface results in an increase in surface pH, causing a decrease in ΔpH and Δp, with a corresponding decrease in cellular ATP. While attachment to the negatively-charged surface demonstrated a finite change in ATP, with the positively-charged surface the cellular ATP continually

decreased over the five-day experiment, indicating that the surfaces were steadily depleting the bacterial energy stores.

There are a number of implications from these findings. First, the results suggest that prolonged attachment to iron (hydr)oxide surfaces will deplete Δp and ATP, and likely lead to cellular death if energy sources are not available to make up for these losses. As shown in Figure 3.5, the cellular ATP concentration for *E. coli* attached to the iron-coated sand did not drop below the planktonic values until near 12 hours of attachment, and it then continued to decrease through the five-day experimental period. These results are supported by the literature. In particular, the studies that found no bacterial inactivation on iron (hydr)oxide surfaces were performed under short time durations from five minutes up to one hour [21-23], while the studies that did identify inactivation were performed for 24 to 48 hours [25, 26]. These results demonstrate that stable iron (hydr)oxide surfaces can lead to cellular inactivation through the charge-regulation process. This leads one to imagine that cells that use iron (hydr)oxide surfaces as electron acceptors may have developed means to remain physically distanced from the surface (Figure 3.8 suggests ~5 nm may be sufficient), while using external electron shuttles and nanowires to complete the redox reactions [74-78]. It should also be noted that this charge-regulated inactivation will be mediated by other positively-charged surfaces, such as cationic polymers, which have been shown to lead to bacterial inactivation [79-81].

One other implication is surface sensing and gene expression. Surface recognition and gene expression for initiating biofilm growth has been shown to be dependent on the

local pH [82-85] and osmolarity [85-88], both of which will change during charge-regulated adhesion. Changes in Δp and cellular ATP concentrations have also been suggested as surface-sensing signals [89], and the cellular concentration of cyclic AMP (cAMP), which is formed from ATP, regulates genes in bacteria, including surface sensing genes [90]. This suggests that appropriate selection of surfaces may allow expression or repression of genes in attached bacteria via changes in Δp and ATP mediated by the charge-regulation process.

3.4 Acknowledgement

This project was funded by the National Science Foundation through Grant 0828356. The authors gratefully acknowledge their valuable support during this work.

3.5 References

[1] K.A. Al-Saad, M.A. Amr, D.T. Hadi, R.S. Arar, M.M. Al-Sulaiti, T.A. Abdulmalik, N.M. Alsahamary and S.H. Al-Yahri, Iron oxide nanoparticles: applicability for heavy metal removal from contaminated water, Journal of Neuclear Sciences and Applications, 2012; 45: 335, 346 (2012).

[2] A. Dąbrowski, Z. Hubicki, P. Podkościelny and E. Robens, Selective removal of the heavy metal ions from waters and industrial wastewaters by ion-exchange method, Chemosphere, 56 (2004) 91-106.

[3] J. Hu, G. Chen and I.M.C. Lo, Selective removal of heavy metals from industrial wastewater using maghemite nanoparticle: performance and mechanisms, J. Environ. Eng., 132 (2006) 709-715.

[4] J.-f. Liu, Z.-s. Zhao and G.-b. Jiang, Coating Fe3O4 magnetic nanoparticles with humic acid for high efficient removal of heavy metals in water, Environ. Sci. Technol., 42 (2008) 6949-6954.

[5] S. Dixit and J.G. Hering, Comparison of arsenic (V) and arsenic (III) sorption onto iron oxide minerals: Implications for arsenic mobility, Environ. Sci. Technol., 37 (2003) 4182-4189.

[6] A. Joshi and M. Chaudhuri, Removal of arsenic from ground water by iron oxide-coated sand, J. Environ. Eng., 122 (1996) 769-771.

[7] D. Rozell, Modeling the removal of arsenic by iron oxide coated sand, J. Environ. Eng., 136 (2009) 246-248.

[8] P. Xu, G.M. Zeng, D.L. Huang, C.L. Feng, S. Hu, M.H. Zhao, C. Lai, Z. Wei, C. Huang and G.X. Xie, Use of iron oxide nanomaterials in wastewater treatment: a review, Science of the Total Environment, 424 (2012) 1-10.

[9] D.H. Phillips, D.B. Watson, Y. Roh and B. Gu, Mineralogical characteristics and transformations during long-term operation of a zerovalent iron reactive barrier, J. Environ. Quality, 32 (2003) 2033-2045.

[10] R.M. Powell, R.W. Puls, D.W. Blowes, R.W. Gillham and D. Schultz, Permeable reactive barrier technologies for contaminant remediation, NASA, (1998).

[11] G.A. Mansoori, T.R. Bastami, A. Ahmadpour and Z. Eshaghi, Environmental application of nanotechnology, in: G. Cao, C.J. Brinker (Eds.) Annual Review of Nano Research, Vol 2, World Scientific, Singapore, 2008.

[12] W.-x. Zhang, Nanoscale iron particles for environmental remediation: an overview, Journal of nanoparticle Research, 5 (2003) 323-332.

[13] X.-Q. Li, D.G. Brown and W. Zhang, Stabilization of biosolids with nanoscale zero-valent iron (nZVI), Journal of Nanoparticle Research, 9 (2007) 233-243.

[14] J. Chorover and X. Gao, Biomolecular complexation affects microbial adhesion to iron (oxyhydr) oxides, in: Proceedings of the 19th World Congress of Soil Science: Soil solutions for a changing world, Brisbane, Australia, 1-6 August 2010. Symposium 2.2. 1 Biogeochemical interfaces in soils, International Union of Soil Sciences (IUSS), c/o Institut für Bodenforschung, Universität für Bodenkultur, 2010, pp. 13-16.

[15] Z. Jin, Bioconjugated magnetic nanoparticles for rapid capture of gram-positive bacteria, Journal of Biosensors & Bioelectronics, (2012).

[16] J. Lukasik, Y.-F. Cheng, F. Lu, M. Tamplin and S.R. Farrah, Removal of microorganisms from water by columns containing sand coated with ferric and aluminum hydroxides, Water Res., 33 (1999) 769-777.

[17] M. Mukherjee and S. De, Reduction of microbial contamination from drinking water using an iron oxide nanoparticle-impregnated ultrafiltration mixed matrix membrane: preparation, characterization and antimicrobial properties, Environmental Science: Water Research & Technology, 1 (2015) 204-217.

[18] A. Omoike, J. Chorover, K.D. Kwon and J.D. Kubicki, Adhesion of bacterial exopolymers to α-FeOOH: Inner-sphere complexation of phosphodiester groups, Langmuir, 20 (2004) 11108-11114.

[19] S.J. Parikh and J. Chorover, ATR-FTIR spectroscopy reveals bond formation during bacterial adhesion to iron oxide, Langmuir, 22 (2006) 8492-8500.

[20] B. Li and B.E. Logan, Bacterial adhesion to glass and metal-oxide surfaces, Colloids and surfaces. B, Biointerfaces, 36 (2004) 81-90.

[21] C. Lee, J.Y. Kim, W.I. Lee, K.L. Nelson, J. Yoon and D.L. Sedlak, Bactericidal effect of zero-valent iron nanoparticles on *Escherichia coli*, Environ. Sci. Technol., 42 (2008) 4927-4933.

[22] M. Diao and M. Yao, Use of zero-valent iron nanoparticles in inactivating microbes, Water Res., 43 (2009) 5243-5251.

[23] M. Auffan, W. Achouak, J. Rose, M.-A. Roncato, C. Chanéac, D.T. Waite, A. Masion, J.C. Woicik, M.R. Wiesner and J.-Y. Bottero, Relation between the redox state of iron-based nanoparticles and their cytotoxicity toward *Escherichia coli*, Environ. Sci. Technol., 42 (2008) 6730-6735.

[24] J. Chen, Z. Xiu, G.V. Lowry and P.J. Alvarez, Effect of natural organic matter on toxicity and reactivity of nano-scale zero-valent iron, Water Res, 45 (2011) 1995-2001.

[25] E.N. Taylor and T.J. Webster, The use of superparamagnetic nanoparticles for prosthetic biofilm prevention, International Journal of Nanomedicine, 4 (2009) 145-152.

[26] A. Azam, A.S. Ahmed, M. Oves, M.S. Khan, S.S. Habib and A. Memic, Antimicrobial activity of metal oxide nanoparticles against Gram-positive and Gram-negative bacteria: a comparative study, International Journal of Nanomedicine, 7 (2012) 6003.

[27] L.S. Albert and D.G. Brown, Variation in bacterial bioenergetics during rapid changes in extracellular pH and implications for the activity of attached bacteria, Colloids Surf. B, doi:10.1016/j.colsurfb.2015.05.020 (2015).

[28] D.G. Brown and Y. Hong, Impact of the Charge-Regulated Nature of the Bacterial Cell Surface on the Activity of Adhered Cells, J. Adhesion Sci. Technol., 25 (2011) 2199-2218.

[29] Y. Hong and D.G. Brown, Alteration of bacterial surface electrostatic potential and pH upon adhesion to a solid surface and impacts to cellular bioenergetics, Biotechnol. Bioeng., 105 (2010) 965-972.

[30] Y. Hong and D.G. Brown, Variation in bacterial ATP level and proton motive force due to adhesion to a solid surface, Appl. Environ. Microbiol., 75 (2009) 2346-2353.

[31] P. Mitchell, Coupling of phosphorylation to electron and hydrogen transfer by a chemi-osmotic type of mechanism, Nature, 191 (1961).

[32] P. Mitchell, Chemiosmotic coupling in oxidative and photosynhetic phosphorylation, Biol. Rev., 41 (1966) 445-502.

[33] P. Mitchell, Possible molecular mechanisms of the protonmotive function of cytochrom systems, J. Theoret. Biol., 62 (1976) 327-367.

[34] M.T. Madigan, J.M. Martinko and J. Parker, Brock Biology of Microorganisms, Ninth ed., Prentice Hall, Upper Saddle River, NJ, 2000.

[35] Y. Hong and D.G. Brown, Electrostatic behavior of the charge-regulated bacterial cell surface, Langmuir, 24 (2008) 5003-5009.

[36] Y. Hong and D.G. Brown, Cell surface acid-base properties of *Escherichia coli* and *Bacillus brevis* and variation as a function of growth phase, nitrogen source and C:N ratio, Colloids Surf. B, 50 (2006) 112-119.

[37] J. Lyklema and J.F.L. Duval, Hetero-interaction between Guoy-Stern double layers: Charge and potential regulation, Adv. Coll. Interface Sci., (2005) 27-45.

[38] D.C. Prieve and E. Ruckenstein, Role of surface chemistry in particle deposition, J. Coll. Interface Sci., 60 (1977) 337-348.

[39] D.C. Prieve and E. Ruckenstein, The double-layer interaction between dissimilar ionizable surfaces and its effect on the rate of deposition, J. Coll. Interface Sci., 63 (1978) 317-329.

[40] D.C. Prieve and E. Ruckenstein, The surface potential of and double-layer interaction force between surfaces characterized by multiple ionizable groups, J. Theoret. Biol., 56 (1976) 205-228.

[41] S. Tseng, T.H. Hsieh, L.H. Yeh, N. Wang and J.P. Hsu, Electrophoresis of a charge-regulated soft sphere: importance of effective membrane charge, Colloids Surf. B, 102 (2013) 864-870.

[42] D. Jones, P.A. Pell and P.H.A. Sneath, Maintenance of bacteria on glass beads at -60°C to -76°C, in: B.E. Kirsop, A. Doyle (Eds.) Maintenance of microorganisms and cultured cells: A manual of laboratory methods, Academic Press, San Diego, 1991.

[43] J.E. Hobbie, R.J. Daley and S. Jasper, Use of nuclepore filters for counting bacteria by fluorescence microscopy, Appl. Environ. Microbiol., 33 (1977) 1225-1228.

[44] S.-B. Kim, S.-J. Park, C.-G. Lee, N.-C. Choi and D.-J. Kim, Bacteria transport through goethite-coated sand: Effects of solution pH and coated sand content, Colloids Surf. B, 63 (2008) 236-242.

[45] S.-B. Kim, S.-J. Park, C.-G. Lee and H.-C. Kim, Transport and retention ofEscherichia coliin a mixture of quartz, Al-coated and Fe-coated sands, Hydrological Processes, 22 (2008) 3856-3863.

[46] H.-U. Bergmeyer, Methods of Enzymatic Analysis, in, Academic Press, USA, 1965.

[47] G. Sposito, The Chemistry of Soils, Oxford University Press, New York, 1989.

[48] M. Kosmulski, The pH-dependent surface charging and points of zero charge: V. Update, J. Coll. Interface Sci., 353 (2011) 1-15.

[49] E.R. Kashket, Stoichiometry of the H+-ATPase of growing and resting, aerobic Escherichia coli, Biochem., 26 (1982) 5534-5538.

[50] P.C. Maloney and F.C. Hansen III, Stoichiometry of proton movements coupled to ATP synthesis driven by a pH gradient in *Streptococcus lactis*, J. Membrane Biol., 66 (1982) 63-75.

[51] D.S. Perlin, M.J.D. San Fransisco, C.W. Slayman and B.P. Rosen, H+/ATP stoichiometry of proton pumps from Neurospora crassa and Escherichia coli, Arch. Biochem. Biophys., 248 (1986) 53-61.

[52] R. Vink, M.R. Bendall, S.J. Simpson and P.J. Rogers, Estimation of H+ to adenosine 5'-triphosphate stoichiometry of Escherichia coli ATP synthase using 31P NMR, Biochem., 23 (1984) 3667-3675.

[53] J.J. Tomashek and W.S.A. Brusilow, Stoichiometry of energy coupling by proton-translocating ATPases: A history of variability, J. Bioenerg. Biomembr., 32 (2000) 493-500.

[54] C.W. Jones, Membrane-associated energy conservation in bacteria: a general introduction, in: C. Anthony (Ed.) Bacterial Energy Transduction, Academic Press, New York, 1988.

[55] W.J. Ball, Jr. and D.E. Atkinston, Adenylate energy charge in Saccharomyces cerevisiae during starvation, J. Bacteriol., 121 (1975) 975-982.

[56] D.N. Dietzler, C.J. Lais and M.P. Leckie, Simultaneous increases of the adenylate energy charge and the rate of glycogen synthesis in nitrogen-starved Escherichia coli W4597, Arch. Biochem. Biophys., 160 (1974) 14-25.

[57] C. Petersen and L.B. Møller, Invariance of the nucleoside triphosphate pools of Escherichia coli with growth rate, J. Biol. Chem., 275 (2000) 3931-3935.

[58] D.E. Atkinson and G.M. Walton, Adenosine triphosphate conservation in metabolic regulation - Rat liver citrate cleavage enzyme, J. Biol. Chem., 242 (1967) 3239-3241.

[59] D.E. Atkinson, The energy charge of the adenylate pool as a regulatory parameter. Interaction with feedback modifiers, Biochem., 7 (1968) 4030-4034.

[60] F.S. Markland and C.L. Wadkins, Adenosine Triphosphate-Adenosine 5'-Monophosphate Phosphotransferase of Bovine Liver Mitochondria: II. General kinetic and structural properties J. Biol. Chem., 241 (1966) 4136-4145.

[61] A.G. Chapman, L. Fall and D.E. Atkinson, Adenylate energy charge in *Escherichia coli* during growth and starvation, J. Bacteriol., 108 (1971) 1072-1086.

[62] G.H. Fynn and J.A. Davison, Adenine nucleotide pool and energy charge during growth of a tyrothricin-producing strain of Bacillus brevis, J. Gen. Microbiol., 94 (1976) 68-74.

[63] A. Kahru and R. Vilu, On characterization of the growth of Escherichia coli in batch culture, Arch. Microbiol., 135 (1983) 12-15.

[64] E.R. Kashket, Effects of aerobiosis and nitrogen source on the proton motive force in growing Escherichia coli and Klebsiells pheumoniae cells, J. Bacteriol., 146 (1981) 377-385.

[65] D. White, The physiology and biochemistry of prokaryotes, Oxford University Press, New York, 2000.

[66] D.G. Nicholls and S.J. Ferguson, Bioenergetics 3, Academic Press, London, 2002.

[67] B.W. Ninham and V.A. Parsegian, Electrostatic potential between surfaces bearing ioniable groups in ionic equilibrium with physiologic saline solution, J. Theoret. Biol., 31 (1971) 405-428.

[68] D. Chan, J.W. Perram, L.R. White and T.W. Healy, Regulation of surface potential at amphoteric surfaces during particle-particle interaction, J. Chem. Soc., Faraday Trans. I, 71 (1975) 1046-1057.

[69] T.W. Healy, D. Chan and L.R. White, Colloidal behaviour of materials with ionizable group surfaces, Pure Appl. Chem., 52 (1980) 1207-1219.

[70] J.-P. Hsu and Y.-C. Kuo, The electrostatic interaction force between a charge-regulated particle and a rigid surface, J. Coll. Interface Sci., 183 (1996) 194-198.

[71] J.F.L. Duval, H.J. Busscher, B. van de Belt-Gritter, H.C. van der Mei and W. Norde, Analysis of the interfacial properties of fibrillated and nonfibrillated oral Streptococcal strains from electrophoretic mobility and titration measurements: Evidence for the shortcomings of the 'classical soft-particle approach', Langmuir, 21 (2005) 11268-11282.

[72] J.F.L. Duval and H. Ohshima, Electrophoresis of diffuse soft particles, Langmuir, 22 (2006) 3533-3546.

[73] H. Ohshima, Electrophoretic mobility of soft particles, Coll. Surf. A, 103 (1995) 249-255.

[74] Y.A. Gorby, S. Yanina, J.S. McLean, K.M. Rosso, D. Moyles, A. Dohnalkova, T.J. Beveridge, I.S. Chang, B.H. Kim, K.S. Kim, D.E. Culley, S.B. Reed, M.F. Romine, D.A. Saffarini, E.A. Hill, L. Shi, D.A. Elias, D.W. Kennedy, G. Pinchuk, K. Watanabe, S.i. Ishii, B. Logan, K.H. Nealson and J.K. Fredrickson, Electrically conductive bacterial nanowires produced by *Shewanella oneidensis* strain MR-1 and other microorganisms, Proc. Nat. Acad. Sci. USA, 103 (2006) 11358-11363.

[75] J.A. Gralnick and D.K. Newman, Extracellular respiration, Molecular microbiology, 65 (2007) 1-11.

[76] D.R. Lovley, Extracellular electron transfer: wires, capacitors, iron lungs, and more, Geobiology, 6 (2008) 225-231.

[77] G. Reguera, K.D. McCarthy, T. Mehta, J.S. Nicoll, M.T. Tuominen and D.R. Lovley, Extracellular electron transfer via microbial nanowires, Nature, 435 (2005) 1098-1101.

[78] Y. Yang, M. Xu, J. Guo and G. Sun, Bacterial extracellular electron transfer in bioelectrochemical systems, Process Biochemistry, 47 (2012) 1707-1714.

[79] L. Cen, K.G. Neoh and E.T. Kang, Surface functionalization technique for conferring antibacterial properties to polymeric and cellulosic surfaces, Langmuir, 19 (2003) 10295-10303.

[80] R. Kügler, O. Bouloussa and F. Rondelez, Evidence of a charge-density threshold for optimum efficiency of biocidal cationic surfaces, Microbiology, 151 (2005) 1341-1348.

[81] A. Terada, A. Yuasa, T. Kushimoto, S. Tsuneda, A. Katakai and M. Tamada, Bacterial adhesion to and viability on positively charged polymer surfaces, Microbiology, 152 (2006) 3575-3583.

[82] L. Ponsonnet, M. Boureanu, N. Jaffrezic, A. Othmane, C. Dorel and P. Lejeune, Local pH variation as an initial step in bacterial surface-sensing and biofilm formation, Materials Science and Engineering: C, 28 (2008) 896-900.

[83] S.-I. Nakayama and H. Watanabe, Involvement of *cpxA*, a sensor of a two-component regulatory system, in the pH-dependent regulaton of expression of *Shigella sonnei virF* gene, J. Bacteriol., 117 (1995) 5062-5069.

[84] D.L. Hung, T.L. Raivio, C.H. Jones, T.J. Silhavy and S.J. Hultgren, Cpx signaling pathway monitors biogenesis and affects assembly and expression of P pili, The EMBO Journal, 20 (2001) 1508-1518.

[85] W.R. Schwan, Osmolarity and pH Growth Conditions Regulate fim Gene Transcription and Type 1 Pilus Expression in Uropathogenic Escherichia coli, Infection and Immunity, 70 (2002) 1391-1402.

[86] C. Prigent-Combaret, O. Vidal, C. Dorel and P. Lejeune, Abiotic surface sensing and biofilm-depeendent regulation of gene expression in Escherichia coli, J. Bacteriol., 181 (1999) 5993-6002.

[87] J.M. Wood, Osmosensing by bacteria: Signals and membrane-based sensors, Microbiol. Molec. Biol. Rev., 63 (1999) 230-262.

[88] Q. Ma and T.K. Wood, OmpA influences Escherichia coli biofilm formation by repressing cellulose production through the CpxRA two-component system, Environmental microbiology, 11 (2009) 2735-2746.

[89] M.A. Kemper, M.M. Urrutia, T.J. Beveridge, A.L. Koch and R.J. Doyle, Proton motive force may regulate cell wall-associated enzymes of Bacillus subtilis, J. Bacteriol., 175 (1993) 5690-5696.

[90] I. Pastan and R. Perlman, Cyclic adenosine monophosphate in bacteria, Science, 169 (1970) 339-344.

Chapter 4

Examination of attachment-induced intracellular ATP variations in both Gram-positive and Gram-negative bacteria using surfaces spanning a range of surface charge functionality.

Chapter 4 Examination of attachment induced intracellular ATP variations in both Gram-positive and Gram-negative bacteria using surfaces spanning a range of surface charge functionality.

4.1 Introduction

Microbial attachment to surfaces plays a critical role in many natural and artificial systems. In any given system, it is characteristic of bacteria to naturally adhere to surfaces. This inclination of bacteria for adhesion is the initial step towards surface colonization and biofilm development which is beneficial in some systems and detrimental in other systems [1-6]. In general, the initial step of biofilm formation is the adhesion of the microorganism to the surface by interactions that are governed by the surface charge and the hydrophobicity of the bacterial and adhering surfaces [7]. Bacterial adhesion to a solid surface can influence various bacterial processes. Of particular interest is the effect of adhesion on the metabolic activity of bacteria which can be either elevated or suppressed, depending on the surface properties of the adhering surfaces. Many studies have focused on identifying surfaces that enhance or inhibit microbial metabolic activity and the reasons for these effects are were ambiguous [8-14] until Hong and Brown developed a hypothesis explaining the underlying mechanism [17]. The same hypothesis is applied here to explore the effect of various surfaces with different functional groups, spanning a range of iso-electric points (IEP's) on the metabolic activity of bacteria. Our findings will facilitate better selection of surfaces for different applications. The hypothesis driving our study indicates a relationship between physiochemical charge regulation that occurs during

bacterial adhesion [15-17] and cellular bioenergetics which centers on energy coupling between catabolic processes and anabolic processes in a living bacterial cell.

4.2 Charge Regulation

The bacterial cell surface contains acidic and basic functional groups like carboxylic, phosphoric, hydroxyl and amine groups [18-20]. As the separation distance between a bacterium and solid surface decrease, there is a variation in the surface charge and potential via the charge regulation effect [17]. The charge regulated nature of the cell surface depends on the type and quantity of functional groups on the bacterial and solid surfaces [21-24]. The degree of ionization of the various functional groups is dependent on the local pH [25, 26]. Adhesion results in a variation in the local pH between the surfaces as a result of electro neutrality. This shift in local pH can directly impact the cellular metabolic activity levels via the proton motive force. The charge-regulation effect is modeled using the Poisson-Boltzmann equation that describes the electrostatic potential as a function of distance from the charged surface. The Poisson-Boltzmann equation can be written as

$$\frac{d^2\psi}{dx^2} = -\frac{1}{\varepsilon_o \varepsilon}\sum_i n_{ri} \cdot z_i \cdot e \cdot \exp\left(\frac{-z_i e\psi}{kT}\right) \qquad (1)$$

Here ψ is the electrostatic potential, ε_o is the permittivity of the vacuum, ε is the dielectric constant of the medium, e is the electron charge, k is the Boltzmann constant, and T is the temperature.

The boundary conditions for the two surfaces are based on Gauss's Law, where the change in potential at the surface is related to the surface charge:

$$\left.\frac{d\psi}{dx}\right|_{surface} = -\frac{1}{\varepsilon_o \varepsilon}\sigma \tag{2}$$

Taking into account the acidic and basic functional groups on the surface, the net surface charge of the cell can be obtained by adding the individual functional groups possessing the positive and negative surface charges:

$$\frac{\sigma}{e} = \sum_j [R_{bj}H^+] - \sum_i [R_{ai}^-] \tag{3}$$

where σ is the surface charge per unit area of the surface, R_{ai} and R_{bj} are the acidic ionizable sites of type i, and the basic ionizable sites of type j. R_{ai} and R_{bj} can be represented as a function of surface pH and their site densities (N_{ai} and N_{bj}). In this case, Equations 2 and 3 lead to the following boundary conditions:

$$\left.\frac{d\psi}{dx}\right|_{surface} = -\frac{e}{\varepsilon_o \varepsilon}\cdot\left\{\sum_j\left[\frac{[H^+]N_{bj}}{[H^+]+K_{bj}\exp\left(\frac{e\psi_s}{kT}\right)}\right] - \sum_i\left[\frac{K_{ai}N_{ai}}{K_{ai}+[H^+]\exp\left(\frac{-e\psi_s}{kT}\right)}\right]\right\} \tag{4}$$

Here, K_{ai} and K_{bj} are the dissociation constants associated with the different acidic and basic functional groups, respectively. Using Equations 1 and 4, the surface charge and surface pH can be modeled as a bacterial cell approaches a surface.

4.3 Bioenergetics

The chemiosmotic theory of Mitchell states that the proton motive force generated during catabolism directly controls the generation of adenosine triphosphate (ATP, which is the energy currency of the cell). The pumping of protons across the cytoplasmic membrane as electrons move down a series of membrane proteins establishes a charge and pH gradient exterior to the membrane. The gradients together constitute the proton motive force that can be represented by the Nernst equation which is expressed as [27,28].

$$\Delta p = \Delta\psi - \frac{2.3RT}{F}\Delta pH \tag{5}$$

The protons are allowed to reenter the bacterial protoplasm through the ATP synthase complex generating an ATP molecule from cytoplasmic ADP and inorganic phosphate for every 2-4 protons. This process is thermodynamically reversible and can aid the generation of ATP via proton entry through ATP synthase or ATP depletion via proton exit through the same ATP synthase. The thermodynamic relationship between Δp and the formation of ATP is expressed as

$$\Delta p = -\frac{\Delta G_p}{nF} = -\frac{1}{nF}\left[\Delta G^o + 2.303RT\log\left(\frac{[ATP]}{[ADP][P_i]}\right)\right] \tag{6}$$

where F is the Faraday constant, n is the number of protons translocated per ATP molecule synthesized, ΔG_p is the phosphorylation potential and [ATP], [ADP], [P_i] are the cellular concentrations of adenosine triphosphate, adenosine diphosphate and

phosphate respectively. The ATP synthase enzyme is reversible in function, and thus an increase in the Δp will result in an enhanced cellular ATP response and a decrease in the Δp will cause a decline in the cellular ATP.

The shift in pH between the two surfaces as a result of the charge regulation process can influence the cellular bioenergetics by providing a proton rich or proton deficit environment. The bacterial surface typically possesses a net negative charge and the pH at the surface is a function of the solid surface functional properties, pH and ionic strength. A decrease in local pH can cause protons to enter the bacterial cell miming that which takes place during chemiosmosis. Thus the ATP concentration within the cell increases and this can encourage bacterial growth and colonization. An increase in pH at the membrane would result in ATP depletion within the cell and thereby decreasing the overall metabolic activity level of cells as result, growth and survival of bacteria may be compromised.

In Chapter 2 we demonstrated that cellular ATP concentration is a function of bacterial surface pH [29]. Following which, in Chapter 3 we demonstrated that adhesion of *E.coli* to a negative and positive surface resulted in an increase and decrease in energy levels as predicted by the governing hypothesis. In this study we explored the effect of a range of acidic and basic surfaces that can induce a wide spectrum of bacterial surface pH conditions during adhesion. The investigation focused on understanding how Gram positive and Gram negative bacteria may respond during attachment to surfaces that span a range of surface functionality, resulting in a varied bacterial surface pH similar to that tested by artificial

manipulation of the bulk pH at the point of adhesion in Chapter 2. We have examined the metabolic response of *E. coli* and *B. subtilis* upon these pH variations induced by charge regulation. As a result of the charge regulation effect between surfaces during attachment, a negativel-charged surface will cause a decline in surface pH impacting the proton gradient. Thus protons can enter the cell at the expense of the generated gradient, resulting in an increase in cellular ATP levels. Alternatively, attachment to a positive surface can increase the surface pH of bacteria resulting in ATP depletion, thus resulting in compromised growth and survival of adhered species. We also anticipated the metabolic response of attached bacteria to be a function of the solid surface functionality.

The hypothesis was explored by identifying and characterizing surfaces with different surface potentials to observe varied metabolic response of adhered bacteria. Following characterization, adhesion experiments were performed to study the effect of surface functional groups on the metabolic activity of bacteria by measuring ATP concentrations.

Experiments were conducted using soda lime glass beads, silica sand, iron hydroxide modified sand, aluminum hydroxide modified sand, feldspar and olivine. Surface modification of glass beads was also successfully performed and the coated glass beads were used for preliminary experiments (Appendix C). Feldspar is one of the most abundant elements found in nature that also serves as a raw material in the manufacture of ceramics and glass. Olivine is a common subsurface mineral associated usually with igneous rocks.

4.4 Materials and Methods

4.4.1 Bacterial Culture

Gram-negative *Escherichia coli* K-12 (ATCC29181) and Gram-positive *Bacillus subtilis* (ATCC23059) were used in this study. Both bacteria were grown in 500 ml of Luria Bertini Broth (LB broth, Fisher Scientific) and stored using the glass bead procedure [38] at -80°C to serve as inoculum for the experiments. In preparation for each experiment, bacteria were cultivated in 500 ml LB broth at 30°C for 20 hr. The bacteria were washed twice by centrifuging for 15 min at 3500×g using phosphate buffer solution solution (PBS, 0.258 g KH_2PO_4 and 0.470 g K_2HPO_4 in 1 L of deionized water with the pH adjusted to 7.2 using 1 M NaOH). After the cultures were incubated for 48 hours they were washed one last time and diluted to a concentration of approximately 10^8 cells, determined via acridine orange direct counts.

4.42 Granular Surface preparation

The different surfaces used in the adhesion experiments were prepared individually. Soda lime glass beads were soaked in 1 M HCl for 12 hr and washed under running tap water for an hour. The beads were then washed for 10 min with deionized water and dried in the oven overnight at 60°C.

Silica sand was washed in deionized water and dried overnight in an oven at 105°C. 200 g was used directly for experiments while separate 200 g batches were coated with iron and aluminum hydroxide based on the method described by Kim et al [30,31]. The method included treating 200 g of sand with 100 mL of either 0.2 M

ferric chloride or 0.2 M aluminum chloride solution ($FeCl_3.6H_20$ and $AlCl_3.6H_20$). Ferric hydroxide (goethite) and aluminum hydroxide were precipitated in the solution by increasing the pH to ~7.5 using 6 M NaOH. The sand was mixed in a shaker at 60°C for 12 hr after which it was dried in the oven for 24 hr at 105°C. The coated sand was then washed using deionized water a minimum of five times, dried in the oven at 105°C for 48 hr and stored in centrifuge tubes until used.

Feldspar and Olivine were washed in deionized water and dried at 60°C in an oven overnight. The minerals were stored in poly propylene containers.

4.4.3 Surface Characterization

The surfaces were observed using SEM and surface elemental mapping was performed using Energy Dispersive X-ray Analysis to confirm coating on the sand. The zeta potential of the bacterial and solid surfaces was measured by titrating across a range of pH values using a Nano Zetasizer ZS (Malvern). For these titrations, the bacterial suspension was washed and resuspended in 10 mM NaCl and fines from the solid surfaces were obtained during the washing procedure and suspended in 10 mM NaCl. Fines for glass beads were obtained by crushing with a mortar and pestle.

4.4.4 Experimental Method

Adhesion experiments were performed by adding 2 g of the surface of interest into and 4 ml of the bacterial suspension into 10 mL round bottomed glass vials. The vials were placed on an Orbitron shaker at 25 RPM and maintained at 30°C. Vials were removed at specific times up to 120 hr for determining bacterial planktonic counts and cellular

ATP concentrations. ATP was extracted from the sample by introducing the vials in boiling water for 3.5 min followed by snap cooling in an ice bucket for 1 min. One mL of the sample was collected from each vial and stored at -20°C. The samples were assayed using the Luciferase-Luciferin solution in the following manner.

4.4.5 Cellular ATP Analysis

ATP concentrations in each vial was determined according to Hong and Brown [17] using a Sirius Luminometer (Titertek-Berthold) and a freshly prepared Luciferin-Luciferase solution. Luciferase solution was prepared in 25 μL aliquots by adding 1 mL of Tris buffer (20 mM Tris and 2 mM EDTA, adjusted to a pH of 7.75) to 1 mg of Luciferase (Sigma) and stored at -20°C. Ten mL of Tris Albumin buffer (20 mM Tris, 2 mM EDTA, 150 mM magnesium acetate, 50 μM dithiothreitol and 1 g bovine serum albumin adjusted to a pH of 7.75) was added to 1 mg of Luciferin (Sigma) and gently mixed with a Luciferase aliquot. The freshly prepared Luciferin-Luciferase solution was incubated at room temperature for 30 min before performing the ATP analysis.

The frozen ATP extract samples were thawed to room temperature using a thermomixer and 100 μL of the bacterial ATP sample was added into a luminometer tube containing 200 μL of Tris Mg^{2+}. The contents of the tube were mixed thoroughly for 15 sec using a vortex mixer. The tube was then placed in the luminometer which was set to automatically inject 100 μL of the Luciferin-Luciferase solution into the sample. The ATP concentration in the vial was obtained in the form of Relative Light

Units (RLU) and was converted to molar ATP concentrations using standard curves with ATP standard solutions (Sigma).

4.5 Results and Discussion

4.5.1 Microscopy of surfaces

Scanning electron microscopy (SEM) was used to study the morphology of surfaces (Figure 4.1) and Energy Dispersive X-ray Analysis patterns (Figure 4.2 and 4.3) and mapping provided compositional information of the minerals and confirmed the presence of coating for modified sand. Figures 4.4 and 4.5 show the elemental mapping of the sand to confirm coating of iron hydroxide (goethite) and aluminum hydroxide on the sand.

4.5.2 Surface Characterization

The zeta potential values across a range of pH for the bacteria and the solid surfaces are presented in Figure 4.6 and Figure 4.7. *E. coli* and *B. subtilis* had an isoelectric point (IEP) of near 2.5 and possessed a net negative surface charge in the pH range of most natural habitats. Sand and glass were shown to have an IEP of ~2 while iron and aluminum hydroxide had an IEP of ~8 and ~9.1, respectively. The IEP of feldspar was determined to be ~3.5. These values are in agreement with data in the literature [18,30-34]. The zeta potential results were used to obtain the pK (pK = -lot(K)) and N values that best represent the pH-dependent charge properties of the surfaces. Zeta potential measurements performed for olivine showed fluctuations over time as reported in literature [35, 36] hence data was obtained from literature for reference and

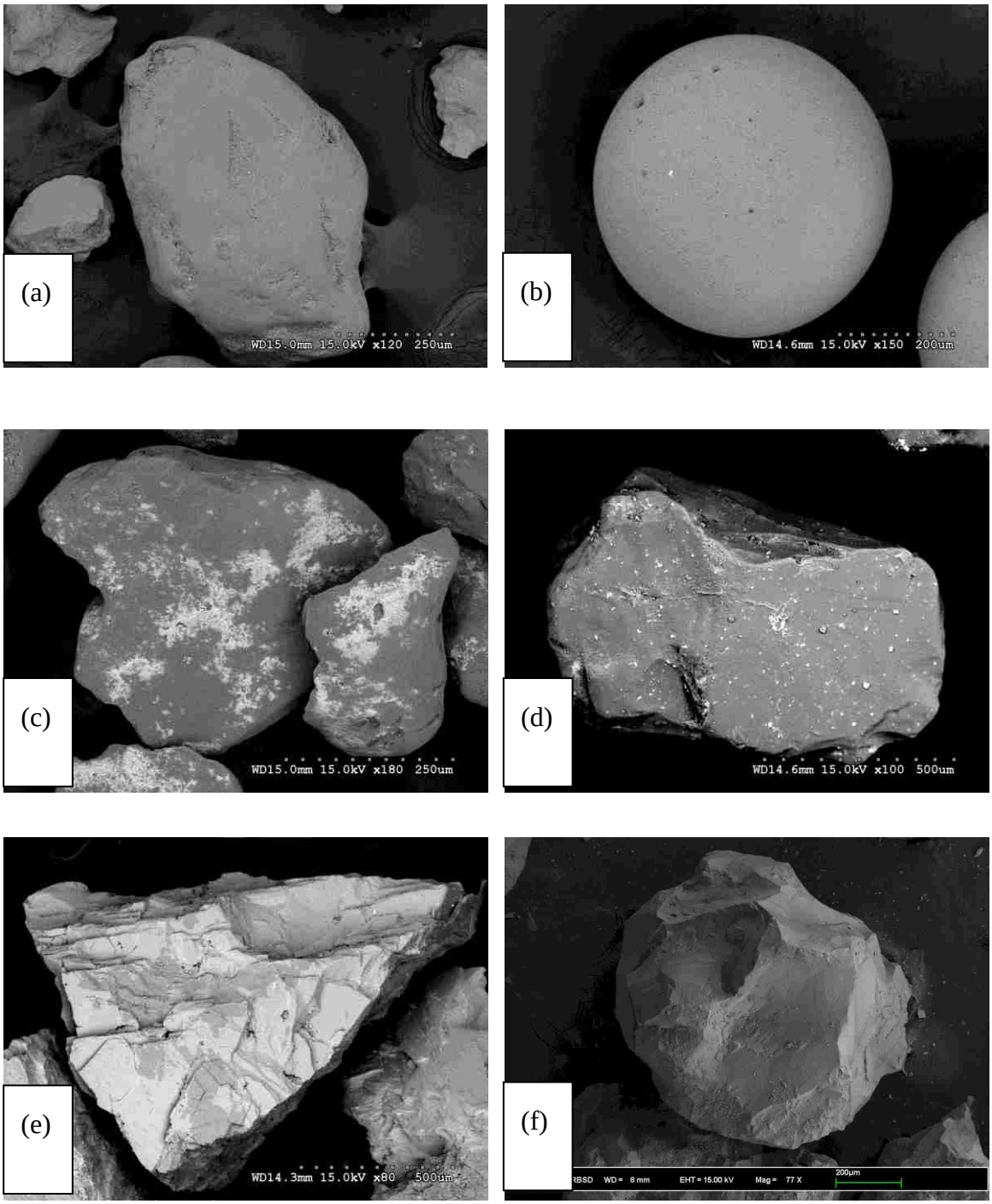

Figure 4.1 – SEM Images of the surfaces used in adhesion experiments. (a)) plain sand; (b) soda-lime glass bead; (c) Iron hydroxide coated sand; (d) Aluminum hydroxide coated sand; (e) Feldspar; (f) Olivine.

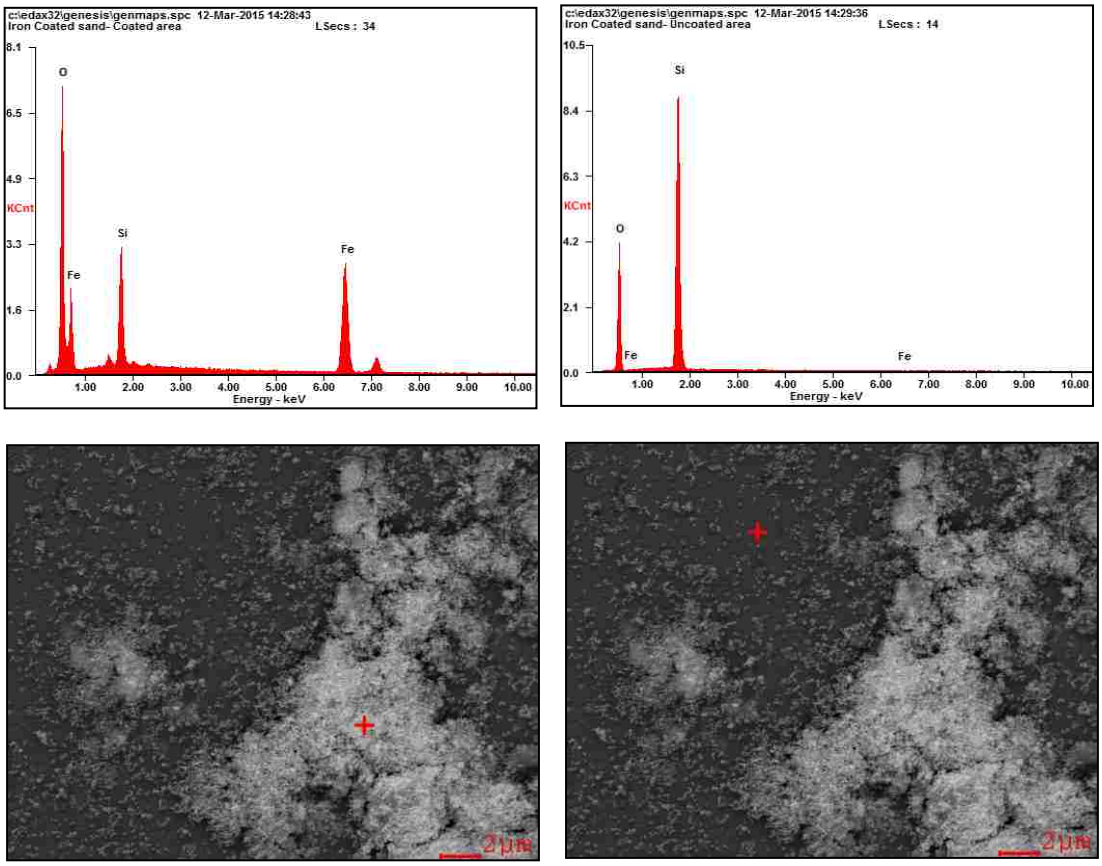

(a) (b)

Figure 4.2 - EDS patterns of the iron hydroxide coated sand showing the presence (a) and absence (b) presence of coating at the designated point.

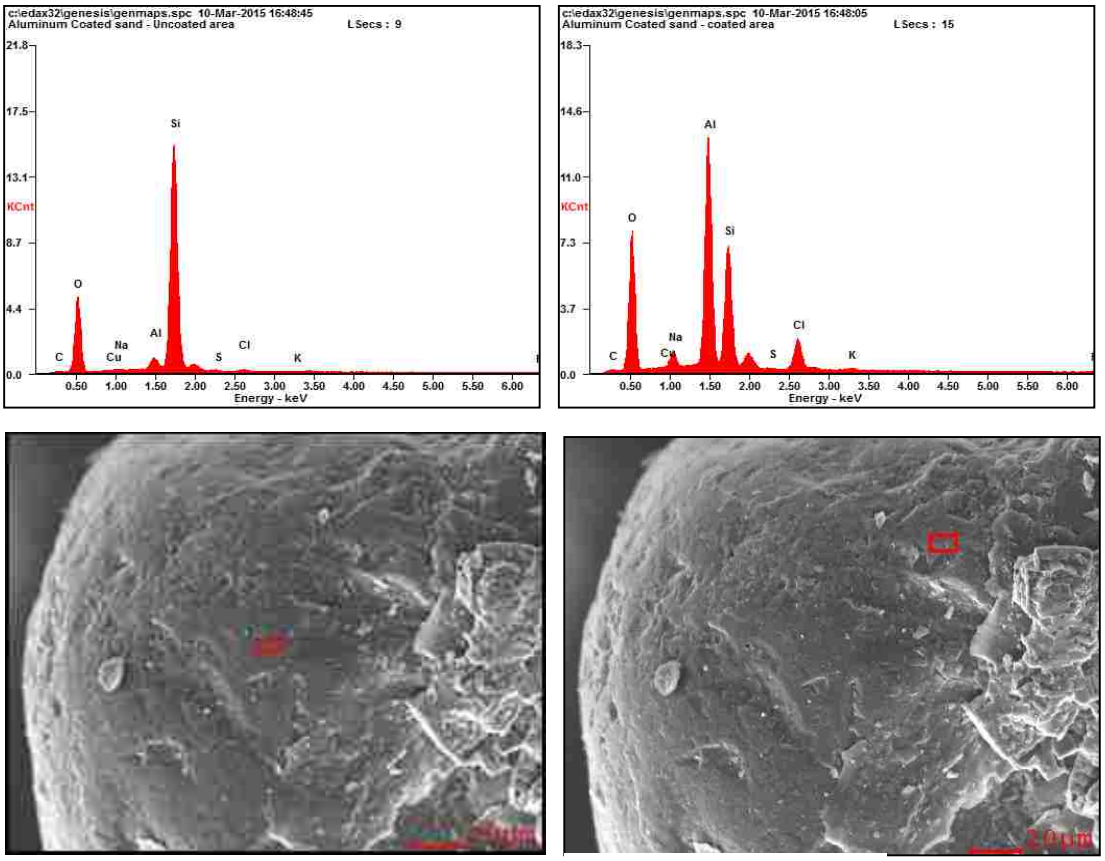

(a) (b)

Figure 4.3 - EDS patterns of the aluminum hydroxide coated sand showing the presence (a) and absence (b) presence of coating at the designated point.

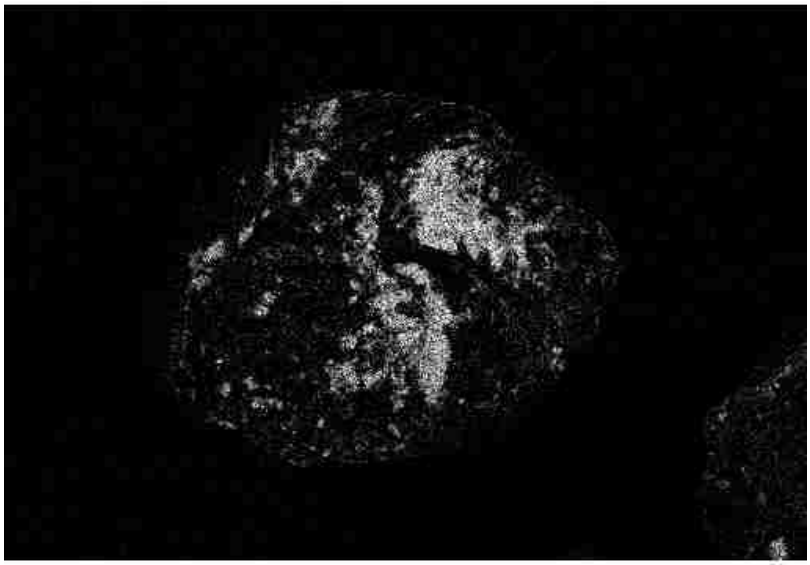

Fe Ka1

Figure 4.4 - An elemental map delineating the presence of iron hydroxide coating on the sand particle is shown above. (Top) SEM image of the iron hydroxide coated sand grain; (Bottom) Image denoting the presence of iron hydroxide on the sand grain.

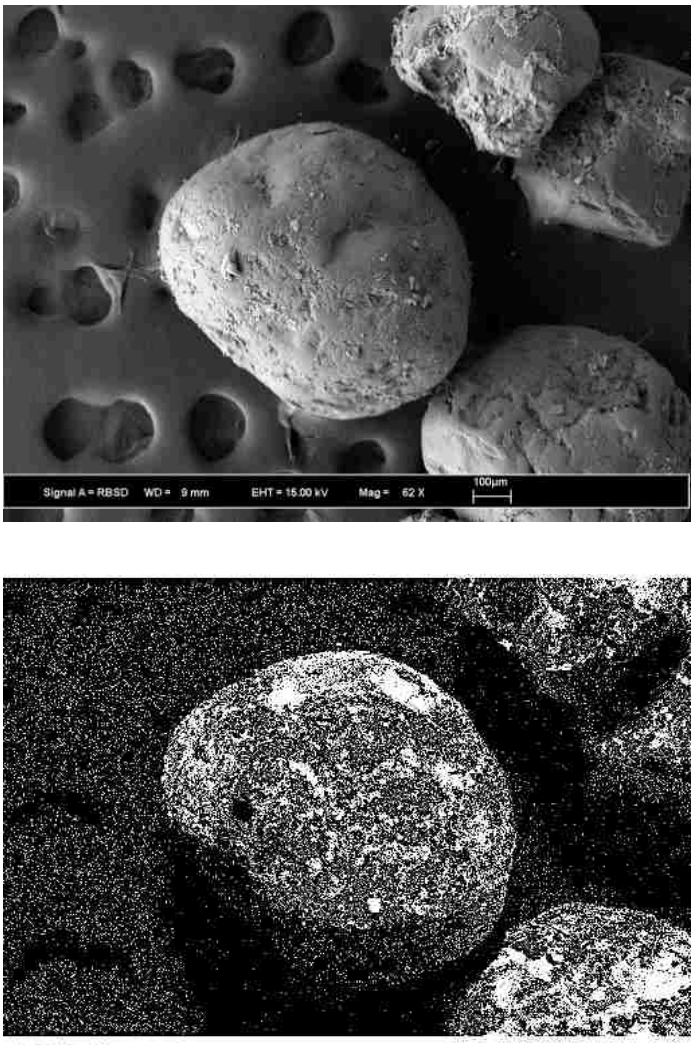

Figure 4.5 - An elemental map delineating the presence of aluminum hydroxide coating on the sand particle is shown above. (Top) SEM image of the aluminum hydroxide coated sand grain; (Bottom) Image denoting the presence of aluminum hydroxide on the sand grain.

not used for modelling purposes [37]. Olivine has been reported to possess a net positive charge across a pH of 2-11. Based on the results glass, sand and feldspar have a net negative charge at neutral pH while iron hydroxide coated sand, aluminum hydroxide coated sand and olivine have a net positive charge at neutral pH.

4.5.3 Bacterial Adhesion

An analysis of the percentage of attached cells for each surface is depicted in Figure 4.8 for *E.coli* and Figure 4.9 for *B. subtilis.* The percentage of attachment varied between surfaces and was highest for the positively-charged surfaces and significantly lesser attachment was observed with the negatively-charged surfaces. The number of planktonic cells in the control vials without surface for attachment remained relatively constant. It was observed that *E.coli* showed a varied degree of attachment with the different surfaces studied, with less than 60% attachment on negative surfaces and greater than 75% of adhesion on positively-charged surfaces. When compared to the *B. subtilis, E.coli* showed a greater degree of variation across the surfaces. *B. subtilis* showed >85% adhesion with all the positively-charged surfaces and ~20% of adhesion with negatively-charged surfaces.

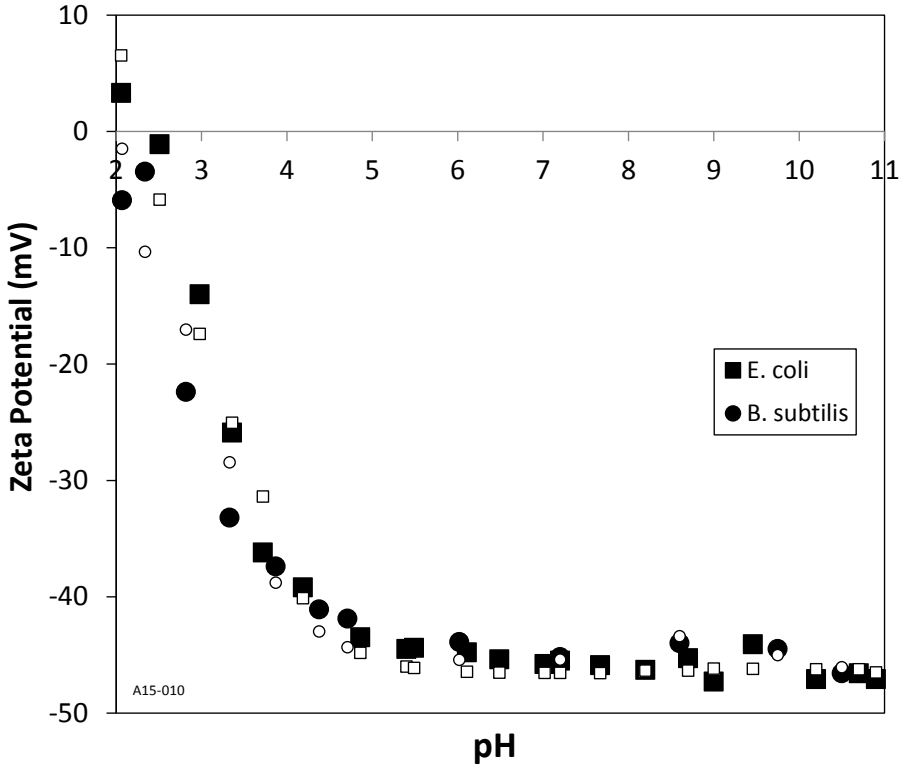

Figure 4.6 - This figure depicts the zeta potential values of *E.coli* and *B. subtilis* obtained experimentally (solid symbols) and that determined via modelling (hollow symbols). Both bacteria were identified to have an IEP of ~2.5.

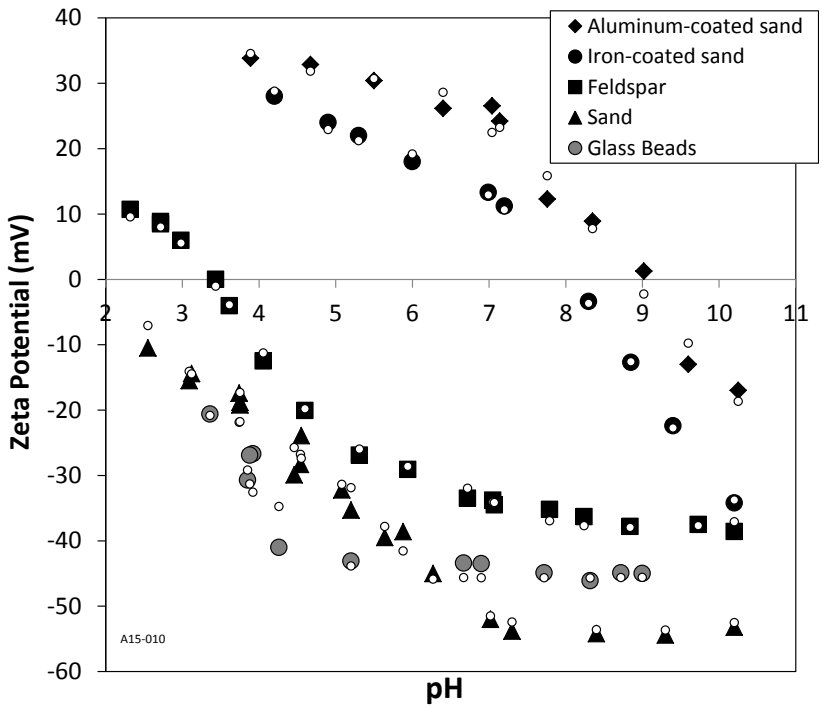

Figure 4.7 - This figure demonstrates the zeta potential measurements (solid symbols) of the different surfaces employed in our experiments. Glass and Sand were observed to have an IEP of ~2; feldspar had an IEP of ~ 3.4. iron hydroxide and aluminum hydroxide had IEPs of ~8.1 and ~9.0 respectively. The model fits (hollow symbols) obtained from pK and N values accurately describes the surface electrostatic properties**.**

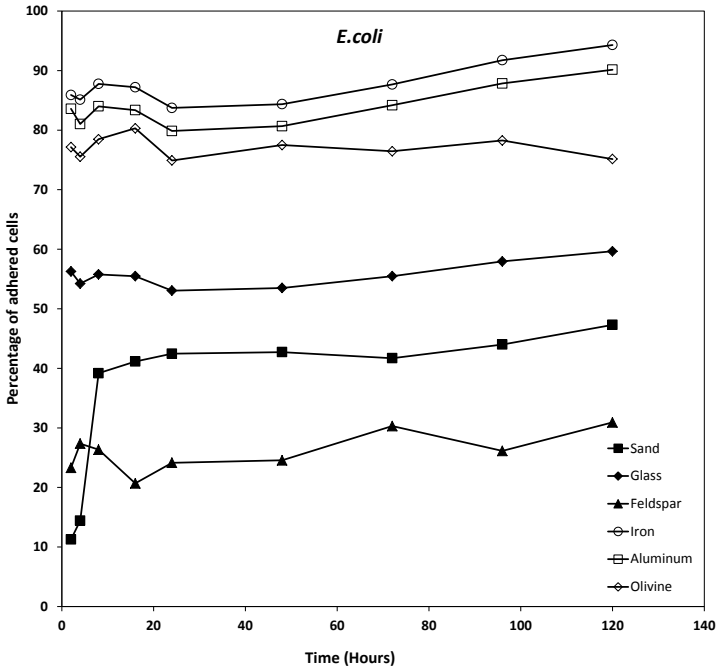

Figure 4.8 – The percentage of adhesion of *E.coli* to the different surfaces used in the adhesion experiments. Overall trends show a greater percentage of attachment with the positively-charged surfaces (adhesion >75%) when compared to the negatively-charged surfaces (adhesion < 60%).

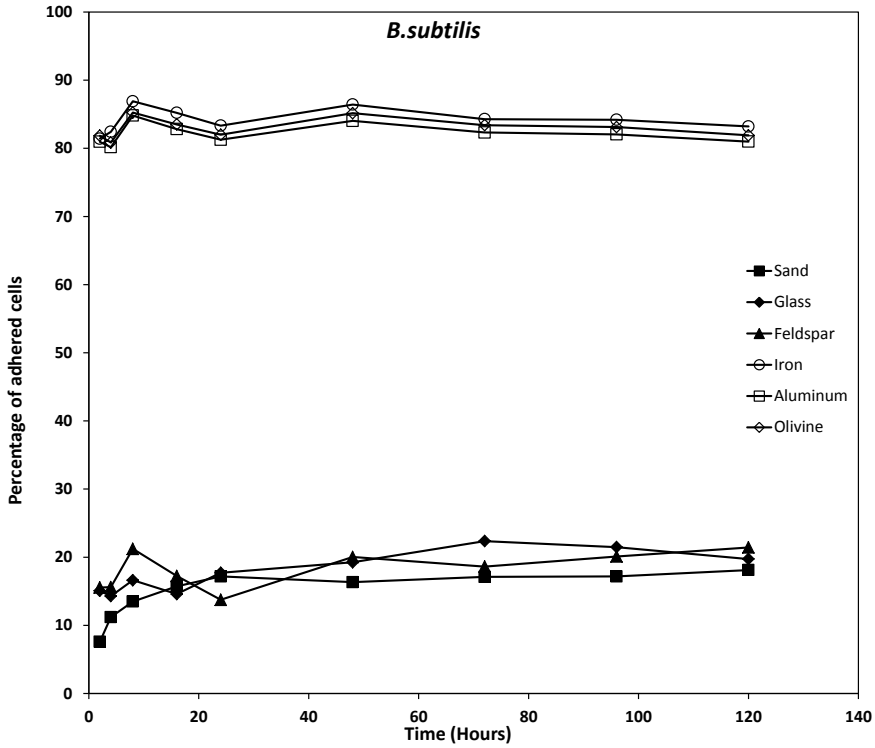

Figure 4.9 – The percentage of adhesion of *B.subtilis* to the different surfaces used in the adhesion experiments. Overall trends show a greater percentage of attachment with the positively-charged surfaces (adhesion of ~85%) when compared to the negatively-charged surfaces (adhesion of ~20%).

4.5.4 Bacterial Energetics

The hypothesis predicts that a variation in surface pH via charge regulation will have a corresponding impact on cellular bioenergetics upon bacterial attachment. A drop in surface pH will result in an enhanced ATP response while an increase in surface pH will result in decreased ATP concentrations.

The total ATP levels per vial for both bacteria are presented in Figure 4.10 and Figure 4.11 indicating a varied response with attachment to different surfaces. Experimental results showed that the total ATP per vial with no surface was fairly constant throughout the course of the experiment. The total ATP of vials containing the acidic sand, glass and feldspar surfaces increased over time and remained higher than the total ATP values in vials without any surface for attachment throughout the length of the experiment. A rapid increase in total ATP per vial was observed for the first 48 hours with glass and sand as expected, after which a gradual decline was observed. Vials containing feldspar also showed an enhanced ATP response which stayed fairly stable after 24 hours. Feldspar showed a less pronounced increase in ATP when compared to glass and sand, owing to its less acidic IEP of ~3.5.

On the other hand; the vials with iron hydroxide coated sand and olivine demonstrated a pronounced decline in cellular ATP values over the first 24 hour period after which a gradual decline was observed. With *E.coli*, the aluminum hydroxide coated sand exhibited ATP values much lower than the plain sand but very similar to the planktonic cells, likely indicating the proportion of sand surface that may have been coated.

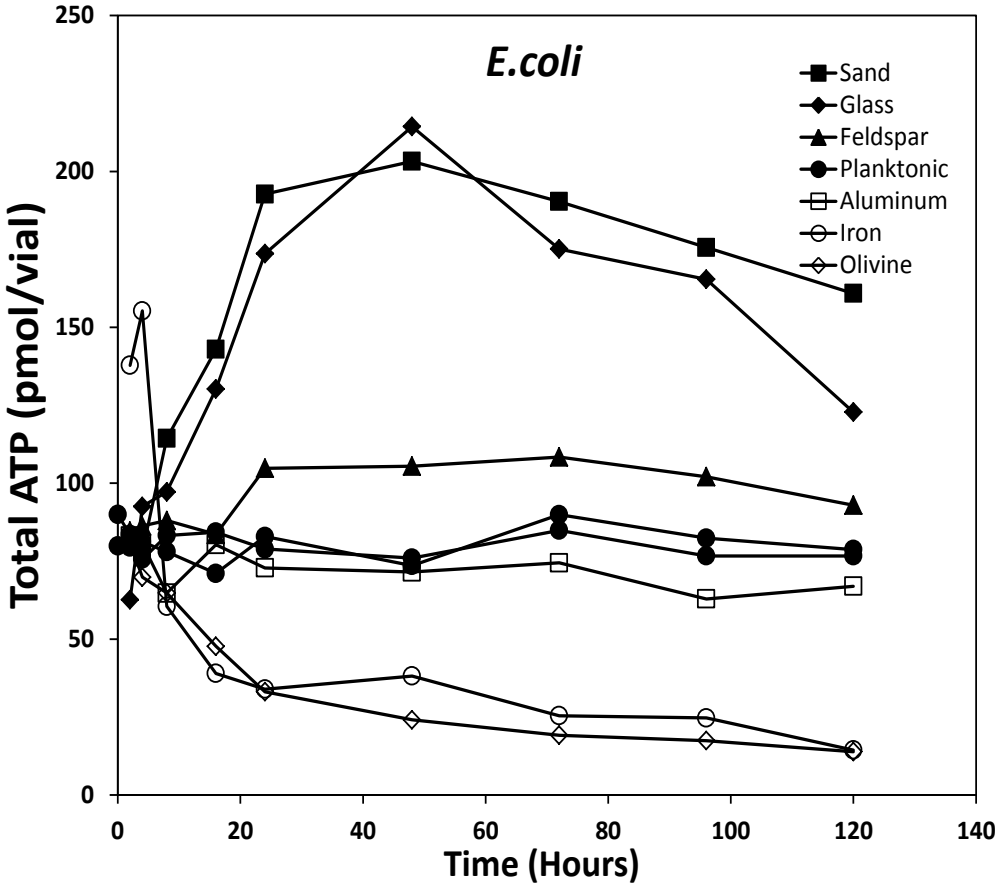

Figure 4.10 - Total ATP per vial of *E.coli* containing the different surfaces of interest.

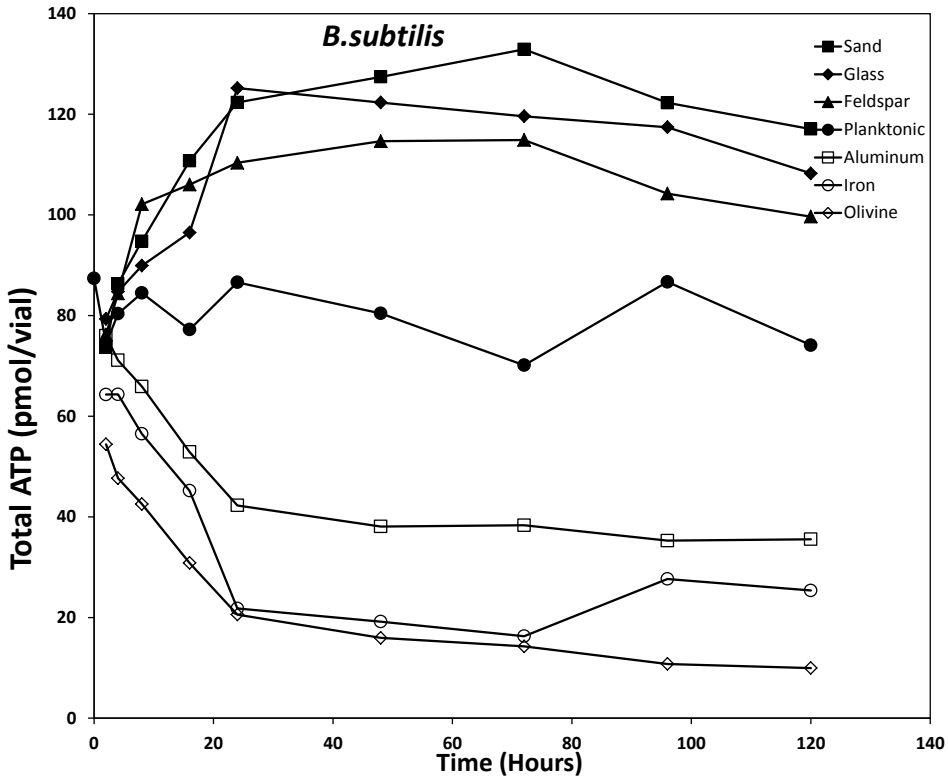

Figure 4.11 - Total ATP per vial of *B. subtilis* containing the different surfaces of interest.

The results imply that the percentage of coating was just enough to balance the decline in ATP upon bacterial attachment to aluminum hydroxide rich area and increase in ATP upon attachment to uncoated areas. For *B.subtilis*, ATP values corresponding to the aluminum hydroxide vials show a more prominent decrease when compared to the ATP values associated with plain sand.

The ATP per planktonic cell and per attached bacterium for the six different surfaces is presented in Figure 4.12 and Figure 4.13. The results illustrate the variation in metabolic activity as a function of the surface functional groups associated with the substrata provided for attachment. The ATP per attached cell for sand was higher than the ATP per planktonic cell closely followed by glass and then feldspar. The attachment resulted in a 2-4 fold increase during the 24 to 48 hour period for all three surfaces. The ATP per attached cell reduced upon adhesion to the positive surfaces in all cases except with E.coli attachment on aluminum hydroxide for which it was close to planktonic values. The reduction in cellular ATP upon bacterial adhesion to all the modified surfaces resulted in ATP concentrations lower than that observed due to adhesion to negative surfaces.

In Figure 4.14, the cellular ATP concentration per attached cell upon incubation for 24 hours and 48 hours is plotted as a function of the surface IEP. The intracellular ATP concentration per planktonic bacterium is indicated by the dotted lines for reference. The ATP concentrations of both bacterial strains were elevated upon adhesion to glass, sand and feldspar demonstrating that a more acidic surface can enhance metabolic activity.

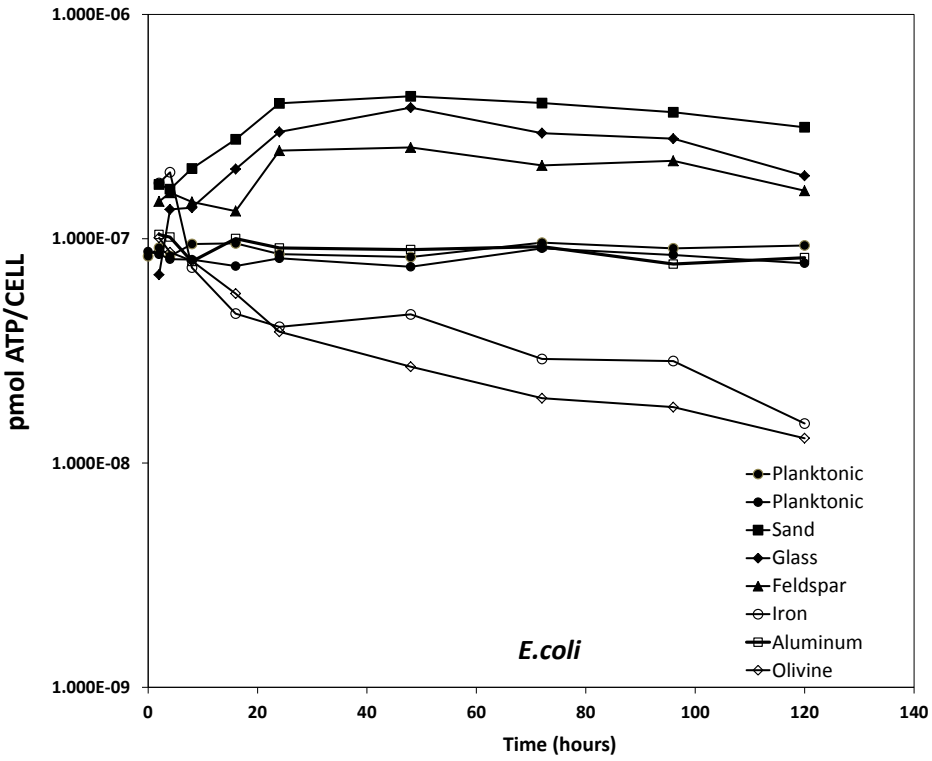

Figure 4.12 – ATP concentrations for planktonic and attached *E. coli* cells. The results demonstrate a variation in ATP as predicted by the hypothesis.

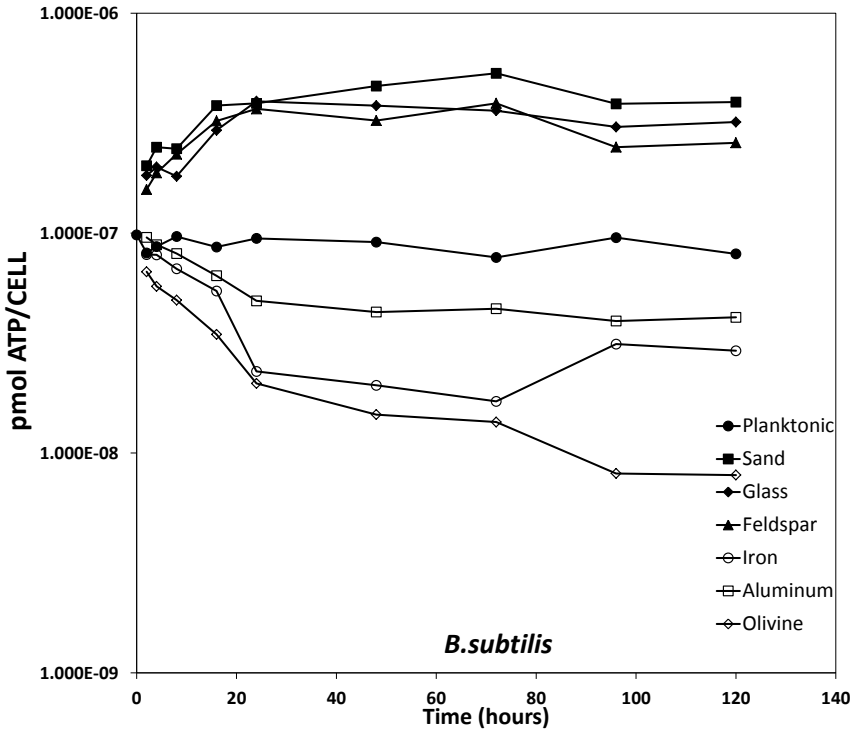

Figure 4.13 - ATP concentrations for planktonic and attached *B. subtilis* cells. The results demonstrate a variation in ATP as predicted by the hypothesis.

The ATP concentrations show a decline for the modified sands, indicating the effect positive surface functional groups have on the cellular metabolic activity. With the modified sand, bacteria may attach to the negatively charged uncoated area of sand or to the positively charged metal hydroxide coated area. The combined effect resulted in a net decline in ATP concentration per attached cell. The ATP concentrations per adhered cell upon attachment to olivine also resulted in a decline in ATP concentrations. The results are similar across the two different bacteria strains studied.

4.5.5 Charge Regulation Modelling

The pK and N values of the surfaces were obtained from the zeta potential data as explained in Chapter 3 and the results are provided in Tables 1 and 2. The charge-regulation model results using these values are presented along with the experimentally obtained zeta-potential measurements in Figures 4.6 and 4.7 and it can be seen that the identified pK and N values were able to accurately represent the surface potential as a function of pH.

The pK and N were used to calculate the bacterial surface pH as a function of separation distance from the surfaces, and the results are shown in Figure 4.15. The figure represents the difference in surface pH during bacterial adhesion to surfaces with different functional groups. In the case of the negative surfaces modelling indicates a drop in pH implying a corresponding increase will be observed in cellular ATP concentrations. This is in agreement with our experimental data. Initial modelling of the positive surfaces suggests that the surface pH of the bacterium is

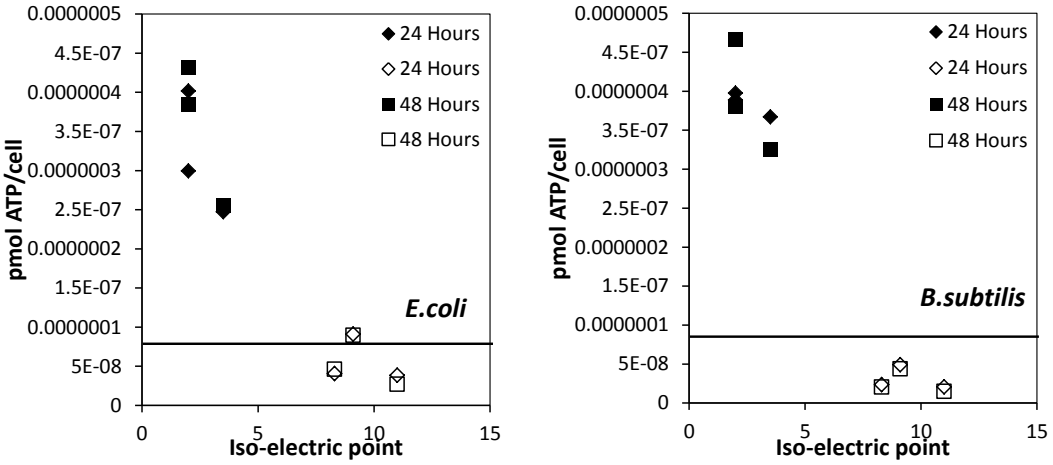

Figure 4.14 - The variation in bacterial ATP as a function of the surface IEP at 24 hr and 48 hr. The dotted lines depict the ATP concentration per planktonic cell for both *E. coli* and *B. subtilis*.

Table 4.1 - Dissociation constants of the bacterial surface functional groups and their corresponding site densities obtained from zeta potential measurements.

Dissociation constants and their site densities obtained for bacterial surfaces			
E. coli			
Parameters	95% Confidence Interval		
	value	Lower	Upper
pK_a	2.60	2.49	2.71
pK_b	11.24	7.70	14.79
$N_{a\ (\#/nm^2)}$	1.18E-01	1.08E-01	1.29E-01
$N_{b(\#/nm^2)}$	4.20E-02	3.22E-02	5.47E-02
B. subtilis			
pK_a	2.48	2.15	2.81
pK_b	9.06	3.94	14.19
$N_{a\ (\#/nm^2)}$	9.96E-02	7.79E-02	1.27E-01
$N_{b(\#/nm^2)}$	2.07E-02	6.21E-03	6.88E-02

Table 4.2 - Dissociation constants of the different solid surface functional groups and their corresponding site densities obtained from zeta potential measurements.

Dissociation constants and their site densities obtained for solid surfaces			
Sand			
Parameters	**95% Confidence Interval**		
	value	**Lower**	**Upper**
pK_{a1}	2.75	2.49	3.02
pK_{a2}	5.16	4.94	5.38
$N_{a1\ (\#/nm^2)}$	3.83E-02	3.40E-02	4.31E-02
$N_{a2(\#/nm^2)}$	5.32E-02	4.60E-02	6.14E-02
Glass beads			
pK_{a1}	3.14	2.93	3.34
$N_{a1\ (\#/nm^2)}$	7.41E-02	6.56E-02	8.38E-02
Feldspar			
pK_{a1}	3.72	3.62	3.82
pK_{b1}	6.42	6.16	6.68
$N_{a1\ (\#/nm^2)}$	6.43E-02	6.29E-02	6.57E-02
$N_{b1\ (\#/nm^2)}$	2.02E-02	1.79E-02	2.27E-02
Iron-coated sand			
pK_{a1}	4.42	4.04	4.81
pK_{a2}	7.52	6.86	8.18
pK_{b1}	9.04	8.40	9.68
$N_{a1\ (\#/nm^2)}$	3.93E-02	2.50E-02	6.15E-02
$N_{a2(\#/nm^2)}$	3.03E-02	1.22E-02	7.52E-02
$N_{b1\ (\#/nm^2)}$	6.87E-02	5.24E-02	9.01E-02
Aluminum-coated sand			
pK_{a1}	4.30	0.83	7.77
pK_{a2}	7.74	6.56	8.91
pK_{b1}	9.41	8.55	10.28
$N_{a1\ (\#/nm^2)}$	1.70E-02	3.05E-03	9.51E-02
na2	3.38E-02	1.26E-02	9.05E-02
nb1	6.41E-02	3.88E-02	1.06E-01

higher during adhesion to the more positive surfaces than the negative surfaces as expected, however the results depict a decline in surface pH as the distance between the bacterium and the solid surface decreases. The modelling results with the positive modified sand deviate from those experimentally determined where a decline in ATP was observed with the positive surfaces via an increase in surface pH. Nonetheless, we know that the modification of sand resulted in only partial coverage of sand with coating; hence, it is reasonable to conclude that the site density of the basic functional groups (N_b) is higher in the coated areas than the average values obtained from the zeta potential experiments. Furthermore, it is essential to recognize that the adhesion results discussed above show elevated levels of adhesion upon attachment to coated surfaces confirming that a great percentage of adhesion occurred onto the coated areas of the sand grains. We can accommodate that knowledge in our modelling by increasing the site density of the basic functional groups associated with the coating. The results presented in Figure 4.16 demonstrate that a doubling of N_b results in an increase in bacterial surface pH values as the bacterium approaches the surface. With iron hydroxide coated sand the pH value increased to ~7.5 and with aluminum hydroxide, the pH value increased to ~8.0. The final modelling results obtained are in agreement with our experimental results.

The modeled surface charge densities of the coated sands are presented in Figure 4.17 for both N_b and $2xN_b$. The IEP associated with the iron hydroxide coated sand

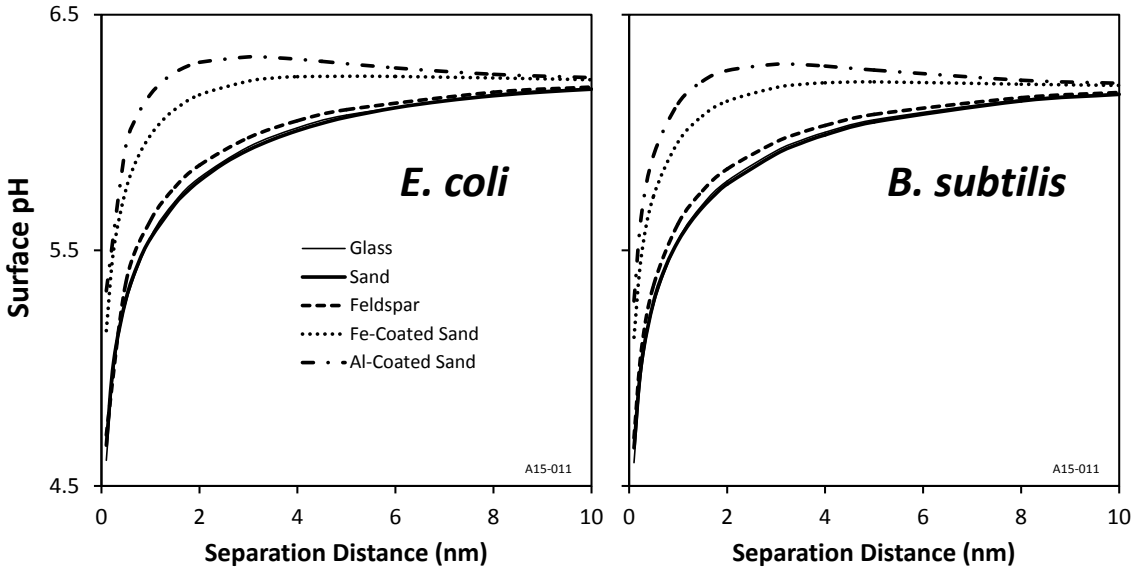

Figure 4.15 - Initial modelling resulted in a decline in surface pH with negatively charged surfaces as expected. Although a higher surface pH was obtained with the positive surfaces when compared to the negative surface, the modelling still suggests a decline in ATP at the surface.

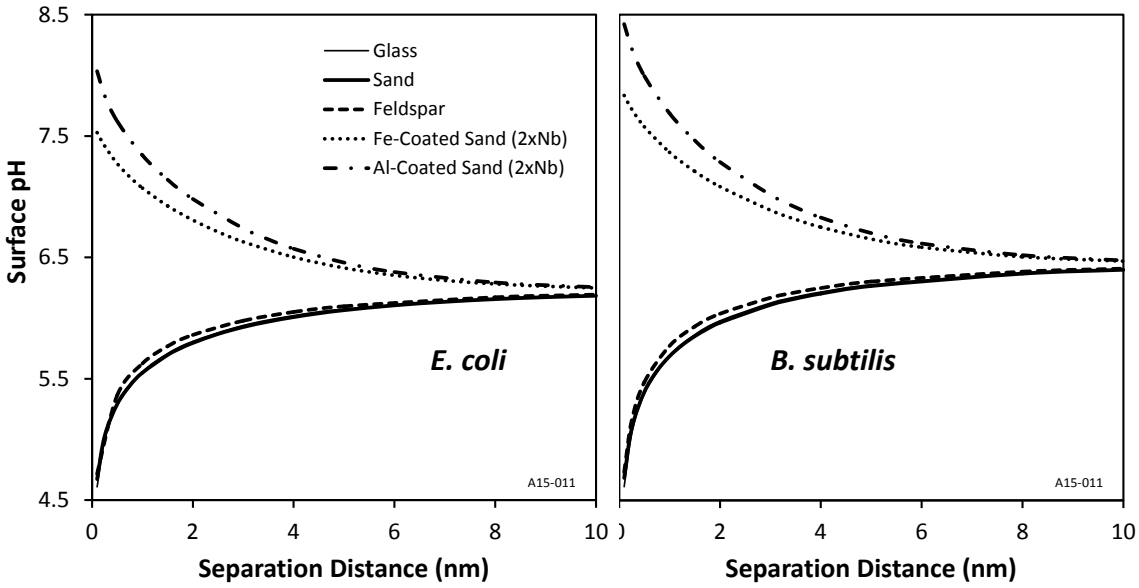

Figure 4.16 – A doubling of N_b for the coated sands results in an increase in surface pH with the positively-charged surfaces during bacterial adhesion. See text for discussion.

increased to ~9 while that of the aluminum hydroxide coated sand increased to ~9.5, and both remain within values obtained from literature. It should be noted that these results provide us with overall trends in surface pH that we can expect during bacterial adhesion to various surfaces and not specific numbers, as modelling assumes that both the bacterial surface and the solid surface are planar surfaces with a uniform distribution of functional groups. Thus, experimental and modelling results indicate that upon bacterial adhesion to a negatively-charged surface, the decline in bacterial surface pH contributes towards the proton motive force manifesting in improved ATP concentrations while adhesion to a positively-charged surface results in an increase in surface pH and a decreased proton motive force, resulting in compromised ATP levels. The ATP of bacteria attached to negative surfaces show a definite increase and remain at those elevated levels or gradually taper down during the duration of the experiment. However, attachment to positive surfaces results in a continual depletion of energy reserves during the course of the experiment.

4.6 Conclusions

The results of the adhesion studies showed a greater degree of attachment with positively-charged surfaces than negatively-charged surfaces. These results are reasonable owing to the greater attraction between the negatively-charged bacterial surface and the positively-charged surfaces. The results obtained from the adhesion experiments and ATP analyses are in agreement with the hypothesis. All the results

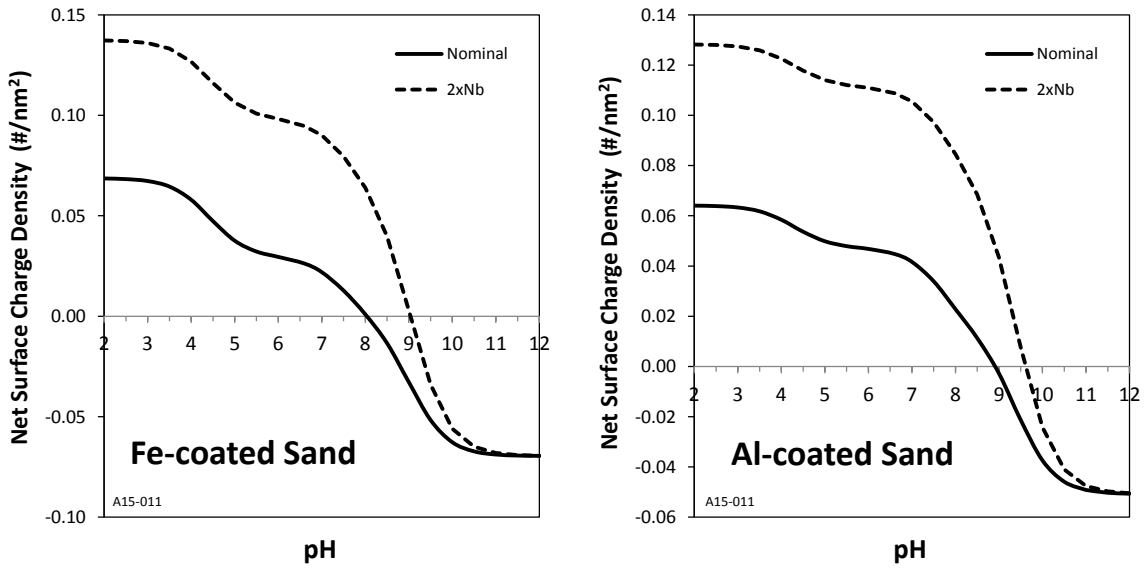

Figure 4.17 - Here we present the surface charge density as a result of variation in pH for the normal site density obtained via modelling and two times the site density of the positive functional group associated with iron hydroxide and aluminum hydroxide coatings. The figure shows that the IEP of the surface results in minor shifts that are in agreement with literature.

demonstrate how different surface functional groups spanning a range of IEPs can induce a characteristic metabolic response during bacterial attachment. The modelling results showed that when two surfaces bearing functional groups approach each other, the pH at the interphase is a function of the surface associated functional groups. The implications of an increase or decrease in pH were shown with a quantifiable variation in ATP indicating that the pH and potential can propagate across the membrane. The effect of testing multiple surfaces across a range of properties is clearly observed in the diverse ATP concentrations measured.

The results of this study have several environmental implications as bacterial adhesion to surfaces is crucial to many systems. The results of this study can serve as a basis in the selection of surfaces for various applications to result in a desired metabolic level in bacteria. Enhancement of ATP concentrations denotes more growth, colonization and biofilm development this can be take advantage of in waste water treatment, biodegradation and bio augmentation. A decline in ATP refers to lower metabolic states that yield relatively compromised activity, biofilm establishment and survival forming a basis for application in controlling microbiologically induced corrosion, biofouling etc. These findings also can form the framework for applications across various disciplines including dentistry, medicine, marine science and food storage.

4.7 Acknowledgement

This project was funded by the National Science Foundation through Grant 0828356. The authors gratefully acknowledge their valuable support during this work.

4.8 Reference List

[1] J. Costerton, G. Gessey, Microbial contamination of surfaces, in: Anonymous Surface Contamination, Springer, 1979, pp. 211-221.

[2] W.M. Dunne Jr, Bacterial adhesion: seen any good biofilms lately? Clin. Microbiol. Rev. 15 (2002) 155-166.

[3] G. Geesey, R. Mutch, J.t. Costerton, R. Green, Sessile bacteria: An important component of the microbial population in small mountain streams 1, Limnol. Oceanogr. 23 (1978) 1214-1223.

[4] T. Ladd, J. Costerton, G. Geesey, Determination of the heterotrophic activity of epilithic microbial populations, Native aquatic bacteria: enumeration, activity and ecology.ASTM STP. 695 (1979) 180-195.

[5] J. Palmer, S. Flint, J. Brooks, Bacterial cell attachment, the beginning of a biofilm, J. Ind. Microbiol. Biotechnol. 34 (2007) 577-588.

[6] P. Moons, C.W. Michiels, A. Aertsen, Bacterial interactions in biofilms, Crit. Rev. Microbiol. 35 (2009) 157-168.

[7] B. Jucker, H. Harms, S. Hug, A. Zehnder, Adsorption of bacterial surface polysaccharides on mineral oxides is mediated by hydrogen bonds, Colloids and Surfaces B: Biointerfaces. 9 (1997) 331-343.

[8] A.A. Dispirito, P.R. Dugan, O.H. Tuovinen, Inhibitory effects of particulate materials in growing cultures of Thiobacillus ferrooxidans, Biotechnol. Bioeng. 23 (1981) 2761-2769.

[9] M. Fletcher, G.I. Loeb, Influence of substratum characteristics on the attachment of a marine pseudomonad to solid surfaces, Appl. Environ. Microbiol. 37 (1979) 67-72.

[10] R. Kugler, O. Bouloussa, F. Rondelez, Evidence of a charge-density threshold for optimum efficiency of biocidal cationic surfaces, Microbiology. 151 (2005) 1341-1348.

[11] A. Terada, A. Yuasa, S. Tsuneda, A. Hirata, A. Katakai, M. Tamada, Elucidation of dominant effect on initial bacterial adhesion onto polymer surfaces prepared by radiation-induced graft polymerization, Colloids and Surfaces B: Biointerfaces. 43 (2005) 99-107.

[12] M.C. van Loosdrecht, J. Lyklema, W. Norde, A.J. Zehnder, Influence of interfaces on microbial activity, Microbiol. Rev. 54 (1990) 75-87.

[13] S. Underhill, J. Prosser, Surface attachment of nitrifying bacteria and their inhibition by potassium ethyl xanthate, Microb. Ecol. 14 (1987) 129-139.

[14] G. Stotzky, Influence of soil mineral colloids on metabolic processes, growth, adhesion, and ecology of microbes and viruses, Interactions of soil minerals with natural organics and microbes. (1986) 305-428.

[15] Y.H. An, R.J. Friedman, Concise review of mechanisms of bacterial adhesion to biomaterial surfaces, J. Biomed. Mater. Res. 43 (1998) 338-348.

[16] M.C. van Loosdrecht, J. Lyklema, W. Norde, A.J. Zehnder, Bacterial adhesion: a physicochemical approach, Microb. Ecol. 17 (1989) 1-15.

[17] Y. Hong, D.G. Brown, Variation in bacterial ATP level and proton motive force due to adhesion to a solid surface, Appl. Environ. Microbiol. 75 (2009) 2346-2353.

[18] Y. Hong, D.G. Brown, Electrostatic behavior of the charge-regulated bacterial cell surface, Langmuir. 24 (2008) 5003-5009.

[19] W. Jiang, A. Saxena, B. Song, B.B. Ward, T.J. Beveridge, S.C. Myneni, Elucidation of functional groups on gram-positive and gram-negative bacterial surfaces using infrared spectroscopy, Langmuir. 20 (2004) 11433-11442.

[20] J.B. Fein, C.J. Daughney, N. Yee, T.A. Davis, A chemical equilibrium model for metal adsorption onto bacterial surfaces, Geochim. Cosmochim. Acta. 61 (1997) 3319-3328.

[21] W.A. Cramer, D.B. Knaff, Energy Transduction in Biological Membranes, Springer-Verlag, 1990.

[22] F.M. Harold, The Vital Force: A Study of Bioenergetics, WH Freeman New York, 1986.

[23] P.C. Maloney, F. Hansen III, Stoichiometry of proton movements coupled to ATP synthesis driven by a pH gradient inStreptococcus lactis, J. Membr. Biol. 66 (1982) 63-75.

[24] P. MITCHELL, Coupling of phosphorylation to electron and hydrogen transfer by a chemi-osmotic type of mechanism, Nature. 191 (1961) 144-148.

[25] T.W. Healy, D. Chan, L. White, Colloidal behaviour of materials with ionizable group surfaces, Pure and Applied Chemistry. 52 (1980) 1207-1219.

[26] Y. Hong, D.G. Brown, Cell surface acid–base properties of Escherichia coli and Bacillus brevis and variation as a function of growth phase, nitrogen source and C: N ratio, Colloids and Surfaces B: Biointerfaces. 50 (2006) 112-119.

[27] E.R. Kashket, The proton motive force in bacteria: a critical assessment of methods, Annual reviews in microbiology. 39 (1985) 219-242.

[28] D.G. Nicholls, S. Ferguson, Bioenergetics, Academic Press, 2013.

[29] L.S. Albert, D.G. Brown, Variation in bacterial ATP concentration during rapid changes in extracellular pH and implications for the activity of attached bacteria, Colloids and Surfaces B: Biointerfaces. (2015).

[30] S. Kim, S. Park, C. Lee, H. Kim, Transport and retention of Escherichia coli in a mixture of quartz, Al-coated and Fe-coated sands, Hydrol. Process. 22 (2008) 3856-3863.

[31] S. Kim, S. Park, C. Lee, N. Choi, D. Kim, Bacteria transport through goethite-coated sand: Effects of solution pH and coated sand content, Colloids and Surfaces B: Biointerfaces. 63 (2008) 236-242.

[32] J.C. Joo, C.D. Shackelford, K.F. Reardon, Association of humic acid with metal (hydr) oxide-coated sands at solid–water interfaces, J. Colloid Interface Sci. 317 (2008) 424-433.

[33] W. Stumm, J.J. Morgan, A. Black, Chemical aspects of coagulation [with discussion], Journal (American Water Works Association). (1962) 971-994.

[34] Y. Hong, D.G. Brown, Cell surface acid–base properties of Escherichia coli and Bacillus brevis and variation as a function of growth phase, nitrogen source and C: N ratio, Colloids and Surfaces B: Biointerfaces. 50 (2006) 112-119.

[35] A. Gueney, S. Atak, Separation of chromite from olivine by anionic collectors, Fizykochemiczne Problemy Mineralurgii. (1997) 99-106.

[36] O.S. Pokrovsky, J. Schott, Forsterite surface composition in aqueous solutions: a combined potentiometric, electrokinetic, and spectroscopic approach, Geochim. Cosmochim. Acta. 64 (2000) 3299-3312.

[37] Y. Ucbas, V. Bozkurt, K. Bilir, H. Ipek, Concentration Of Chromite By Means Of Magnetic Carrier Using Sodium Oleate And Other Reagents, Physicochemical Problems Of Mineral Processing. 50 (2014) 767-782.

[38] Jones, D.; Pell, P. A.; Sneath, P. H. A., Maintenance of bacteria on glass beads at -60°C to -76°C. In Maintenance of microorganisms and cultured cells: A manual of laboratory methods, Kirsop, B. E.; Doyle, A., Eds. Academic Press: San Diego, 1991.

Chapter 5

Summary and Conclusions

CHAPTER 5 Summary and Conclusions

5.1 Overall Results and Conclusions

The study provides an understanding of how surfaces containing a range of ionizable functional groups can impact bacterial bioenergetics during adhesion. We have examined the results within our hypothesis that connects physiochemical surface processes and cellular bioenergetics via the proton motive force. Changes in metabolic activity in bacteria were quantified as the cellular ATP concentration using the Luciferase-Luciferin assay.

Based on modelling methods, we predicted variation in the metabolic activity of bacteria upon adhesion to surfaces, with an increase in cellular ATP for acidic (negatively-charged) surfaces and a decrease in cellular ATP for basic (positively-charged) surfaces. The experimental results demonstrated that the ATP response in adhered bacteria was in agreement with our predictions. Thus, the hypothesis has been tested and holds true for Gram positive and Gram negative neutrophilic bacteria. The major contributions of the study are summarized below.

5.1.1 The bacterial ATP concentration is directly affected by changes in the local pH

We have demonstrated that pH variation at the bacterial surface can alter the cellular bioenergetics within the framework of chemiosmosis. Our investigation has demonstrated that surface changes in pH that occur during adhesion play a pivotal role

in the metabolic state of bacteria. We have demonstrated in particular that variation of surface pH of bacteria can drive ATP synthesis or ATP hydrolysis based on ΔpH across the membrane. The results show a 2- to 4-fold increase in ATP concentrations when the external pH was decreased to 3.5 and showed a 20-70% decline when the external pH was increased to 10.5.

Comparative analysis of four different neutrophillic bacteria showed an exponential relationship between surface pH of bacteria and cellular ATP concentrations. The responses were similar for the different starvation times studied (1 day and 1 week). An interesting deviation in ATP response was observed with *S. epidermidis,* which showed no change in ATP with a decrease in pH but showed a more prominent decline in ATP when the pH was increased, implying that alkaline formulations may be ideal in controlling *S, epidermis* colonization of surfaces. This study also paves way to predict cellular ATP concentration of bacteria as a function of the local pH.

5.1.2 Bacterial adhesion to positively-charged surfaces results in a decline in cellular ATP and adhesion to negatively-charged surfaces results in an increase in ATP, with both results following our hypothesis

The major contribution of this study was the demonstration that variation in pH at the interface during bacterial adhesion affects cellular ATP concentration. The results show that planktonic bacteria had relatively constant ATP concentrations over the experimental duration, whereas the ATP levels varied during attachment. Modelling results showed an anticipated decrease or increase in surface pH, depending on the electrostatic properties of the surface. The experimental results are coherent and in

accordance to predictions, with bacterial adhesion to negatively-charged surfaces showing an enhanced metabolic state when compared to their planktonic counterparts and adhesion to positively-charged surfaces resulting in a decline in ATP. Thus, sessile bacteria in many systems have a different metabolic profile in comparison to free living species.

5.1.3 While attachment to the negatively-charged surfaces demonstrated a finite change in ATP, with the positively-charged surfaces the cellular ATP continuously decreased over the five-day experiment, indicating that the surfaces were steadily depleting the bacterial energy stores.

Experimental results showed that bacterial attachment to negatively-charged surfaces resulted in a finite increase in ATP. In some cases the bacteria maintained an enhanced metabolic profile throughout the length of the experiment and in other cases a gradual decline in metabolic activity of the bacteria was observed. The results with the positively-charged surfaces demonstrated that bacterial ATP continually declined over the course of the experiment, implying that the adhesion resulted in a steady depletion of bacterial energy reserves by the reverse function of ATP synthase.

5.1.4 The magnitude of the change in bacterial ATP upon adhesion is directly related to the acid/base properties of the adhering surface

A primary contribution of this thesis was identifying the varied response of bacteria upon attachment to surfaces that have a range of IEPs. Model predictions indicated an increase in cellular metabolic activity when bacteria are in close proximity to acidic surfaces. This was experimentally demonstrated by adhesion experiments with

negatively-charged sand, glass and feldspar, where elevated ATP concentrations were measured. Moreover, the measured ATP concentrations were found to vary as a function of the surface IEP, as predicted by the charge-regulation modeling. This implies that the charge regulation process directly impacted Δp. Bioenergetic modeling indicated that upon bacterial attachment to positive surfaces, Δp will decline resulting in a simultaneous decrease in ATP. This effect of basic surfaces on cellular ATP concentrations was demonstrated with adhesion experiments using iron hydroxide coated sand, aluminum hydroxide coated sand and olivine. Conversely, bioenergetic modeling of negatively-charged surfaces indicated that Δp will increase, resulting in an increase in ATP and this was demonstrated with glass beads, sand and feldspar. The results indicate that the surface charge of attachment substratum plays an integral role in defining the metabolic state of adhered bacteria.

5.1.5 The required variation in ΔpH that results in the experimentally-observed ATP variations is less than 0.6 pH units and this can be achieved via the charge-regulation process upon bacterial adhesion.

The results indicate that a variation of less than 0.6 pH units across the membrane is sufficient to achieve the enhance ATP response observed. This pH shift was demonstrated to be attainable by charge regulation by modelling the variation in surface pH during bacterial adhesion. With goethite coated sand, it was observed that a minor shift of 0.25 pH units was sufficient to achieve the declined ATP response obtained experimentally and modelling has shown that this decline in pH can be

readily achieved during adhesion. Thus, minor changes in ΔpH are satisfactory to obtain the observed ATP variations.

5.1.6 The results were similar for both the Gram-negative E. coli and the Gram-positive B. subtilis, demonstrating that the hypothesis is valid for both types of bacterial cell walls.

Our experiments with both the Gram-negative *E.coli* and the Gram-positive *B. subtilis* yielded results with similar trends. Bacterial ATP decreased upon attachment to positively charged surfaces and increased upon adhesion to negatively charged surfaces thereby, indicating that the observed metabolic response of the bacteria triggered via the charge regulation effect is common. It is interesting to note that bulk pH manipulation experiments with the neutrophilic *S. epidermidis*, which is able to grow at pH levels below 5, demonstrated no effect on ATP levels during a decrease in extracellular pH. This indicates that bacteria can evolve to overcome the effects of extracellular pH.

5.2 Future research

The experimental results obtained in his study are meaningful and clearly describe the effect of solid surface properties on metabolic activity of bacteria upon bacterial adhesion. The following sections discuss potential future research based on this study.

5.2.1 Examining effects of solid surface properties on growth and colonization

We have shown that the metabolic activity of bacteria varies upon bacterial adhesion to surfaces. It is desirable to understand how the metabolic activity of attached

bacteria during growth will change as a function of solid surface properties. This understanding of how surface growth and colonization of bacteria is impacted via changes in metabolic activity can be potentially useful.

5.2.2 Exploring the impact of the charge-regulated bacterial surface in the formation and growth of biofilms

Bacteria commonly form complex microbial communities, micro-colonies and biofilms in natural and engineered systems following initial adhesion. All our experiments have focused on the initial adhesion of bacteria to surfaces, it will be beneficial to take steps in learning the effect of the charge regulated bacterial surface interacting with other bacterial surfaces via modelling and experiments. The results can find application across a range of disciplines to which microbial adhesion is crucial.

5.2.3 Examining the impact of conditional films on bacteria-surface interactions

Conditioning layers consisting of organic and inorganic particles form on surfaces in most environments. Incorporating natural conditioning of surfaces in experiments to study the effect of conditioning films on bacterial metabolic states during adhesion and characterizing them can provide a greater understanding of details involved in metabolic effects of adhesion in various systems.

5.2.4 Examining the implications of the hypothesis on natural and engineered systems (e.g., bacterial evolution of nanowires for electron transfer to iron surfaces).

It can be advantageous to study the implications of the hypothesis in natural and man-made systems. Certain bacteria have been identified to produce nanowires that help them use alternate external surface-associated molecules (eg., metal oxides) as terminal electron acceptor during limited presence of oxygen. This facilitates electron transfer from bacteria without direct contact with the surface and also facilitates electron transfer to surfaces inaccessible for adhesion. The hypothesis can be extended to examine if the charge regulated surface triggers the development of nanowires. Another area to explore is charge regulated surface signaling for surface recognition and to examine the possibility of charge regulation serving as an indicator to surface proximity.

5.2.5 Determination of the changes in $\Delta\psi$ and ΔpH during charge-regulated bacterial adhesion

As discussed in the previous chapters, the proton motive force consist of a charge and pH gradient. Determining the effect of charge regulation on each of the two components of the proton motive force during bacterial adhesion and their corresponding influence on cellular bioenergetics using selective ionophores can be extremely useful. This will provide us with a more holistic understanding of the charge regulated metabolic response of bacteria.

5.2.6 Developing paints/coatings that can aid in improving biofilm/colonization control

Eradication of biofilms has proved to be a great challenge as they render selective advantages for survival and resistance over free swimming bacteria. It is also known that initial surface colonization rates are influenced by the chemical nature of surfaces involved. Thus, developing paints or coatings that can provoke a decline in cellular bioenergetics upon adhesion can go a long way in the control of biofilms. This can be beneficial in many fields, such as developing paints minimize biofilm growth in distribution pipeline systems. Also it can be used in the pharmaceutical field, where often high doses of antibiotics are administered over extended periods to control pathogenic biofilm formation on medical implants and devices. It is necessary to however understand how conditioning can change the surface properties in these systems.

Appendix A

Standardization of the ATP extraction Protocol

Appendix A: Standardization of the ATP extraction Protocol

The most popular assay for ATP estimation is the firefly luciferase- luciferin bioluminescence assay using a luminometer. It is essential to initially extract ATP from intact living cells prior to performing the quantification of ATP. Several methods for ATP extraction are practiced and it was required to identify an appropriate method to conduct our experiments. The initial method adopted for ATP extraction was by means of a Nucleotide Releasing Buffer (NRB). The agent of choice was benzalkonium Chloride and our method of extraction was identical to that used in prior experiments by Hong and Brown.

The NRB method served as an excellent ATP extraction procedure, however in experiments in which extracted ATP samples had to be stored over a long period of time at -20°C before collective analysis, it was noticed that the Relative Light Units (RLU) obtained from the luminometer were significantly lower. The RLU is a direct estimation of the ATP concentration in the sample. ATP measurements performed immediately after extraction showed high RLU values whereas those for samples that were stored at -20°C dropped. Moreover samples treated with NRB showed a decline in NRB 3 minutes post treatment. For this purpose experiments were performed to identify alternate extraction methods to be used when samples were not analyzed immediately post extraction.

Several procedures were investigated and modified (example with/without sonication, with/without freezing) to compare final concentrations of ATP. Some of the methods explored were the TCA method, microwave method, boiling method etc. The boiling method was selected for experiments that required storage of samples owing to its simplicity, stability and reproducibility. The NRB method was used in experiments that did not require freezing and thawing of samples. The following results indicate the pronounced decline in RLU post freezing and thawing of bacterial samples incubated with glass beads of varying mass (Figure A1.1). The results with the boiling method on the other hand showed consistent RLU in samples that were frozen and thawed and those that were not (Figure A1.2). However, it was identified that it was required that all samples be at the same temperature during analysis. This was ensured by using placing thawed samples in a thermomixer at 27° C for 20 minutes prior to analysis.

The finalized protocol involved placing the bacterial sample in a boiling water bath on a hot plate for 3.5 minutes followed by snap cooling in an ice bucket for 1 minute. 1 ml of sample was immediately pipetted into micro centrifuge tubes and stored at -20°C until analysis. Prior to ATP analysis, the samples were thawed by placing at room temperature for 30 minutes followed by thawing in a thermomixer for 20 minutes at 27° C. The ATP concentration of samples was then determined as usual. The method can be modified as per experimental requirements.

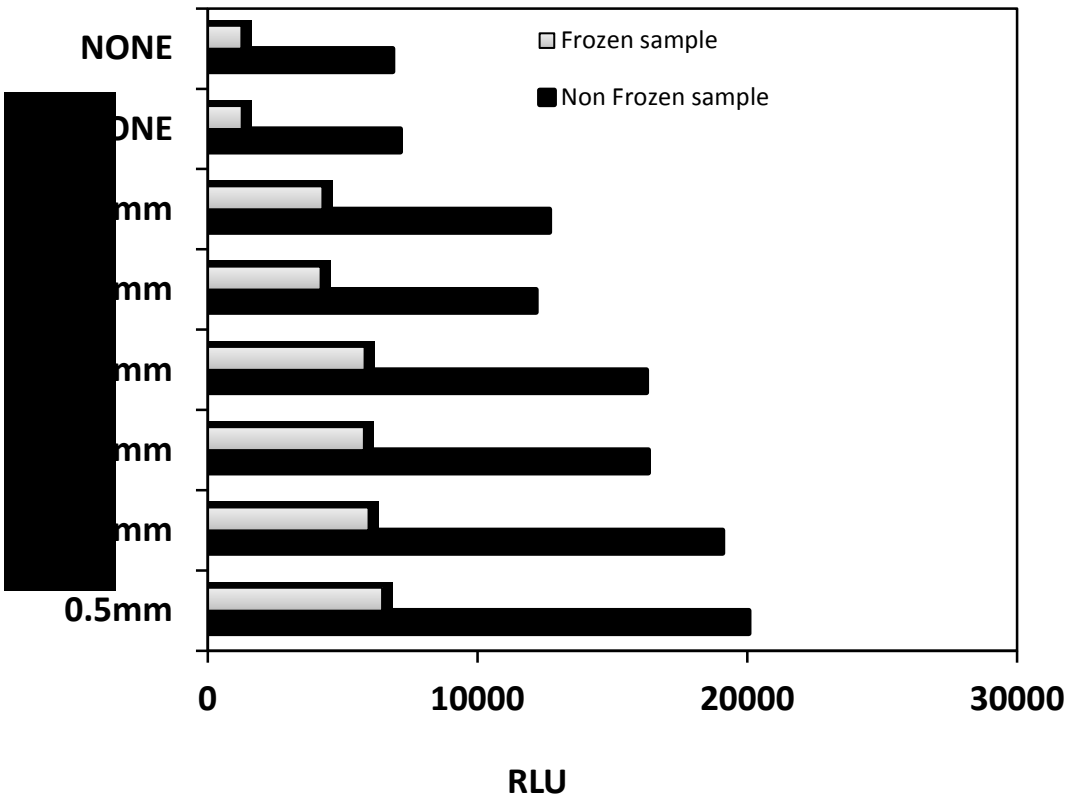

Figure A1.1 - The figure demonstrates the drop in RLU upon freezing and thawing of bacterial ATP samples post NRB treatment. Experimental results show a gradual increase in ATP concentrations per vial with an increase in surface area of negatively charged glass beads. The experiment was preliminary with the goal of studying the effects of freezing and thawing of ATP samples. The unfrozen samples exhibit higher RLU values compared to the frozen samples.

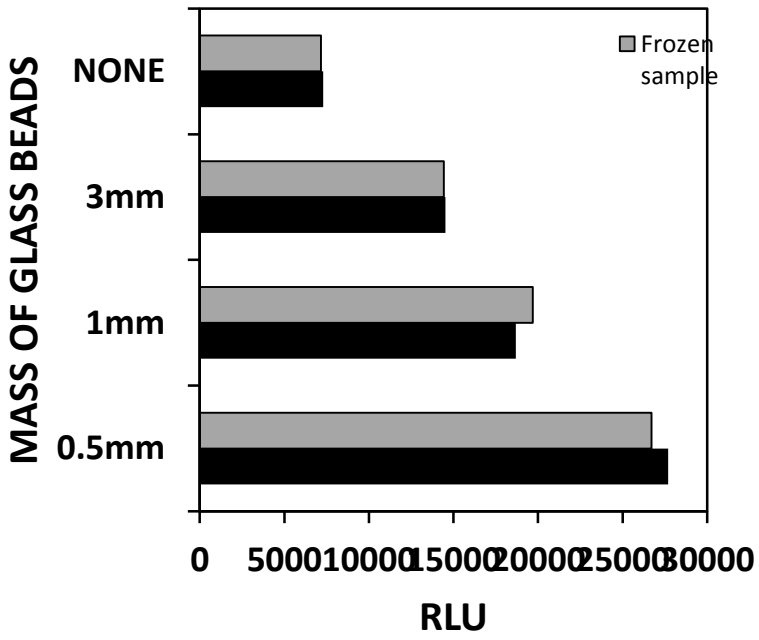

Figure A1.2 - The figure demonstrates the effect of freezing and thawing on bacterial ATP samples post boiling treatment. Experimental results show a gradual increase in ATP concentrations per vial with an increase in surface area of negatively charged glass beads. The experiment was preliminary with the goal of studying the effects of freezing and thawing of ATP samples. The unfrozen samples exhibit RLU values similar to the frozen samples indicating that freezing and thawing samples subject to boiling treatment did not affect ATP concentrations.

Appendix B

Bioenergetics of bacteria is impacted during adhesion to surfaces

Appendix B: Bioenergetics of bacteria is impacted upon adhesion to surfaces

We have presented our results depicting bacterial ATP variation upon adhesion to different surfaces with a range of surface properties in chapter 3 and 4. To ensure that adhesion impacted these energy variations, we conducted experiments using dialysis tubing in which surfaces of interest were delimited forming dialysis sacs, with surfaces. Experiments were conducted identical to the procedure described in chapter 3 and chapter 4. The exception was that here, the surface was limited within a dialysis sac ensuring that bacteria did not adhere to the surface under study.

Experiments were performed with no dialysis tubing, with dialysis tubing and with surfaces limited within the dialysis tubing. The experiment was performed over the regular length of time of our adhesion experiments *E.coli* served as model organism.

The results obtained depicted in Figure B1.1showed minimum variation between the different experimental conditions, implying that the adhesion is critical to obtaining significant bioenergetics changes in bacteria.

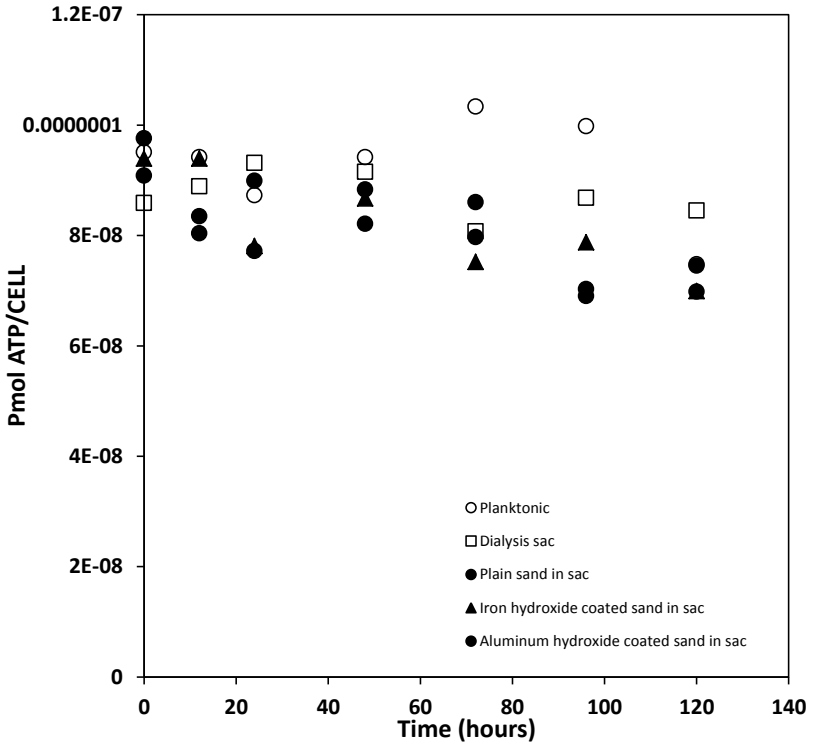

Figure B1.1 - The results presented in this figure show minimum variation in ATP concentrations across the different experimental conditions. Experiments were conducted with *E.coli* in the absence of membrane sac and surface, in the presence of membrane sac alone, in the presence of surfaces (plain sand, iron hydroxide coated sand, aluminum hydroxide coated sand) delimited by a membrane sac.

Appendix C

Effect of plain and coated glass beads on the metabolic activity of adhered bacteria

Appendix C Effect of plain and coated glass beads on the metabolic activity of adhered bacteria

The effect of charge regulation on the metabolic activity of bacteria upon adhesion to glass beads and iron hydroxide coated glass beads was tested experimentally. Based on the hypothesis, surface pH and charge variation as the result of charge regulation during adhesion can impact cellular ATP levels of the adhering bacterium. An increase in surface pH can negatively impact the proton motive force resulting in a decrease in ATP concentration. Alternatively, with a decrease in surface pH, the proton motive force increases and results in ATP synthesis. Thus, the effect of adhesion on metabolic activity was explored for negatively charged glass and positively charged iron hydroxide coated glass.

It was expected that upon *E.coli* adhesion to negatively charged glass, an increase in proton motive force would result in an increased cellular ATP response and with the positively charged iron hydroxide coated glass a decline in proton motive force and a corresponding ATP concentration decline will be observed. The results obtained are in agreement with the hypothesis with ATP enhancement upon adhesion to glass and ATP decline upon adhesion to iron coated glass and demonstrated in Figure C1.1 and Figure C1.2.

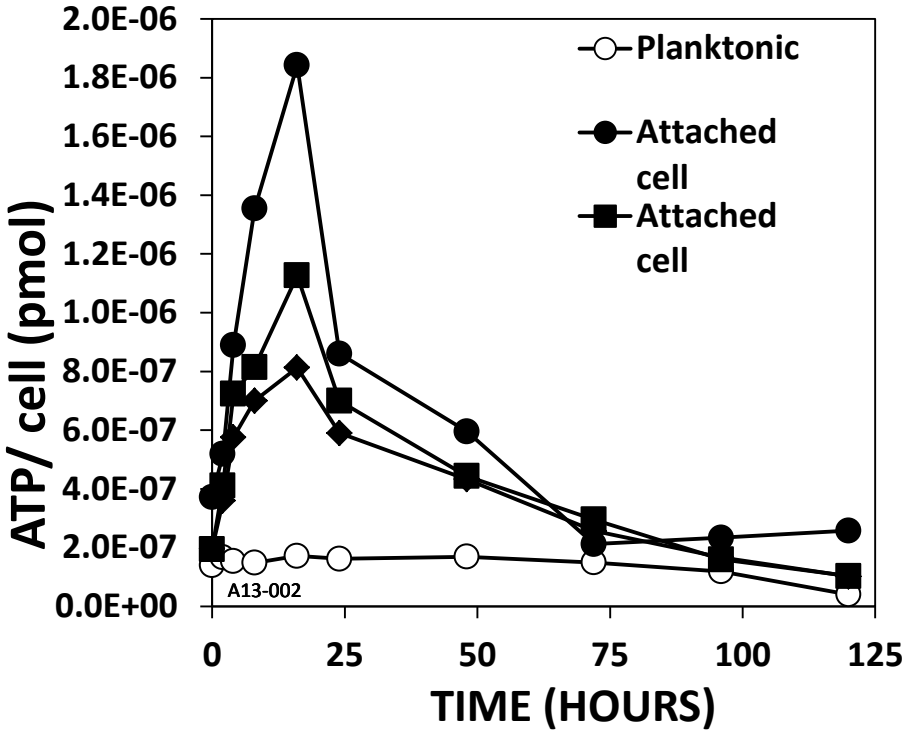

Figure C1.1 - The figure depicts an increase in ATP per attached *E.coli* when compared to planktonic cells. This is the result of an enhanced proton motive force due to charge regulation during bacterial adhesion to a negatively charged glass surface.

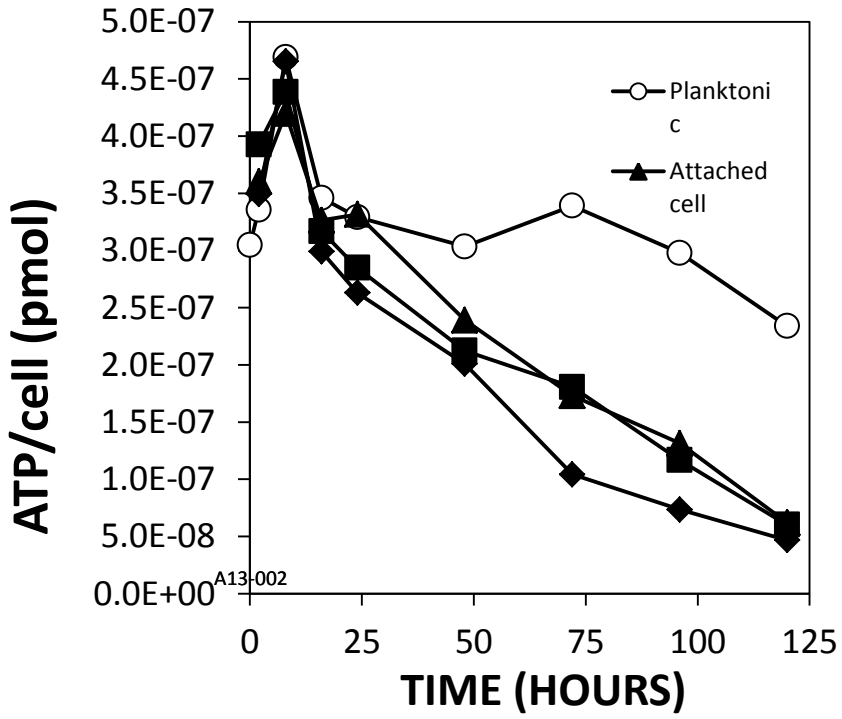

Figure C1.2 - The figure depicts a decrease in ATP per attached *E.coli* when compared to planktonic cells. This is the result of a decline in proton motive force due to charge regulation during bacterial adhesion to a positively charged iron hydroxide surface.

Appendix D

Preliminary exploration of adhesion induced metabolic activity variation of *S. epidermidis*

Appendix D Preliminary exploration of adhesion induced metabolic activity variation of *S. epidermidis*

As part of testing the hypothesis correlating surface changes via charge regulation and cellular bioenergetics variation, the effect of bulk pH on ATP concentration was tested. The alteration of bulk pH enabled artificially manipulating the surface pH to mimic the effect of charge regulation on the surface pH during adhesion. The details are provided in chapter 2 of this dissertation. The results obtained showed that with a decline in bulk pH the ATP concentration of bacteria increased and with an increase in surface pH by increasing the bulk pH, the cellular ATP concentration decreased. Four neutrophilic bacterial strains were used in this study, including the Gram-Negative strains *Escherichia coli* K-12 (ATCC29181) and *Pseudomonas putida* (ATCC12633) and the Gram-Positive strains *Bacillus subtilis* (ATCC23059) and *Staphylococcus epidermidis* (ATCC 35984). The results obtained were similar across the strains, indicating that this is a common mechanism by which ATP synthesis or hydrolysis occurs. The one exception was observed with *S. epidermidis* which showed no alteration in cellular ATP when the pH of the bulk solution was decreased but showed a more steeper decline in ATP when the bulk pH of the solution was increased. This deviation from normal behavior suggested that *S. epidermidis* adhesion to a negatively changed surface may not result in changes in metabolic activity of the bacteria.

A quick experiment was performed to test the effect of *S. epidermidis* attachment onto negatively charged glass beads and iron hydroxide coated glass beads. Vials were set

up with 0.5, 1.0 and 2.0 grams of glass beads. The experiment was conducted with E.coli bacteria alongside to allow comparison. In Chapter 4 we presented results of how the ATP concentration of *E. coli* and *B. subtilis* increase upon adhesion to glass beads. However, preliminary experiments with *S. epidermidis* did not indicate that the bacterial ATP was enhanced upon adhesion to the glass beads. Experimental results upon adhesion of *S. epidernidis* to positively charged glass beads indicated a decline in cellular ATP concentrations. To allow comparison of the change in ATP across both the bacterial strains the results are presented in Figure D1.1 and Figure D1.2 in the form of normalized RLU. Here, RLU values obtained with different masses of beads were normalized by the RLU value obtained for planktonic bacteria.

Currently the results are preliminary in nature and conducting experiments over longer periods of time can provide insight to *S. epidermidis* adhesion behavior.

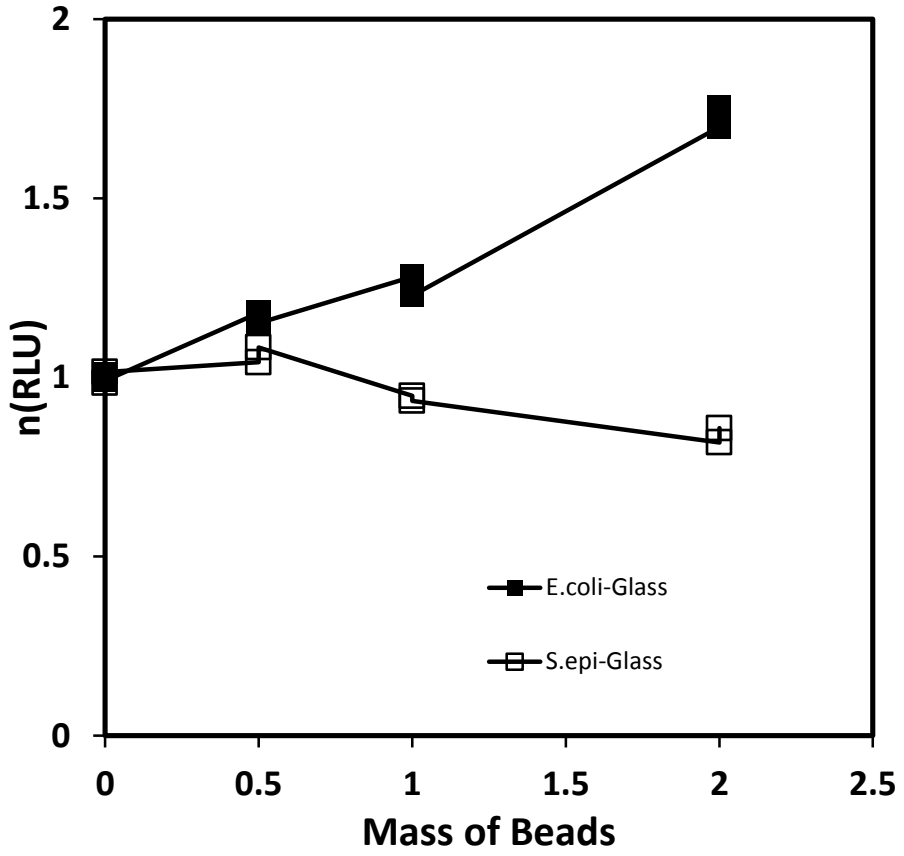

Figure D1.1 - This figure depicts the increase in ATP corresponding to an increase in the mass of glass beads with *E.coli* (solid symbols). Results with *S. epidermidis* (hollow symbols) do not exhibit an increase in ATP concentration with an increase in mass of beads.

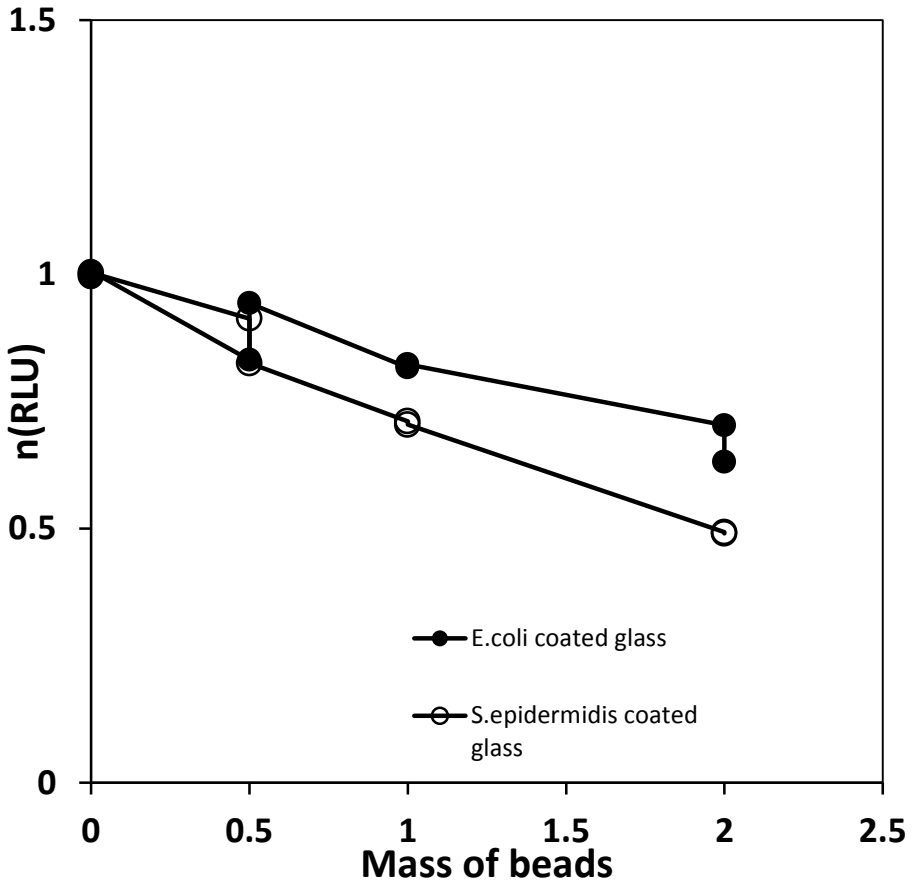

Figure D1.2 - This figure depicts the decline in ATP corresponding to an increase in the mass of coated glass beads with *E. coli* (solid symbols) and *S. epidermidis* (hollow symbols).

VITA

EDUCATION

- **PhD. (Expected: June 2015),** Environmental Engineering (Department of Civil and Environmental Engineering) **Lehigh University**, PA, USA. Advisor: Dr. Derick. G. Brown
- **M.S in Biotechnology**, University of Madras, Chennai, India (2006)
- **B.S in Biochemistry**, University of Madras, Chennai, India (2004)

TEACHING EXPERIENCE

As Instructor

- CEE 170, Introduction to Environmental Engineering (2015)

As Teaching Assistant

- CEE 12 Civil Engineering Statistics (2010)
- CEE 375/477 Environmental Engineering Processes (2010-2013)
- CEE 378/478 Hazardous Waste Management (2011)
- CEE 271/472 Environmental Risk Assessment (2011 and 2014)
- CEE 222 Hydraulic Engineering (2013 and 2014)
- CEE 376/476 Environmental Biotechnology (2013)
- CEE 275 Environmental Microbiology Lab (2012 and 2014)

PEER-REVIEWED PAPERS

- **Albert, L.S. and Brown, D.G. 2015.** "Variation in bacterial bioenergetics during rapid changes in external pH and implications for the activity of attached bacteria." *Colloids and Surfaces B: Biointerfaces*,132:111-116.

PEER-REVIEWED PAPERS IN PREPARATION

- **Albert, L.S. and Brown, D.G.** (In preparation). "Variation in *E. coli* energy levels during attachment to iron hydroxide (goethite) coated sand: Identification of a charge-regulated mechanism for bacterial inactivation." To be submitted to *Environmental Science & Technology*.
- **Albert, L.S. and Brown, D.G.** (In preparation). "Examination of attachment induced intracellular ATP variations in both Gram-positive and Gram-negative bacteria using surfaces spanning a range of surface charge functionality." To be submitted to *Environmental Science and Technology*.
- **Zhu, H., Albert, L.S. and Brown, D.G**. (In preparation). "Method for quantifying surface functional group equilibrium constants and site densities using zeta potential titration data." To be submitted to *Langmuir*.
- **Zhu, H., Dong, H., Lu, H., Xia, W., Albert, L.S, Sheets, S., Fox, J., Redding, A., and Brown, D.G., (In preparation).** "Charge regulated bioavailability of

sorbed organic substrates." To be submitted to *Environmental Science and Technology*.

CONFERENCE PRESENTATIONS

- **Albert, L.S., Zhu, H. and Brown, D.G.,** "Charge-regulated variation in local pH and its effects on the bioenergetics of attached bacteria under non-growth conditions." Presented to the Ninth International Symposium on Subsurface Microbiology, Pacific Grove, CA, 5-10 October 2014.
- **Zhu, H., Albert, L.S. and Brown, D.G.,** "Impacts of the charge-regulation effect on the growth of attached bacteria and the bioavailability of ionizable substrates." Presented to the Ninth International Symposium on Subsurface Microbiology, Pacific Grove, CA, 5-10 October 2014.
- **Zhu, H., Albert, L.S. and Brown, D.G.,** "Impacts of the physiochemical charge-regulation effect on the growth of attached bacteria." Presented to the 88th ACS Colloid and Surface Science Symposium, Philadelphia, PA, 23-25 June, 2014.
- **Albert, L.S., Zhu, H. and Brown, D.G.,** "Charge-Regulated Variation in pH between Two Adhering Surfaces and Its Ability to Affect Bioenergetics of Attached Bacteria under Non-Growth Conditions", Presented to the 88th ACS Colloid and Surface Science Symposium, Philadelphia, PA, 23-25 June, 2014.

- **Albert, L.S., Zhu, H. and Brown, D.G.,** "Effects of localized surface pH on the metabolic activity of attached bacteria", Presented to the 4TH North American International Society of Electrochemistry and Microbiology, Penn State University, 13-15 May, 2014.
- **Albert, L.S., Zhu, H. and Brown, D.G.,** "Impact of surface functional groups on the metabolic activity of adhered bacteria." Presented to the 244th ACS National Meeting, Philadelphia, PA, 19-23 August, 2012.
- **Zhu, H., Albert, L.S. and Brown, D.G.,** "Effects of adhesion on bacterial growth kinetics". Presented to the 244th ACS National Meeting, Philadelphia, PA, 19-23 August, 2012.